COMPARISON OF METHODS FOR ESTIMATING FOREST OVERSTORY COVER

INTEGRATED WILDLIFE INTENSIVE FORESTRY RESEARCH

BC

A cooperative project between the Ministries of Environment and Forests

COMPARISON OF METHODS FOR ESTIMATING FOREST OVERSTORY COVER

David J. Vales
Fred L. Bunnell

Forestry Wildlife Group
Faculty of Forestry
The University of British Columbia
Vancouver, B.C. V6T 1W5

November 1985

This Publication is IWIFR-20

Ministry of Forests, Research Branch EP 923
Ministry of Environment, Wildlife Bulletin B-36

This report received peer review prior to publication and may be considered refereed.

Research supported by the Science Council of British Columbia and the National Sciences and Engineering Research Council of Canada.

Copies of this report may be obtained, depending on supply, from:

Research Branch
Ministry of Forests
1450 Government Street
Victoria, B.C.
V8W 3E7

Wildlife Branch
Ministry of Environment
Parliament Buildings
Victoria, B.C.
V8V 2X5

The contents of this report may not be cited in whole or in part without the approval of the Director of Research, B.C. Ministry of Forests, Victoria.

Citation:

Vales, D.J. and F.L. Bunnell. 1985. Comparison of methods for estimating forest overstory cover. Research, Ministries of Environment and Forests. IWIFR-20. Victoria, B.C.

SUMMARY

Nine techniques for estimating forest overstory cover were tested for precision and differences in mean overstory cover above plots. Two observers were used to test repeatability and possible interactions of four techniques with the overstory. The most precise instrument is the spherical densiometer, but it gives higher estimates of overstory cover than all except one of the other techniques tested. There was an interaction of person and plot with the convex spherical densiometer. Techniques that project wider angles result in higher mean estimates of overstory cover. Techniques using angles greater than 10° are biased with respect to direct overhead (vertical) overstory cover. Over all plots (sample size differences aside), the moosehorn was the most precise instrument among unbiased techniques for the sample design used. Point by point comparisons indicated that the 10° arc of the concentric grid from hemispherical photographs was the most precise, unbiased technique.

ACKNOWLEDGMENTS

P. Wallis helped acquire measurements for tests of technique interactions. J.B. Nyberg of the British Columbia Ministry of Forests provided the hemispherical lens, camera body, and tripod used in this study. Dr. J. Petkau, F. Hovey, B. Wong, Dr. M. Greig, and Dr. Y. El Kassaby made helpful suggestions on the statistical analyses. The British Columbia Ministry of Forests provided services to develop and print the hemispherical photos. The Natural Sciences and Engineering Research Council of Canada and Science Council of British Columbia provided financial assistance. J.B. Nyberg, L.D. Peterson, and S.M. Northway made helpful comments on a draft manuscript.

TABLE OF CONTENTS

SUMMARY iii

ACKNOWLEDGMENTS iv

TABLE OF CONTENTS v

LIST OF TABLES vii

LIST OF FIGURES ix

1 INTRODUCTION 1

1.1 Review of Techniques in Use 3

1.1.1 Ocular 3

1.1.2 Vertical projection, dot 4

1.1.3 Vertical projection, grid 5

1.1.4 Photography or light regime 7

2 STUDY AREA 15

3 METHODS 16

3.1 Definition of Techniques Evaluated 18

3.2 Statistical Methods 21

4 RESULTS 22

4.1 Normality and Equality of Variance 22

4.2 Clearcuts 32

4.3 Gimbal on Microplots 34

4.4 Observer Effects 37

4.5 Technique Effects 51

4.5.1 ANOVA on individual observations 51

4.5.2 ANOVA on plot means 62

4.6 Means and Confidence Intervals 66

4.7 Sample Size Estimates 68
4.8 Correlation of Horizontal Plane of Interception with Means and Standard Deviations 76
4.9 Variation in Relation to Height to Base of Live Crown 77
5 DISCUSSION 77
6 CONCLUSION 90
7 LITERATURE CITED 91

APPENDICIES

1 Paired t-tests and Wilcoxon rank-sum statistics for plot means and all pair combinations 94
2 Descriptive statistics for all techniques on untransformed observations for plot 95

LIST OF TABLES

1 Angle of view for each technique and area of view for a hypothetical 20-m tall canopy with a point of measurement height of 1.2 m 14

2 Mean crown completeness for a clearcut of stand age 10 years and tree height 1.5-2.0 m 34

3 ANOVA comparing gimbal on microplot plot means with plot means for other techniques 35

4 Means, standard deviations, and Duncan's multiple range test at 5% probability for gimbal on microplot plot means and top row plot means for other techniques 37

5 Two-way contingency tables for comparing observers' measurements from ocular and gimbal sight estimation of mean crown completeness 38

6 ANOVA comparing observers' measurements with the spherical densiometer 43

7 Paired comparisons of spherical densiometer estimations of mean crown completeness between observers for all plots ..45

8 ANOVA comparing different observers' measurements from the moosehorn 47

9 Paired comparisons of moosehorn estimation of mean crown completeness between observers for all plots 48

10 Summary of analyses comparing observers' measurements from the moosehorn 49

11 ANOVA comparing techniques generating continuous variables 53

12 Means, standard deviations, and Duncan's multiple range test at 5% probability for all techniques using individual observations as input 54

13 ANOVA comparing 50 mm and 100 mm photographic lenses 55

14 Paired comparisons of 50 mm and 100 mm photographic estimations of mean crown completeness for all plots 57

15 ANOVA comparing observers' measurements from the moosehorn with those from 100 mm photography 58

16 ANOVA comparing observers' measurements from the moosehorn with those from concentric grids of hemispherical photographs 59

17 ANOVA comparing diffuse and direct site factors 61

18 ANOVA comparing observers' measurements from the spherical densiometer with diffuse site factor 62

19 ANOVA comparing all techniques across all plots, using plot means 64

20 Overall means, standard deviations, and Duncan's multiple range test at 5% probability for all techniques using plot means as input 65

21 Univariate statistics on untransformed observations for all techniques across all plots, ranked from lowest to highest MCC 67

22 Univariate statistics on untransformed observations measured at hemispherical photo points only, across all plots 68

23 Approximate maximum sample sizes for selected techniques to obtain a precision of ± 5% mean crown completeness at 95% confidence 76

LIST OF FIGURES

1 Grid for estimating diffuse site factor obtained from from hemispherical photographs 10

2 Concentric ring dot grid used for estimating mean crown completeness from hemispherical photographs 12

3 Solar track diagram used for estimating direct site factor obtained from hemispherical photographs 13

4 Plot layout and location of sampling points for overstory measurements 17

5 Cumulative frequency distribution of observations using four techniques for estimating mean crown completeness ...24

6 Histograms of frequency distributions of observations using four techniques for estimating mean crown completeness 25

7 Histograms of frequency distribution for angular transformed observations for two techniques used to estimate mean crown completeness 26

8 Cumulative frequency distribution for one observer's moosehorn observations within a single plot 27

9 Cumulative frequency distribution of plot means obtained from two techniques used for estimating mean crown completeness 28

10 Relationship between plot variance and plot mean for moosehorn observations of two observers 30

11 Relationship between plot variance and plot mean for all techniques (except concentric grids) and all plots 31

12 Hypothetical example of mean crown completeness estimates versus ranked plots. There is no interaction between observer and plot 40

13 Measurements of mean crown completeness versus ranked plots for two observers using ocular canopy estimation ...41

14 Measurements of mean crown completeness versus ranked plots for three observers using gimbal sight canopy estimation 42

15 Measurements of mean crown completeness versus ranked plots for two observers using the spherical densiometer ..46

16 Measurements of mean crown completeness versus ranked plots for two observers using the moosehorn 51

17 Influence of mean crown completeness on the estimated number of moosehorn samples necessary for a precision of ± 5% with 95% confidence 69

18 Influence of mean crown completeness on the estimated number of spherical densiometer samples necessary for a precision of ± 5% with 95% confidence 70

19 Influence of mean crown completeness on the estimated number of 50 mm photography samples necessary for a precision of ± 5% with 95% confidence 71

20 Influence of mean crown completeness on the estimated number of 100 mm photography samples necessary for a precision of ± 5% with 95% confidence 72

21 Influence of mean crown completeness on the estimated number of diffuse site factor samples necessary for a precision of ± 5% with 95% confidence 73

22 Influence of mean crown completeness on the estimated number of ocular and gimbal sight samples necessary for a precision of ± 5% with 95% confidence 74

1 INTRODUCTION

Estimates of forest overstory cover have been used to study precipitation interception by forests (e.g., Church 1912; Kittredge 1948; Null 1969; Harestad and Bunnell 1981); light transmittance (Miller 1959); habitat of forest dwelling birds (Emlen 1967); and several forest stand characteristics (e.g., Brown and Worley 1965). Predictive relationships using forest overstory cover as the independent variable are useful for estimating timber volume (Garrison 1949) or forest overstory-understory relationships (e.g., Dodd et al. 1972).

Many terms have been used to define the proportion of sky covered by the canopy. Canopy closure, crown closure, and canopy density are often used as synonyms. Bunnell et al. (1985) recently defined crown completeness as the "proportion of sky obliterated by tree crowns within a defined angle . . . from a single point." Crown completeness is a point measurement that takes into account spaces between crowns as well as within crowns. Mean crown completeness (MCC) is a stand measurement derived from a number of crown completeness measurements. Canopy measurements in this study are defined as MCC.

Mean crown completeness is an abstract concept for which no true value can be determined. Studies in which MCC is measured are usually concerned with the relationship of a variable to MCC. Accuracy is desired in a technique selected to index MCC. Because no true value for MCC can be measured,

determining accuracy of MCC as measured by different techniques is not possible. The accuracy of indexing MCC by each technique can only be tested against a variable of interest. Different studies have different parameters of interest, and the way to determine which technique is most accurate for a specific parameter is to evaluate instruments against a predicted variable by using the standard error of regression (e.g., Bunnell et al. 1985; Bunnell and Vales[1]).

Most instrument and technique errors are small in comparison with inherent tree variation and sampling error (Smith 1969). Nevertheless, careful definition and standardization of techniques are essential. Instruments should eliminate operator bias and be precise. Different instruments may give different estimates of MCC in the same stand when used at the same points, and thus some evaluation of accuracy is important. Bonnor (1967) assumed that MCC estimates derived from single vertical dot projection were the true, unbiased plot MCC's. He determined that projection angles of single dots were biased if they resulted in MCC estimates significantly different from the vertical projection estimate. His assumption may be misleading when the canopy measurement is meant to be a predictor variable for rain or snow interception, light transmittance, or understory biomass.

---

[1] Bunnell, F.L. and D.J. Vales. [1985]. Comparison of methods for estimating forest overstory cover, II. Bias and accuracy in predicting snow interception and understory cover. B.C. Min. For., Victoria, B.C. In preparation.

In the former two cases the trajectory of the dependent variables are not vertical and specific overstory measurement techniques are unlikely to incorporate consistent bias, but rather, error associated with variable trajectories. In the latter case the canopy is assumed to be a surrogate for either light interception or some form of competition. Again, departures from vertical are unlikely to be associated with consistent bias, but instead with several scales of variation and with error.

Specific objectives of this study were to: 1) briefly review techniques used to estimate overstory cover; 2) evaluate observer effects within instruments; 3) document differences in MCC among instruments and in interactions between operators, instrument, and canopy; 4) evaluate precision of techniques used to index MCC; and 5) examine the nature and distribution of canopy measurements.

1.1 Review of Techniques in Use

Many techniques have been used to index MCC. The most common methods are ocular, single vertical dot projection, vertical grid projection, or photography.

1.1.1 Ocular

Ocular MCC estimates have been poorly defined, little used, and are subjective. Such estimates can be put into classes or recorded as either open or closed above a point.

Young et al. (1967) ocularly estimated MCC as being in one of three classes above each plot. Robinson (1947) determined ocular estimates to be too unreliable for accurate work.

1.1.2 Vertical projection, dot

Vertical projection of a single dot is often associated with measuring tree crown diameter (Walters and Soos 1962; Ormerod 1968). Bonnor (1967) tested bias and precision of single dot projection for indexing MCC and concluded that the vertical dot projection is useful in estimating MCC, but that a large number of readings is necessary. Emlen (1967) developed a vertical viewing tube with mirrors and a nail suspended as a plumbob to get a single point. Lindroth and Perttu (1981) describe an instrument similar to a Cajanus cylinder that uses a brass tube with a mirror at the bottom for sighting through the tube, and is mounted on a universal joint to hang vertically. Walters and Soos (1962) developed a self-leveling gimbal sight with crosshairs etched on the lens surface. The gimbal sight was originally designed to measure tree crown diameters. It was later modified (Ormerod 1968) to be smaller, lighter, and easier to use. The current version uses a gimbal-mounted Asahi Pentax right-angle camera viewfinder with crosshairs and a small circle in the center of the lens to sight on the crown. Ormerod (1968) concluded that for measuring crown diameters, the gimbal sight showed no difference between operators. However, use of the gimbal

sight for MCC measurements is subjective; the observer must determine how much of the center circle is covered by canopy to record the point as open or closed.

1.1.3 Vertical projection, grid

A commonly used vertical projection of a grid is the moosehorn developed by Robinson (1947). Modifications were recommended by Garrison (1949) to later develop the Hillborn moosehorn. A similar instrument was designed by Hale (1980), which has a grid of open cells rather than a grid of dots as in the moosehorn. The moosehorn does not have a means for leveling so care must be taken to point it vertically. Robinson (1947) stated that normally 20 moosehorn readings are taken on a 0.25-acre (0.1-ha) plot and if time permits, 40 are preferable. Garrison (1949) used 15 randomly located moosehorn readings on 0.25-acre (0.1-ha) plots. Bonner (1967) evaluated precision, bias, and sample size requirement for the moosehorn over a range of MCC from 25 to 93% on plots 100 x 100 ft. (0.09-ha). He felt that the moosehorn was not significantly biased, that it was more precise than single vertical dot projection, and that the number of readings required depended on canopy density (MCC) and crown distribution. Because crown distribution was unknown for a particular plot, he fitted a parabola approximating the maximum sample size necessary to give a desired precision. To be within ± 5% mean MCC at 95% probability, he estimated that

a maximum of 300 readings at 50% MCC and 192 at 80% MCC were necessary.

Lemmon (1956) developed both convex and concave mirror spherical densiometers. The convex spherical densiometer is widely used in forestry to index MCC. Concave mirrors give a narrow view of the overhead canopy compared to convex, wide-view mirrors. A grid of 24 quarter-inch squares is etched on the convex mirror of Lemmon's spherical densiometer. Within each square, four equi-spaced dots are imagined and counted where they represent canopy openings. Lemmon (1956) designed the instrument to have the properties of a 6-inch (15.2-cm) sphere. This proved satisfactory for him in western coniferous forests of unspecified age and height. Due to the way the instrument is held, the angle projected is greater in front of the observer than behind. That is, more than half of the canopy viewed is away from the center of the instrument. Leveling is achieved with a circular spirit level mounted beside the mirror. Determination of canopy openings is subjective. Lemmon (1956) felt that operators needed training to be consistent in using the instrument. He felt that judgement and experience were needed to differentiate between overstory areas that were completely open and areas that were thin; and that training and experience were needed for different forest species or types, because of differences in overstory characteristics.

1.1.4 Photography or light regime

Photographic methods for studying the canopy date back to the 1920's when the Hill camera was introduced (Hill 1924). Wide-angle photography has been used to study the light regime under canopies (Evans and Coombe 1959; Anderson 1964). Interception and transmittance of diffuse and direct radiation have received considerable attention in forest regeneration and crop growth study. Lindroth and Perttu (1981) presented methods for calculating radiation extinction through forest canopies from hemispherical photographs having estimates of MCC from vertical dot projections. Lenses covering less than 180° can be used to index MCC (e.g., Null 1969).

Obtaining consistent exposure is one difficulty in photographing a forest canopy. To examine differences in canopy among points and among forest stands, it is necessary to have uniform exposure giving uniform contrast between sky and foliage. Opportunistic sampling does not allow for consistent sky conditions. Sunny days overexpose thin areas of foliage, giving lower MCC estimates than would be obtained during uniform cloudy days. There is potential for bias among persons interpreting photographs. Estimating cover class within a grid of cells is subjective and confounded by exposure on sunny days. Computer scanning of photographs is possible, but exposure of all photos must be similar (Olsson et al. 1982). Dot grids are subjective but more precise than computer scans of variably exposed photographs. Error can

result from overexposed photos, the size of dots in relation to the size of canopy openings, and interpreter definition of what constitutes open canopy.

Newer hemispherical lenses such as the one produced by Nikon are fully color corrected, have reasonable image definition at the horizon, and give an exact reproduction on a flat plane of all objects encompassed within the 180° field. Lower quality lenses with angles less than 180° may give a distorted image around the edges of photographs. Given his equation of accuracy with vertical projection, Bonnor (1967) found bias with single dots projected at angles greater than 7.2° of vertical. He recommended that only the central 10% of hemispherical photos and projection angles less than 6° of vertical be used. The central 10% of hemispherical photographs, however, represent a projection angle of approximately 15° of vertical.

An advantage of photography is that the image is permanent. This permanent record allows for evaluation of the photograph in different ways. Different interpreters can evaluate the photograph and redefine open canopy to get a more precise MCC index. An index of MCC at different angles from the zenith also is possible. Cost and time required are major disadvantages.

Null (1969) studied throughfall precipitation using a 135 mm focal length lens with 18° coverage to estimate MCC. He sampled the central 8.3% of each photograph with a dot grid.

Different interpreters gave slightly different results (Null 1969). Lenses with a focal length greater than 50 mm are rarely used in determining MCC.

Estimates of diffuse light with hemispherical photos use a concentric grid of rings divided by radii (Fig. 1). The grid, as suggested by Anderson (1964), is constructed so that each segment contributes an equal proportion of total illuminance from a standard overcast sky. The diffuse site factor (Anderson 1964), sky obscuration factor (Lindroth and Perttu 1981), and view factor (Steyn 1980) all are derived using a hemispherical grid technique. Anderson's (1964) definition of diffuse site factor refers to openings in the canopy which allow diffuse light to pass through. In this study, "diffuse site factor MCC" (hereafter referred to as diffuse s.f.) represents closed canopy and is defined as 1 minus the diffuse site factor sensu Anderson (1964), to represent closed canopy. Diffuse s.f. grids can be composed of a different number of rings and radii to meet the user's needs.

Mean crown completeness can be analyzed at different angles from the zenith of hemispherical photos. Brown and Worley (1965) used a dot grid laid over a diffuse s.f. grid to estimate MCC from the central 30% of each hemispherical photograph. Studies of snow and rain interception concentrate on the central portion of hemispherical photographs. A grid of five concentric rings with 50 dots per ring and each ring

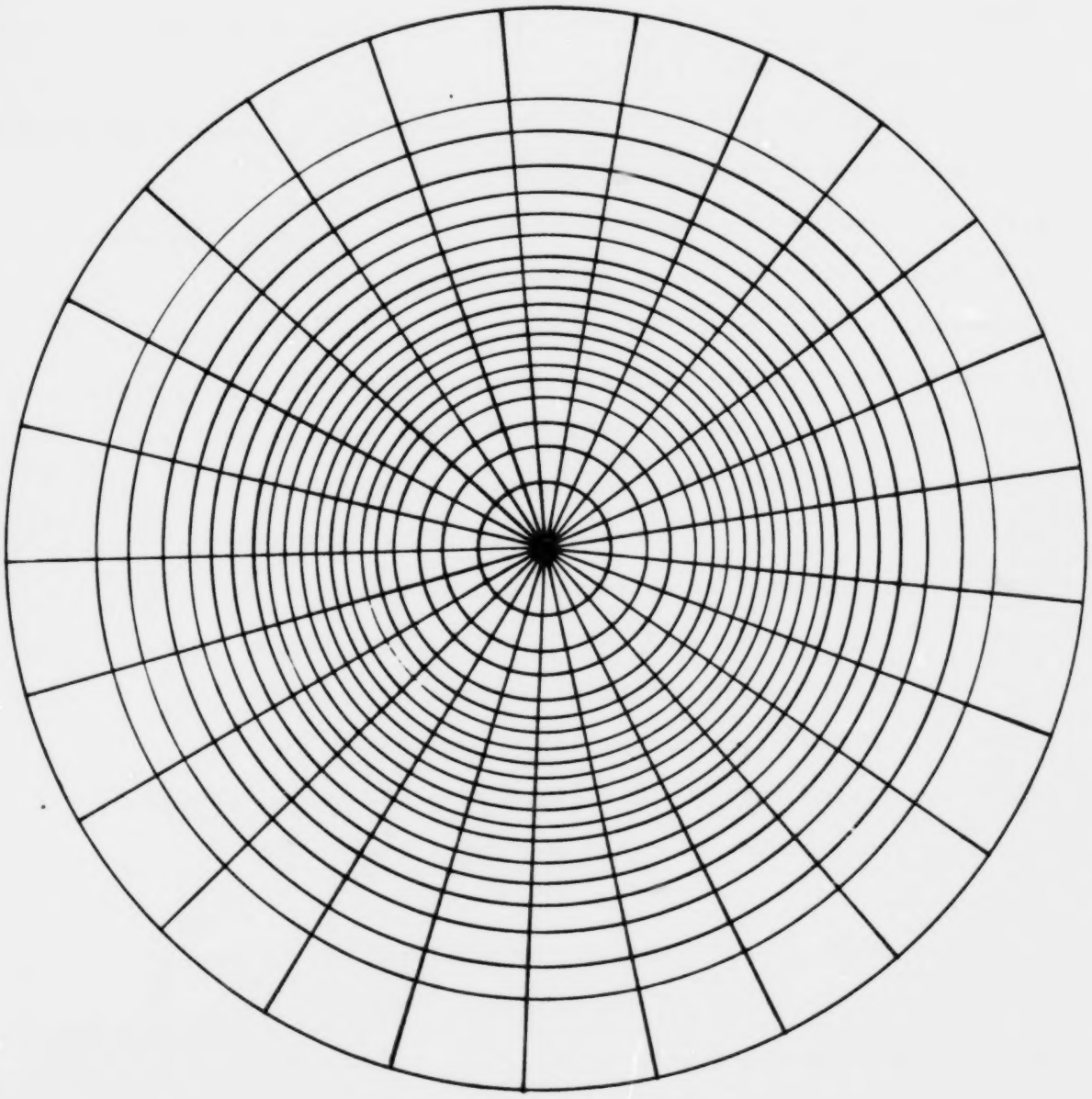

FIGURE 1. Grid for estimating diffuse site factor obtained from hemispherical photographs.

representing an additional 5° increment in angle from zenith (10° arc; Fig. 2) is used by the B.C. Ministry of Forests to estimate snow interception by the canopy (J.B. Nyberg, pers. comm., B.C. Ministry of Forests).

A second method of studying the light regime under a canopy is to determine MCC in the direct path of the sun. A solar track (Fig. 3) for the latitude and period of interest (such as growing season or snowmelt) is placed over the photo and the amount of light passing through the canopy in the path of the sun determined (Evans and Coombe 1959). Anderson's (1964) direct site factor is the percentage of direct light reaching the point where the photograph was taken. "Direct site factor MCC" in this study (hereafter referred to as direct s.f.) is the proportion of sky obstructed by canopy in the solar path during the summer months of May to September.

The angle of view differs for each technique (Table 1). The area viewed by an instrument depends on the height to base of live crown (HBLC) and the height of the point of projection of the angle. The area of horizontal plane of interception (HPI) is defined as the area of the base of live crown intercepted by the projected angle from a certain height, usually 1.2 m (eye level) above ground. Areas of HPI for a plot averaging 20 m HBLC are presented in Table 1.

FIGURE 2. Concentric ring dot grid used for estimating mean crown completeness from hemispherical photographs.

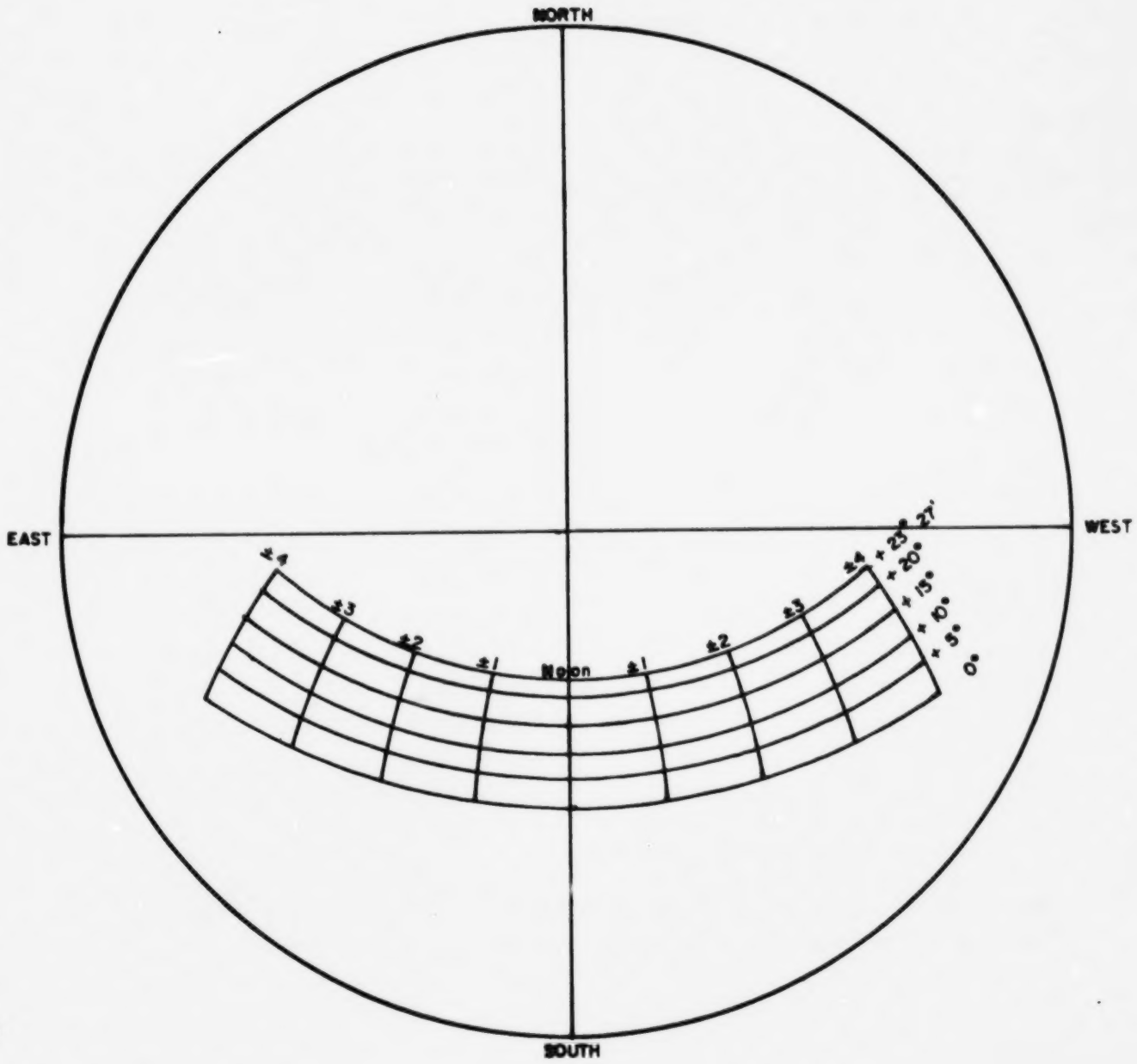

FIGURE 3. Solar track diagram (for 50^{o} N latitude) used for estimating direct site factor obtained from hemispherical photographs. East and west are interchanged to represent the true canopy view.

TABLE 1. Angle of view for each technique and area of view for a hypothetical 20-m tall canopy with a point of measurement height of 1.2 m

Technique	Degree of arc	Geometry	Area of HPI[a]
Ocular	variable	variable	variable
Gimbal sight	0.67°	circular	0.04 m^2
Moosehorn	10.2°	square	11.3 m^2
Spherical densiometer	≈60°	circular/convex but divided into squares	620.0 m^2
50 mm lens	37° x 25°	rectangular	104.9 m^2
100 mm lens	18.5° x 12.5°	rectangular	25.2 m^2
Diffuse[b]	180°	circular	>1018.0 m^2
Concentric grid[b]	10°	circular	8.5 m^2
Concentric grid[b]	20°	circular	34.5 m^2
Concentric grid[b]	30°	circular	79.7 m^2
Concentric grid[b]	40°	circular	147.1 m^2
Concentric grid[b]	50°	circular	241.4 m^2
Direct[b]	depends upon period of interest	curved path	variable

[a]Horizontal plane of interception 18.8 m from the instrument.
[b]derived from hemispherical photography.

2 STUDY AREA

Sampling was done at the University of British Columbia Research Forest near Haney, B.C., 45 km east of Vancouver. Overstory species on the plots included western hemlock (Tsuga heterophylla), Douglas-fir (Pseudotsuga menziesii), and occasionally western redcedar (Thuja plicata). A western redcedar midstory was common. Dominant trees were 75-90 years old, with heights between 20 and 45 m and height to base of live crown between 10 and 25 m. Slopes ranged between 2 and 70%, aspect between 177° and 283°, and altitude between 89 and 447 m.

Three ecotypes within one plant association (Klinka 1976) were covered in sampling. Ten plots, with one in a 10-year-old clearcut, were placed in the Gaultheria-Western Hemlock-Douglas-fir plant association of the Coastal Western Hemlock dry biogeoclimatic subzone (CWHa; ecotypes included loamy sand Lithic Orthic Humo-Ferric Podzol on moraine veneer, Lithic Podzol on moraine veneer, and Lithic Folisol from organic veneer). Ten plots, with one in a 3-year-old clearcut, were located in the Gaultheria-WH-DF plant association of the CWHa dry subzone found on ecotypes with sandy loam Mini Humo-Ferric Podzol on moraine blanket. Five plots were located in the Mahonia-Gaultheria-WH-DF ecotype of the Gaultheria-WH-DF plant association in the CWHa subzone found on sandy loam Mini and Orthic Humo-Ferric Podzols developed from colluvial veneer.

3 METHODS

Plots were selected to encompass a range of MCC within each ecotype. A 2 x 10 m rectangular plot (Fig. 4) was laid out along slope contours. Ocular, gimbal, moosehorn, and spherical densiometer canopy measurements were taken at 1-m intervals along each edge and along the center line of each plot for a total of 33 observations per plot (except two plots in which there were 20 observations). Gimbal on microplot (gimmp) readings were taken at four corners of twenty 0.5 x 0.5 m quadrats along the top inside edge of each plot (N = 42 per plot). Canopy classes ranged from 0 to 4 for each individual microplot, representing MCC above the microplot as 0,25,50,75, and 100%. Photos with 50 mm and 100 mm lenses were taken at the corners of the macroplot and at the 3-m and 7-m mark of each side (8 photos/lens/plot). A *t*-test on one plot (G3, MCC 0.91 with 50 mm lens) showed no significant difference in mean MCC between photos taken on all 33 points, versus photos taken on the 8 points ($P > 0.05$). Two hemispherical photographs were taken along the center line of each plot at the 3-m and 7-m mark. Two observers (denoted by DV and PW) independently sampled the canopy using ocular, gimbal, moosehorn, and spherical densiometer. Ocular estimates for each observer were always made first. An additional observer used the gimbal sight on the same plots and at the same points 7 months prior to this study (BWgimbal). For all readings each observer stood facing

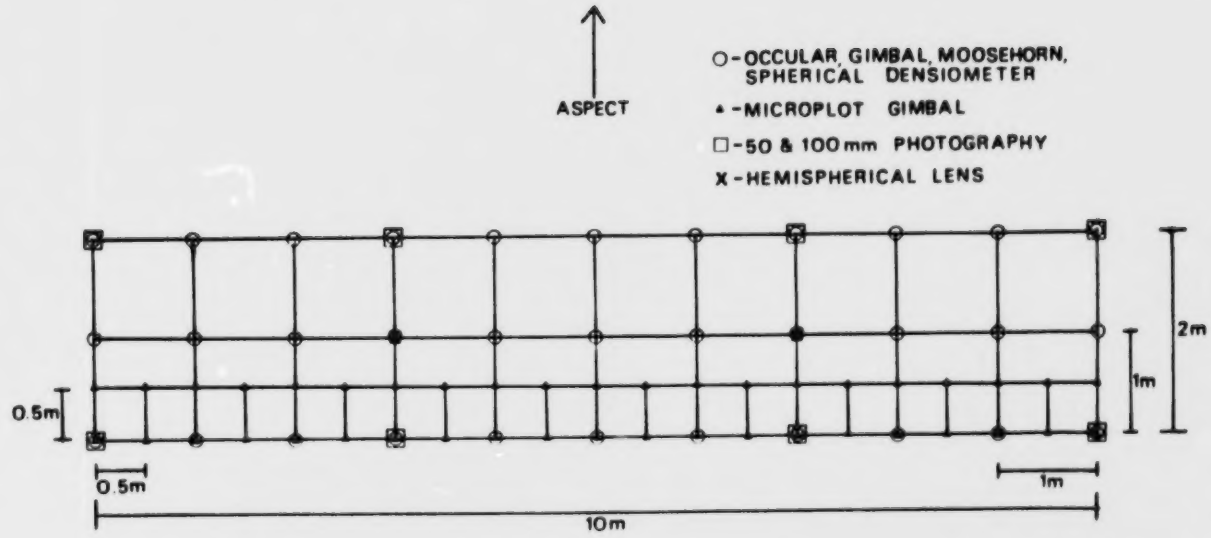

FIGURE 4. Plot layout and location of sampling points for overstory measurements.

downslope.

3.1 Definition of Techniques Evaluated

Ocular estimates were made from a point where the observer simply looked vertically up through the canopy and decided if the point was reasonably covered by the tree canopy. Each observer was allowed to define his angle of view and decide if the point was open or closed.

The gimbal sight was held at eye level directly above each point. When the canopy covered greater than 50% of the center circle, the point was recorded as closed. For gimbal on microplots, gimbal sight readings by one observer were taken at the corner of each microplot. The MCC class above each microplot was the sum of the four corner gimbal readings.

The moosehorn was held at eye level directly above each point. The number of dots that fell on open spaces in the canopy were counted, subtracted from 25 possible dots, and then divided by 25 to give a proportion MCC above each point (0.0-1.0 in increments of 0.04).

The convex spherical densiometer was held at elbow level and far enough away from the observer so he would not be in the field of view. Twenty-four squares with four imaginary equi-spaced dots per square were systematically scanned. Dots that fell where open canopy was seen on the grid were counted, subtracted from 96 possible dots, and divided by 96 to give a proportion MCC above each point.

Photographs using 50 and 100 mm focal length lenses were taken 1.2 m above ground, oriented vertically, and mounted on a tripod with levels. Lenses were changed at each point. The 50 mm lens had a yellow filter and the 100 mm lens a red No. 25A filter to improve contrast between trees and sky with black and white film. No difference was noted between the two filters. Photographs were underexposed two full f-stops to improve contrast. The aperture was fixed at a desired f-stop (f8.0 or f11.0) and shutter speed changed to achieve the desired exposure. Tree movement due to wind was not a problem. Developing and printing of all photographs were done by the same processing lab, which was requested to print the photos darker than normal.

Each photo was analyzed with an acetate dot grid having 32 dots per square inch (6.45 cm^2). Photographs were a standard size 3-1/2 x 5 inch (8.9 x 12.7 cm) 35 mm print, which represented 560 possible dots per photo. The entire photograph was analyzed. Time constraints did not permit additional analyses of the photos in different ways. Dots that fell on open sky were counted, subtracted from 560, and divided by 560 to give a proportion MCC for each photo.

Hemispherical photographs were taken 1.2 m above ground, oriented vertically, and mounted on a tripod with levels. A Nikon fisheye lens (8 mm focal length) was mounted on a Nikon F2AS body and a yellow No. 52 filter was used to improve contrast. North-south orientation was obtained using lights

mounted on the lens. Custom developing and printing was done by the B.C. Ministry of Forests lab in Victoria, B.C., to obtain consistency in print quality and image size. Prints were 19 x 24 cm with the hemispherical image being 17 cm in diameter.

Diffuse and direct site factor estimates were derived using the technique described by Anderson (1964) and J.B. Nyberg (pers. comm., B.C. Ministry of Forests). A 500-cell "spider web" grid (Fig. 1) of 25 radii and 20 concentric circles on acetate was laid over each photo. An ocular estimate was made of the number of cells in each cover class (0, 0-33, 33-66, 66-90, and 90-100% of sky obstructed). The sum for each cover class was multiplied by 1 minus the contribution of the total possible illuminance for each cover class (0, 0.25, 0.50, 0.75, and 1.00) and then averaged for the entire photo (Anderson 1964).

To derive direct site factors, an acetate sheet (Fig. 3) with a solar track for the period between 21 March to 3 September at 50° N latitude was laid over each photo. An ocular estimate was made of the cover class for each of 40 cells. Each cell was multiplied by 1 minus the contribution to the total possible illuminance for that cover class and then averaged to give an average direct site factor for each photograph.

The central 50° of each hemispherical photo was evaluated with a concentric ring dot grid (Fig. 2), used to estimate

snow interception by the canopy (J.B. Nyberg pers. comm., B.C. Ministry of Forests). Five rings, each representing a 5° angle from the zenith (10° arc) and each containing 50 dots, were evaluated for the proportion of MCC within each ring. Each 5° increment in angle from the zenith was obtained by adding dots in the inner rings and dividing by the total possible number of dots. The MCC's for the outer rings were therefore dependent upon values derived for the inner rings.

3.2 Statistical Methods

Means, standard deviations, confidence intervals, measurements of skewness and kurtosis, and analyses of variance (ANOVA) were calculated for those techniques which provided continuous or near-continuous variables. Duncan's multiple range test at 5% probability was used to compare means when the ANOVA was significant. Although Duncan's test is liberal and has been criticized (for review, see Jones 1984), the Type I error rate for adjacent means is maintained (Jones 1984). Ocular and gimbal measurements were discrete and were treated with proportion sampling methods for a binomial distribution (Cochran 1977). Two-way and multi-way tables were used where appropriate. Nonparametric analyses included Wilcoxon rank-sum statistics for paired observations, Friedman's method for randomized blocks, and the ranking of observations from which the normal scores of the adjusted ranks were then taken and the rank-transformed observations

analyzed (Conover and Iman 1981). Data analysis was carried out at The University of British Columbia on an Amdahl V8 computer, using the statistical analysis programs BMDP, MIDAS, ANOVAR, GENLIN (for an unbalanced ANOVA), and SPSSx (for additivity).

4 RESULTS

Analyses initially examined homogeneity of variance among samples, the distribution of measurements, and transformations to increase normality in the distribution and reduce heteroscedasticity among sample variances. Then potential observer effects and technique effects were evaluated. Recent clearcuts and the gimbal on microplot technique represented special cases. Sample sizes required for a specified level of precision were estimated for most techniques. General relationships associated with the angle of projection for each technique and height to base of live crown were documented.

4.1 Normality and Equality of Variance

Basic assumptions for analysis of variance are that the observations are normally distributed around a sample mean; that sample means are normally distributed around a population mean; and that the variance is homogeneous between factors. Bartlett's test for homogeneity of variance is sensitive to departures from normality, but Layard's Chi-square is less so (M. Greig, pers. comm., University of B.C.). The results of

Layard's Chi-squared test were used to evaluate homogeneity of variance. Transformation of observations to obtain homoscedastic variance often results in their distribution approaching normality (Sokal and Rohlf 1981:418). The F-test used in ANOVA is robust. Only very skewed distributions have a large effect on the significance level of the F-test (Sokal and Rohlf 1981:414), and consequences of non-normality of error and moderate heterogeneity of variance are not serious (Sokal and Rohlf 1981:408).

All techniques for overstory measurements were examined for normality across all plots by: plotting the cumulative frequency distribution (Fig. 5; an S-shaped curve is indicative of a normal distribution); examining histograms (Fig. 6); and examining residuals. Observations were consistently skewed to the left. The moosehorn histogram was bimodal, with peaks at 0 and between 0.85 to 1.0. Square root, reciprocal of square root, natural logarithm, reciprocal, power, and angular (arcsine square root) transformation of the data were tried, but none of them approached normal distributions notably better than the original data (Fig. 7). The within plot distribution was generally non-normal (e.g., Fig. 8). Distributions of plot means for individual techniques also were not normal (Fig. 9), and transformations had no effect on the distribution. However, the distribution of residuals for plot means of all techniques combined did approximate normality.

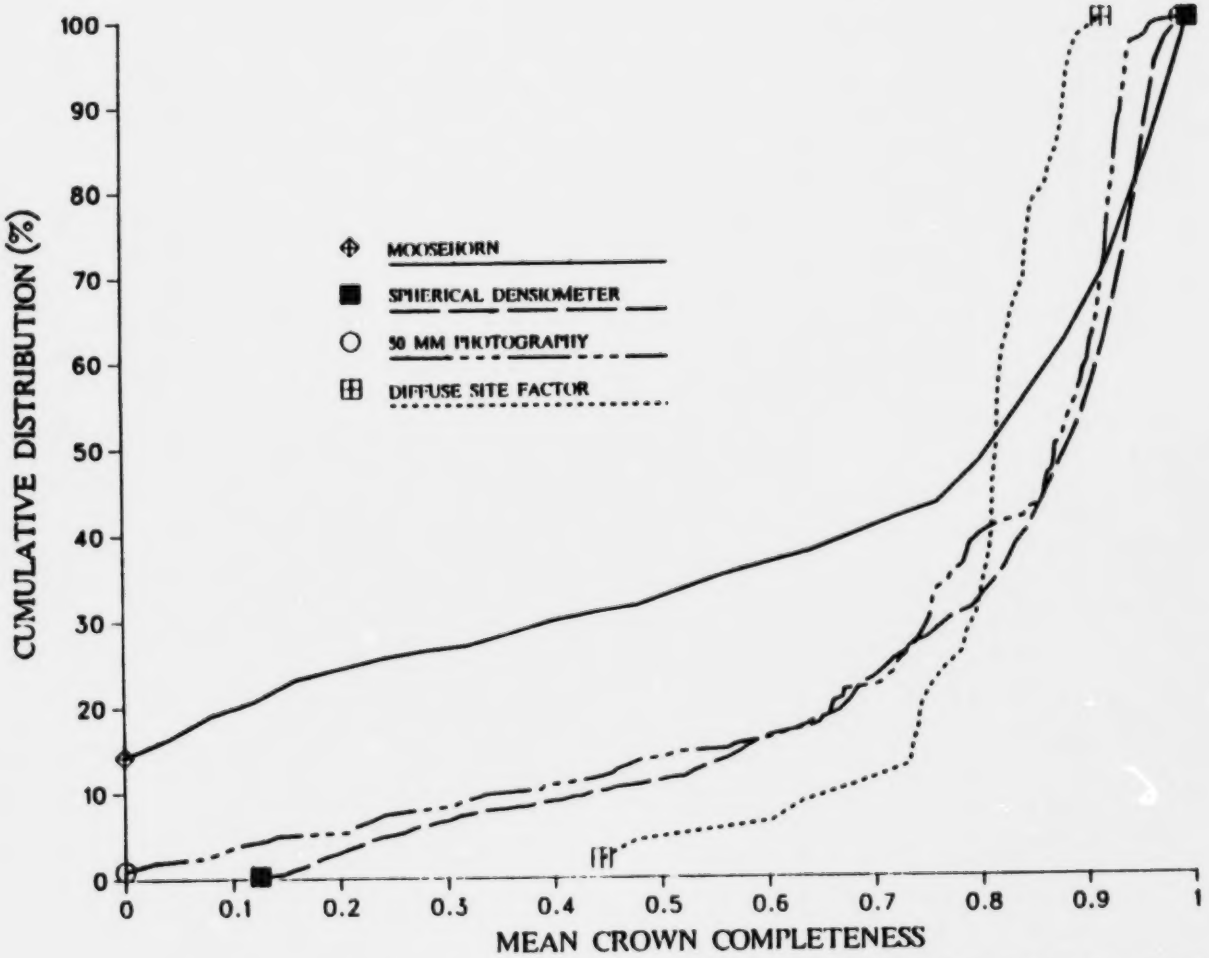

FIGURE 5. Cumulative frequency distribution of observations using four techniques for estimating mean crown completeness.

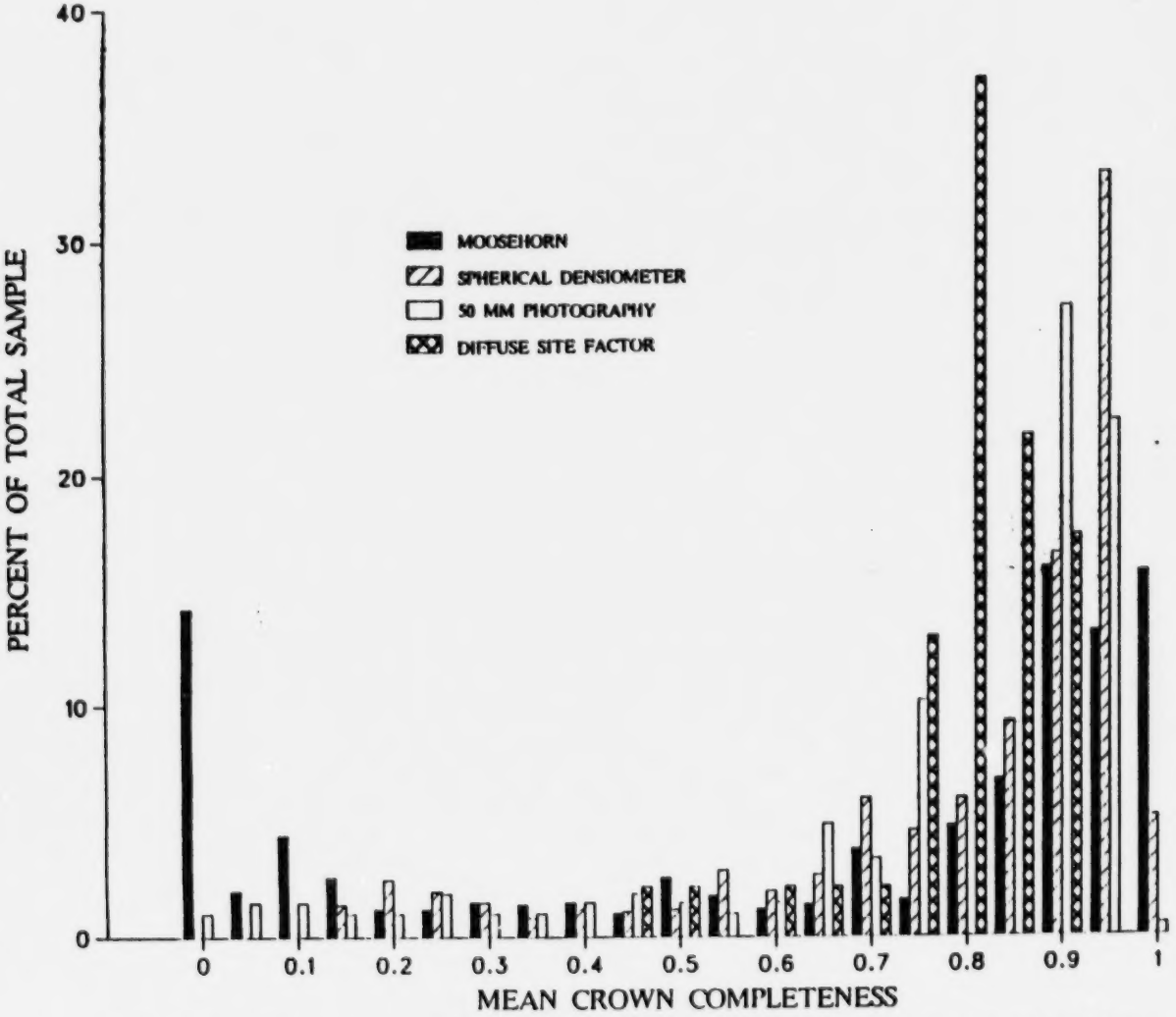

FIGURE 6. Histograms of frequency distributions of observations using four techniques for estimating mean crown completeness.

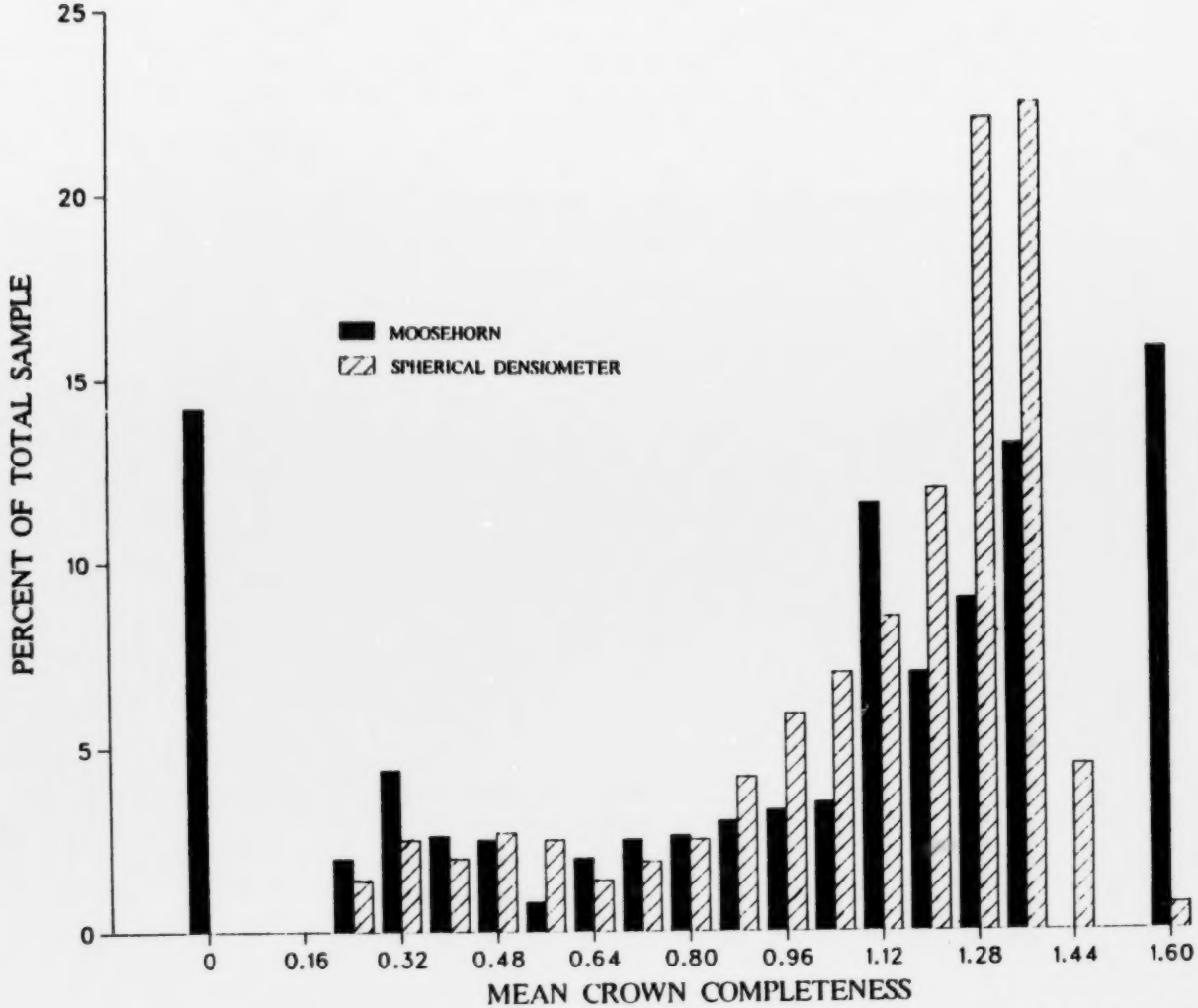

FIGURE 7. Histograms of frequency distributions for angular transformed observations for two techniques used to estimate mean crown completeness.

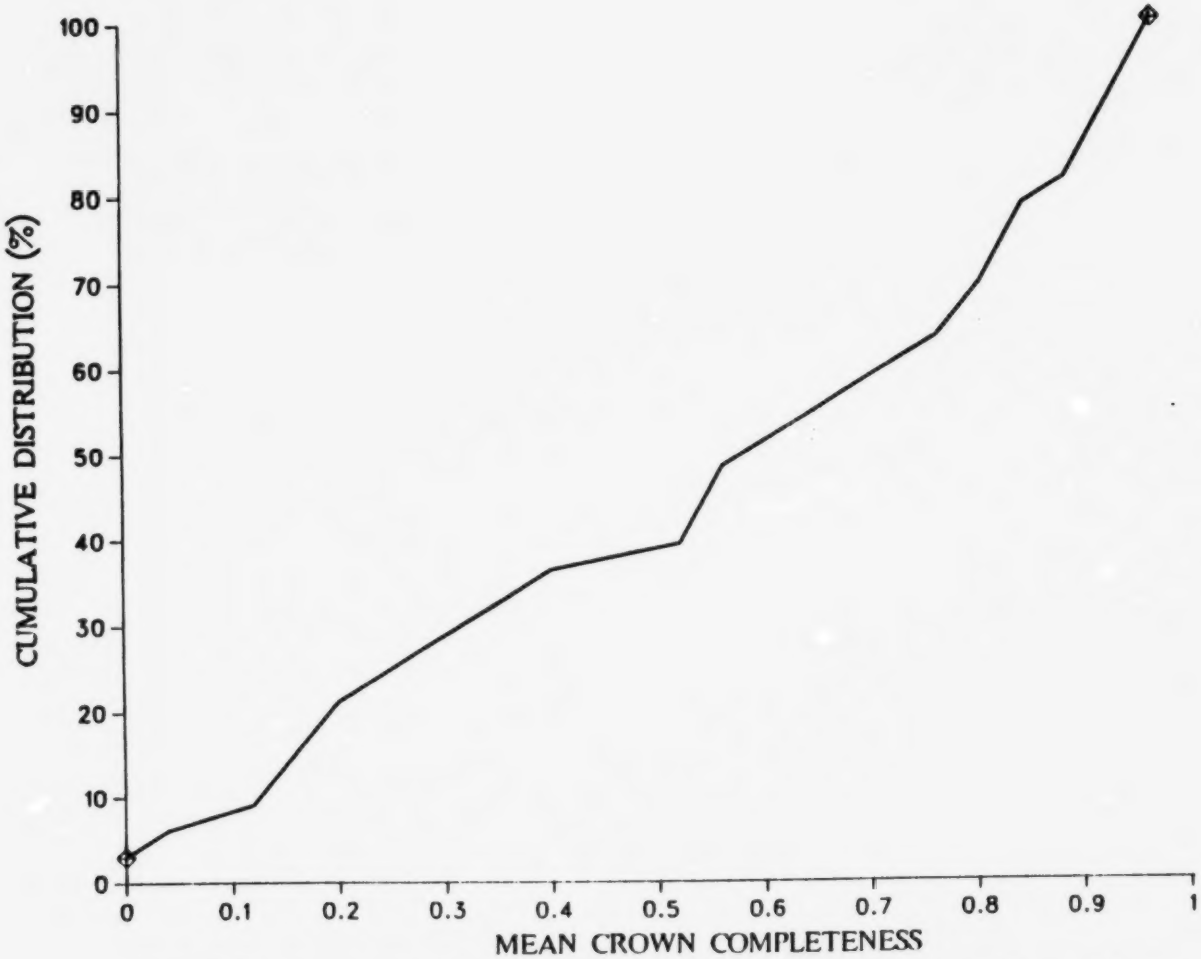

FIGURE 8. Cumulative frequency distribution for one observer's moosehorn observations within a single plot.

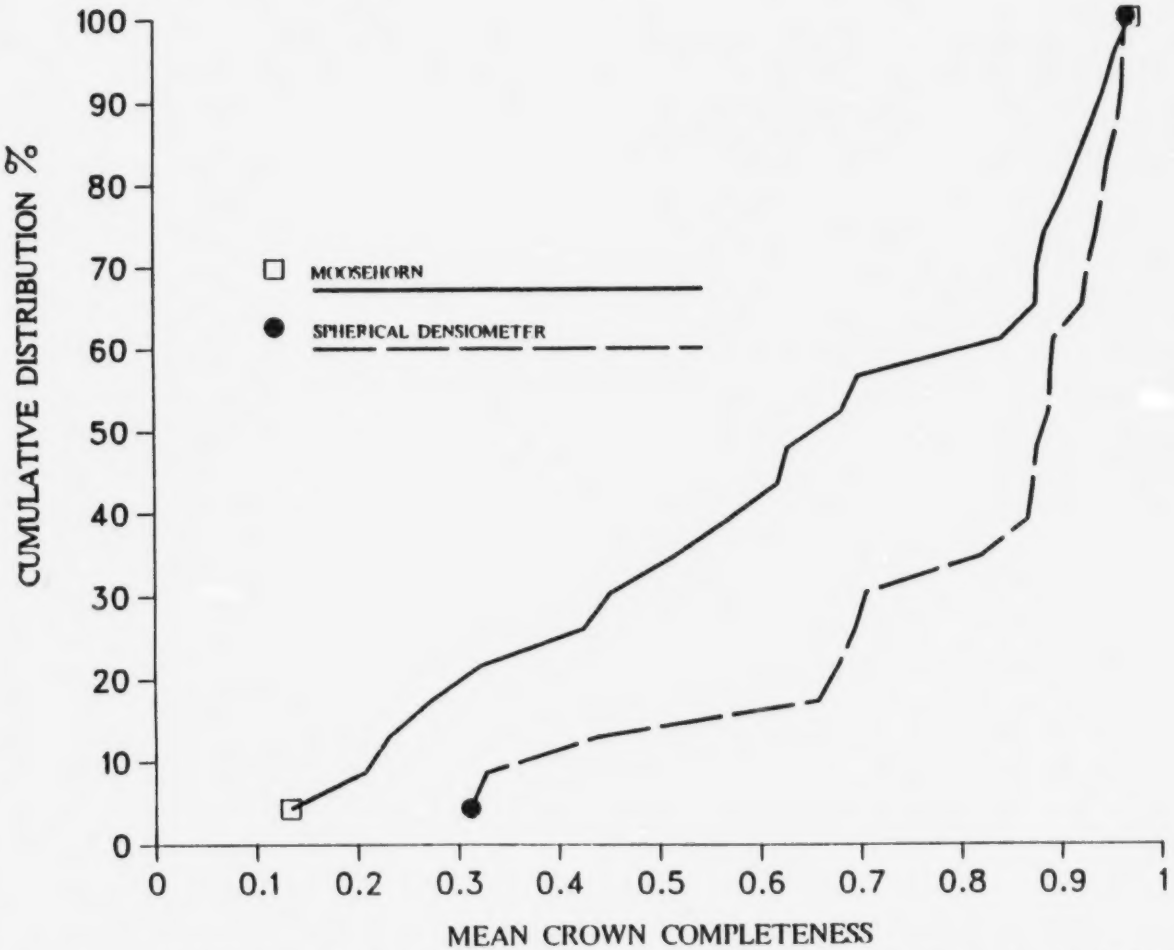

FIGURE 9. Cumulative frequency distribution of plot means obtained from two techniques used for estimating mean crown completeness.

Means and variances were computed within each plot for all techniques and graphed for all plots. Figure 10 illustrates the relationship between estimates of variance and means for untransformed moosehorn readings of both observers; Figure 11 illustrates the relationship for all but the concentric grid techniques. There is a peak of greatest variance around 50% MCC, typical of binomial distributions. The angular transformation had a slight effect, but failed to yield homogeneous variance. Attempts to transform the variance and mean to find a relationship between the two and then integrate the relationship to develop a transformation failed.

The ANOVA's used were mixed model, nested ANOVA's treated as a factorial design. Ecotype effects were fixed, plots were nested in ecotypes and plot effects were random, and techniques were crossed among all plots. Analyses were highly unbalanced when individual observations of all techniques were compared, but nearly balanced for analysis of plot means.

Because two of the basic assumptions of ANOVA were not met, nonparametric tests were considered. The appropriate nonparametric test had to analyze an unbalanced nested factorial design and provide a test of the interactions. Ranked analysis of individual observations was confined to analyzing the variables regarded as continuous. Ranked ANOVA's were computed where significance levels of parametric analyses were not highly significant or insignificant ($0.01 \leq$

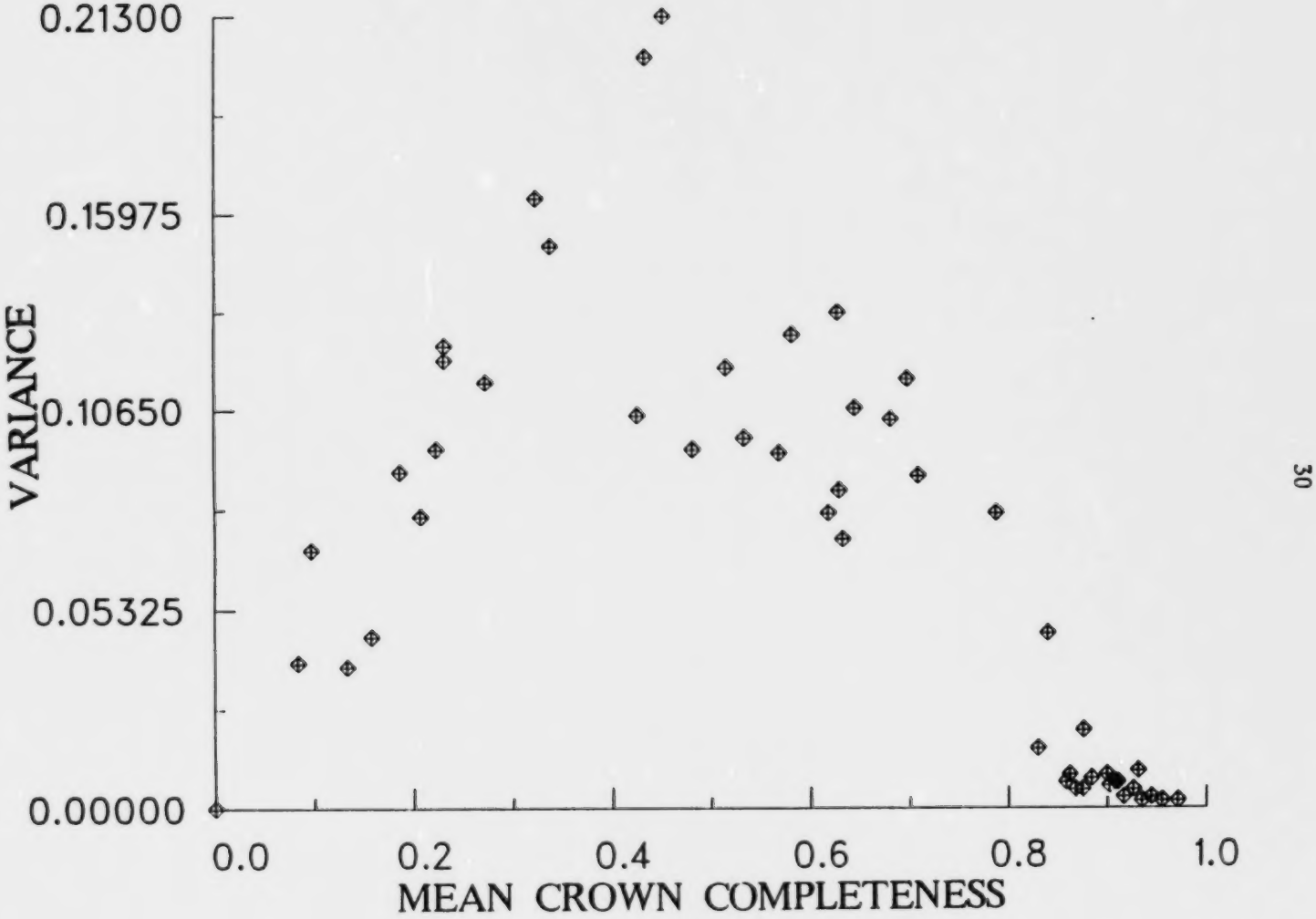

FIGURE 10. Relationship between plot variance and plot mean for moosehorn observations of two observers.

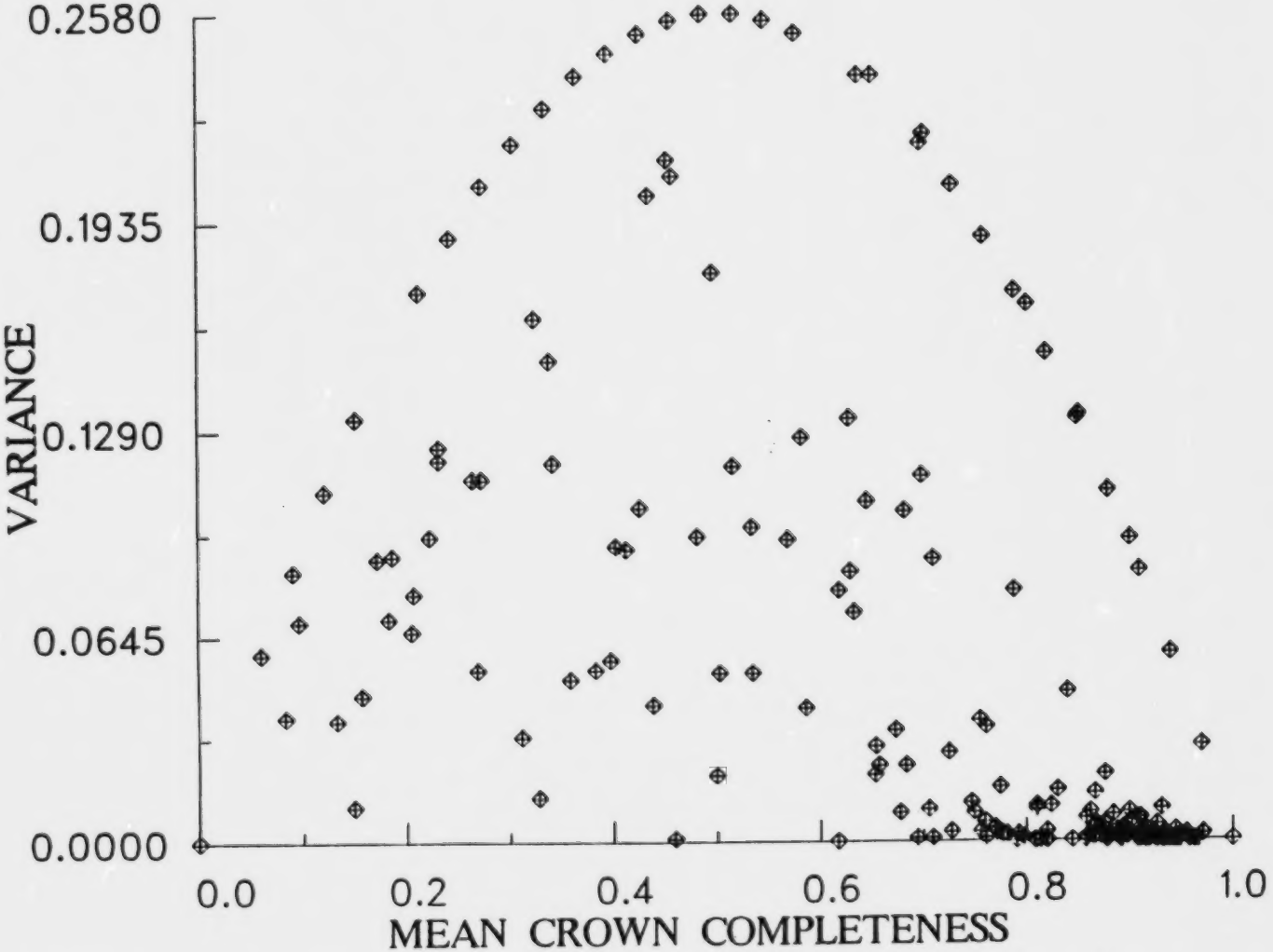

FIGURE 11. Relationship between plot variance and plot mean for all techniques (except concentric grids) and all plots.

$P \leq 0.10$). For the ranked ANOVA's, observations were ranked across all techniques and all plots (Scheirer et al. 1976; Conover and Iman 1981; Errico[2]; M. Greig, pers. comm., University of B.C.). Ties were broken by a random process. The ranked observations were adjusted by subtracting 0.5 and dividing by the total number of observations (M. Greig, pers. comm., University of B.C.). The ranked observations were transformed to normal scores. The normal scores resulted in normality (observations combined for all plots) for all techniques. Wilcoxon's matched-pair rank-sum statistics were calculated to compare to the results of paired t-tests. Two-way and multi-way contingency tables were used where appropriate to test for differences between observers and techniques.

4.2 Clearcuts

One of the clearcut plots contained seedlings approximately 3 years old and did not have any trees taller than 0.5 m. The other clearcut plot in 10-year-old regeneration had trees between 1.5 and 2.0 m tall, with approximately 12 000 stems per hectare. The younger stand had an MCC of 0%. The older stand had a canopy taller than the height of the point of measurement. This resulted in some techniques recording a partial canopy. The MCC for each

[2] Errico, D. 1982. Unpublished memorandum. B.C. Min. For., Victoria, B.C.

technique in the older plot is shown in Table 2, presented in order of increasing MCC.

Some techniques gave an MCC of 0%. The spherical densiometer gave the highest MCC estimate, probably because it was used throughout the plot (and so included the outer edge excluded by the hemispherical lens), and likely because it included trees from outside the plot.

A young stand will have a low average tree HBLC. The MCC estimate will depend on the difference between the HBLC and the height of the MCC measurement. Because this study was concerned with testing different instruments for estimating overhead MCC in older stands, and because some techniques estimated 0% canopy for the plot (estimate of variance=0), the two recent clearcuts were excluded from further analyses.

4.3 Gimbal on Microplots

The gimbal on microplot (gimmp) technique was compared to other techniques for all plots. Only canopy measurements taken along the row closest to the microplots (top row) were used for comparison. Gimmp measurements for each microplot fall into five discrete classes: no corners with closed canopy, one, two, three, or all four corners measured as closed. To compare other techniques to gimmp, plot means of the MCC measurements for the techniques were calculated and used in an ANOVA.

The analysis (Table 3) indicated significant differences

TABLE 2. Mean crown completeness for a clearcut of stand age 10 years and tree height 1.5-2.0 m

Technique[a]	N	Mean	S.D.	1/2 width 95% conf. int.
Gimmp	20	0.0		
50 mm photo	8	0.0		
100 mm photo	8	0.0		
10° grid	2	0.0		
20° grid	2	0.0		
30° grid	2	0.0		
40° grid	2	0.0		
50° grid	2	0.0		
Direct s.f.	2	0.0		
PWmoosehorn	33	0.08	0.198	0.07
PWocular	33	0.09	0.292	0.10
PWgimbal	33	0.09	0.292	0.10
DVmoosehorn	33	0.10	0.263	0.09
BWgimbal	33	0.12	0.331	0.12
Diffuse s.f.	2	0.15	0.103	0.92
DVocular	33	0.15	0.364	0.13
DVgimbal	33	0.15	0.364	0.13
PWsph. dens.	33	0.18	0.264	0.09
DVsph. dens.	33	0.21	0.257	0.09

[a]DV, BW, and PW refer to observers used.

TABLE 3. ANOVA comparing gimbal on microplot plot means with plot means for other techniques

Source	df	MSE	*F*-ratio	*P*	Test term
Ecotype	2	1.36	1.53	0.452	Plot
Plot(ecotype)	18	0.89	43.44	<0.001	Residual
Technique	11	0.13	6.44	<0.001	Residual
Technique x ecotype	22	0.01	0.65	0.884	Residual
Residual	195	0.02			
Total	248				

in plots and techniques, but not among ecotypes. There was no technique x ecotype interaction. Variances were homoscedastic and standardized residuals were normally distributed. Table 4 shows backtransformed means, standard deviations, and Duncan's multiple range test at 5% probability. Only BWgimbal was not significantly different from the gimbal on microplot technique. Means for other techniques were greater than the mean for gimmp. Because gimmp only covered a small portion of the plot, and means for other techniques measured close to gimmp measurements were significantly different, the gimbal on microplot sampling technique was excluded from further analyses.

4.4 Observer Effects

Four techniques were tested for differences between observers and interaction with plots. The ocular and gimbal techniques were tested with two-way tables and the G-test. There were no apparent differences between observers for ocular and gimbal methods or between observers and techniques when they were combined (Table 5). Plot-observer interactions for these two techniques were tested with log-linear models. The results showed no interaction of observers with plots or ecotypes ($P = 0.30$). Potential interaction can be evaluated graphically by plotting the means obtained by each observer against plot number as ranked by any specific observer. If no interaction is present, values of plot means for each

TABLE 4. Means, standard deviations, and Duncan's multiple range test at 5% probability for gimbal on microplot plot means and top row plot means for other techniques

Duncan's test	Technique[a]	N	Observed mean (backtransformed)	Standard dev. (backtransformed)
	Gimmp	21	0.61	0.094
	BWgimbal	18	0.64	0.098
	PWmoosehorn	21	0.70	0.097
	DVocular	21	0.70	0.127
	DVgimbal	21	0.71	0.113
	DVmoosehorn	21	0.72	0.113
	PWocular	21	0.73	0.129
	100 mm photos	21	0.74	0.068
	PWgimbal	21	0.78	0.143
	50 mm photos	21	0.78	0.051
	DVsph. dens.	21	0.82	0.061
	PWsph. dens.	21	0.85	0.040

[a]DV, BW, and PW refer to observers used.

TABLE 5. Two-way contingency tables for comparing observers' measurements from ocular and gimbal sight estimation of mean crown completeness. Expected values are in parenthesis.

Observer[a]	Canopy class		*G*	*P*
	Open	Closed		
DVocular	296 (283)	437 (450)	1.95	0.163
PWocular	270 (283)	463 (450)		
BWgimbal	269 (258)	391 (402)		
DVgimbal	291 (287)	442 (446)	2.10	0.351
PWgimbal	272 (287)	461 (446)		
DVocular	296 (285)	437 (448)		
PWocular	270 (285)	463 (448)		
BWgimbal	269 (257)	391 (403)	4.14	0.386
DVgimbal	291 (285)	442 (448)		
PWgimbal	272 (285)	461 (448)		

[a]DV, BW, and PW refer to observers used.

technique will be approximately the same distance apart (see Fig. 12 for an example). An interaction would show crossing of the lines connecting points, with one technique giving a higher mean in one plot and a lower mean in a different plot than another technique. Figure 13 shows plot means versus ranked plot for ocular estimates of two observers. There is very little crossing, and it occurs only in the 0.50-0.65 MCC range. The potential interaction of observer and plot for the gimbal sight is graphed in Figure 14. There is little interaction between observer and plot for DVgimbal and PWgimbal. BWgimbal shows a large number of crossings and possible interaction. This could indicate that measurements of DVgimbal and PWgimbal were not made at exactly the same point as the earlier BWgimbal measurements. Statistical analyses by log-linear models, however, indicated no interaction, probably because of the large variation within plots and the discrete nature of the data.

Observer differences for the spherical densiometer were tested with a 3-factor, nested factorial to remove ecotype and plot effects and simultaneously test for an interaction. Although transformations had little effect on homoscedascity or normality, the angular transformation for percentage data was used to reduce heteroscedascity where possible. There was a significant difference between observers ($P = 0.01$) and a significant person x plot interaction ($P < 0.01$; Table 6). All factors showed heteroscedastic variance. Paired tests

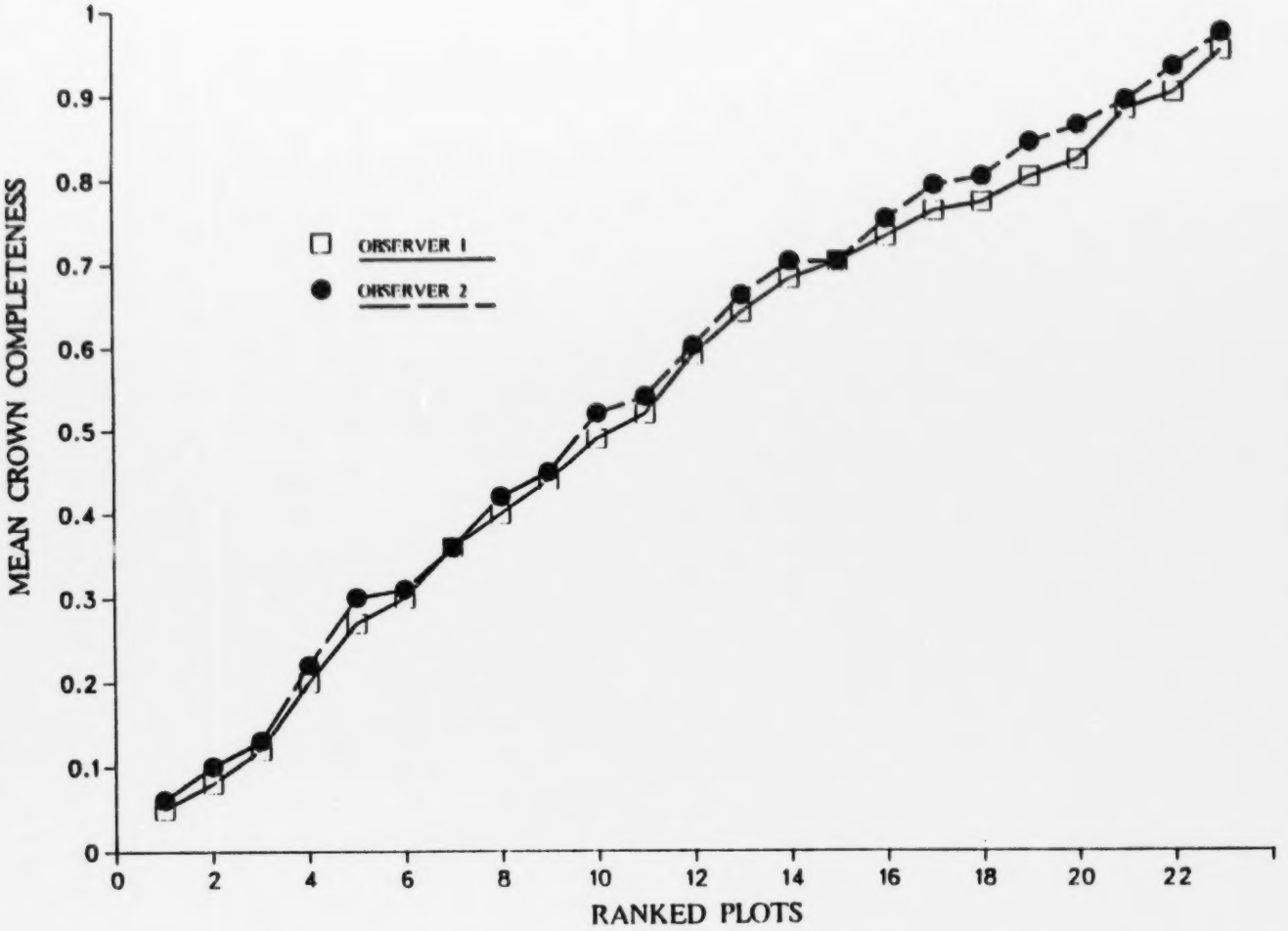

FIGURE 12. Hypothetical example of mean crown completeness estimates versus ranked plots. There is no interaction between observer and plot.

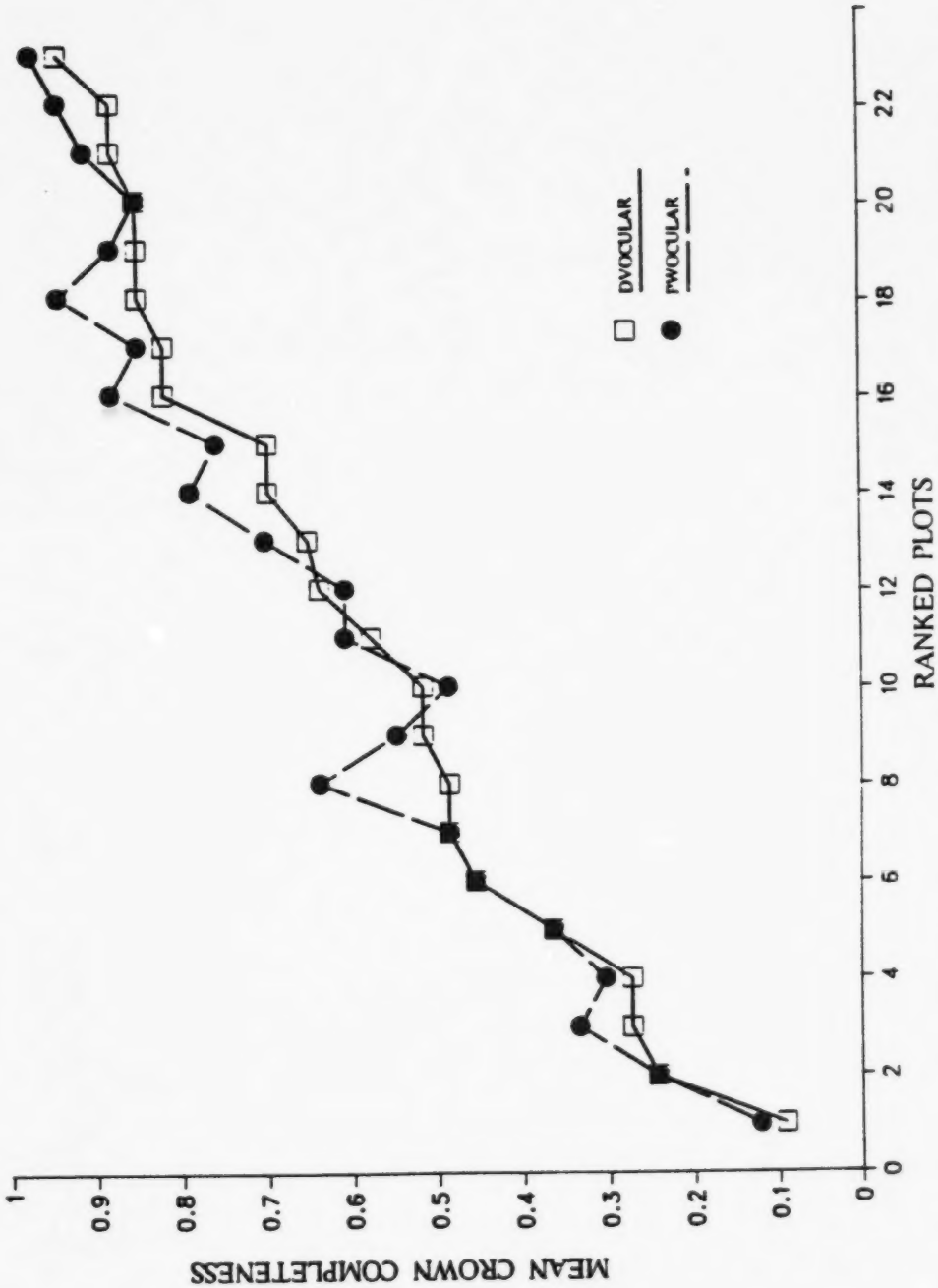

FIGURE 13. Measurements of mean crown completeness versus ranked plots for two observers using ocular canopy estimation. Plot ranking follows DV.

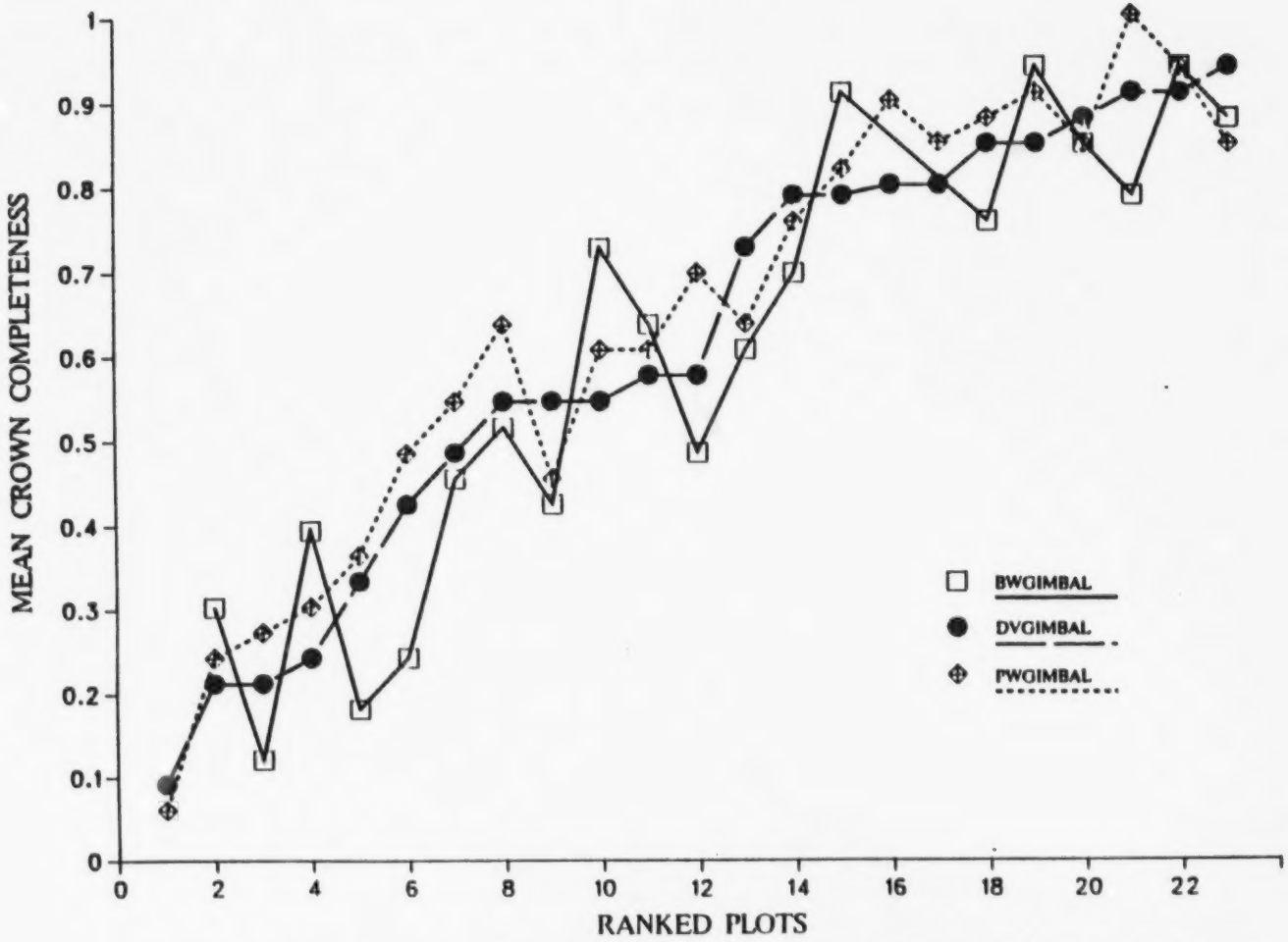

FIGURE 14. Measurements of mean crown completeness versus ranked plots for three observers using gimbal sight canopy estimation. Plot ranking follows DV.

TABLE 6. ANOVA comparing observers' measurements with the spherical densiometer. Data angular transformed.

Source	df	MSE	*F*-ratio	*P*	Test term
Ecotype	2	4.97	1.67	0.214	Plot
Plot(ecotype)	20	2.98	250.52	<0.001	Residual
Person	1	0.78	7.94	0.011	Person x plot
Person x ecotype	2	0.02	0.17	0.842	Person x plot
Person x plot	20	0.10	8.29	<0.001	Residual
Residual	1420	0.01			
Total	1465				

	DVsph. dens.	PWsph. dens.
Number of observations	733	733
Observed mean (backtransformed)	0.829	0.863
Standard deviation (backtransformed)	0.067	0.051

within plots found 16 plot pairs to be significantly different ($P < 0.05$; Table 7) and an overall paired test was significant, confirming results of the ANOVA. The interaction is illustrated in Figure 15. Although there seems to be very little interaction, the spherical densiometer with low variance caused the ANOVA test for interaction to be significant. Because the F value was highly significant, no further analyses were necessary to test for observer differences.

The moosehorn was also tested for observer effects with ANOVA (Table 8). Data were angular transformed. No significant difference was found between observers ($P = 0.10$) and there was no plot x person interaction ($P = 0.93$). Ecotype and person variances were homogeneous, but plot variances were not. Because of the lack of normality with the moosehorn and marginal significance level, a ranked ANOVA was computed on individual observations (Table 8). The ranked ANOVA indicated a significant difference between observers ($P = 0.017$). An ANOVA using transformed plot means was also computed and indicated no significant difference between observers ($P = 0.085$). Paired tests by plot found seven plots different at $P < 0.05$ (Table 9). Only the parametric ANOVA and overall paired t-test analyses indicated no significant difference between observers at 5% probability when all moosehorn observations were analyzed (Table 10). All tests indicated no significant difference between observers when

TABLE 7. Paired comparisons of spherical densiometer estimations of mean crown completeness between observers for all plots

Plot	N	Plot MCC		Diff	*P*	
		Observer DV	Observer PW		*t*-test	Wilcoxon
M1	33	0.31	0.36	0.05	0.014*	0.150
J2	33	0.33	0.59	0.26	<0.001**	<0.001**
N2	33	0.44	0.50	0.06	<0.001**	<0.001**
C2	33	0.66	0.68	0.02	0.111	0.050*
C1	33	0.68	0.75	0.07	<0.001**	<0.001**
N1	33	0.69	0.80	0.11	<0.001**	<0.001**
J1	33	0.71	0.81	0.10	<0.001**	<0.001**
D1	33	0.82	0.89	0.07	<0.001**	<0.001**
F1	33	0.87	0.92	0 05	<0.001**	<0.001**
H1	33	0.87	0.87	0.00	0.663	1.000
D2	33	0.88	0.94	0.06	<0.001**	<0.001**
H2	33	0.89	0.90	0.01	0.185	0.851
A1	20	0.89	0.89	0.00	0.825	0.481
C4	33	0.89	0.92	0.03	<0.001**	<0.001**
JM	33	0.92	0.95	0.03	<0.001**	<0.001**
A2	20	0.93	0.91	0.02	0.003**	0.008**
G1	33	0.94	0.95	0.01	0.167	0.345
C3	33	0.94	0.94	0.00	0.053	0.052
E1	33	0.95	0.95	0.00	0.123	0.201
G3	33	0.96	0.94	0.02	0.015*	0.019*
B2	33	0.96	0.93	0.03	<0.001**	<0.001**
JB	33	0.96	0.94	0.02	<0.001**	<0.001**
F2	33	0.97	0.96	0.01	0.016*	0.004**
All	733	0.80	0.84	0.04	<0.001**	<0.001**

* significant at $P \leq 5\%$.
** significant at $P \leq 1\%$.

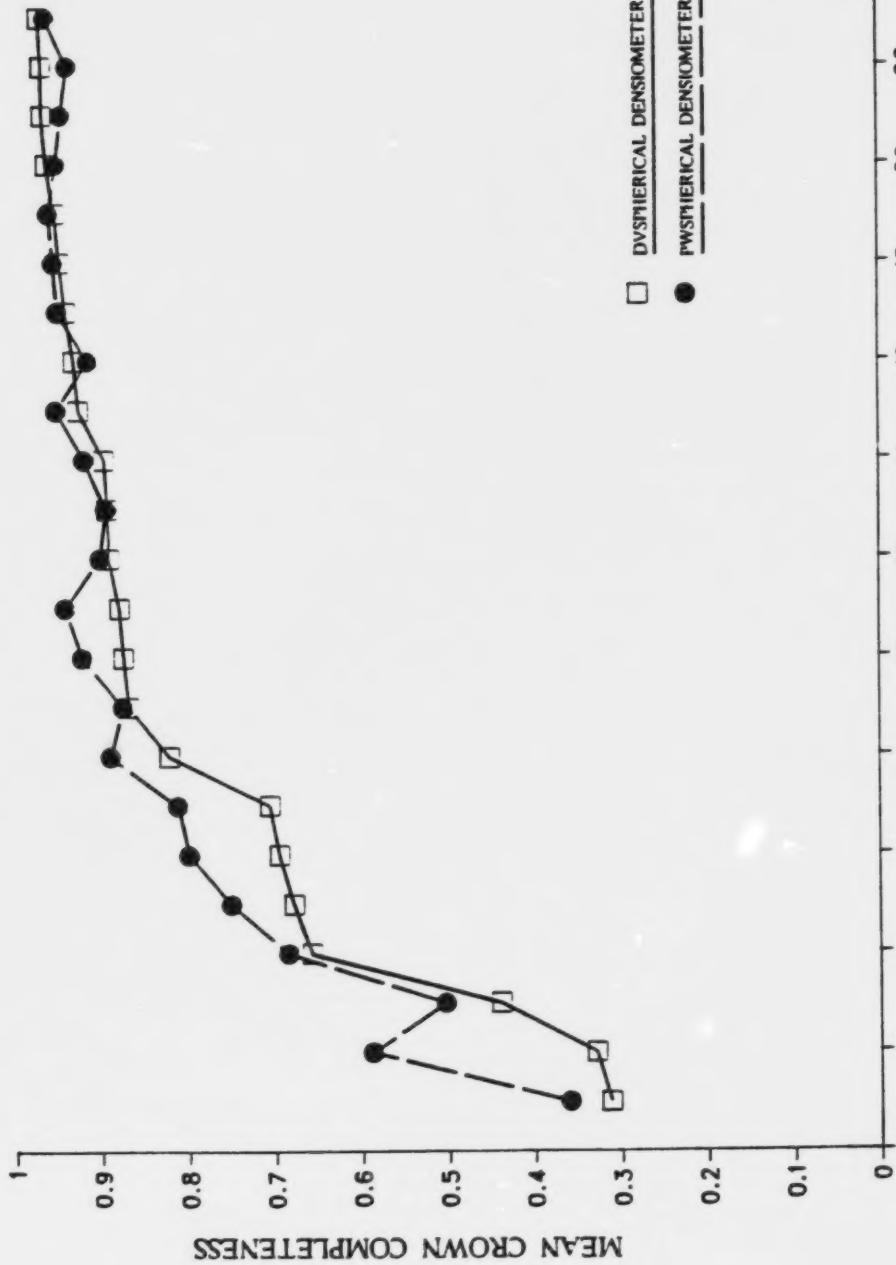

FIGURE 15. Measurements of mean crown completeness versus ranked plots for two observers using the spherical densiometer. Plot ranking follows IV.

TABLE 8. ANOVA comparing different observers' measurements from the moosehorn

A. Parametric analysis

Source	df	MSE	*F*-ratio	*P*	Test term
Ecotype	2	5.24	0.55	0.583	Plot
Plot(ecotype)	20	9.45	69.72	<0.001	Residual
Person	1	0.23	2.94	0.102	Person x plot
Person x ecotype	2	0.02	0.32	0.733	Person x plot
Person x plot	20	0.08	0.58	0.931	Residual
Residual	1420	0.14			
Total	1465				

	DVmoosehorn	PWmoosehorn
Number of observations	733	733
Observed mean (backtransformed)	0.663	0.638
Standard deviation (backtransformed)	0.255	0.237

B. Ranked observations

Ecotype	2	20.24	0.75	0.481	Plot
Plot(ecotype)	20	26.92	58.89	<0.001	Residual
Person	1	2.78	6.71	0.017	Person x plot
Person x ecotype	2	0.11	0.26	0.774	Person x plot
Person x plot	20	0.42	0.91	0.577	Residual
Residual	1420	0.46			
Total	1465				

C. Plot Means

Ecotype	2	0.11	0.56	0.579	Plot
Plot	20	0.20	119.73	<0.001	Residual
Person	1	0.005	3.29	0.085	Residual
Person x ecotype	2	0.001	0.75	0.487	Residual
Residual	20	0.002			
Total	45				

TABLE 9. Paired comparisons of moosehorn estimation of mean crown completeness between observers for all plots

Plot	N	Plot MCC		Diff	*P*	
		Observer DV	Observer PW		*t*-test	Wilcoxon
N2	33	0.13	0.16	0.03	0.207	0.383
M1	33	0.21	0.19	0.02	0.429	0.238
J2	33	0.23	0.23	0.00	1.000	0.754
C1	33	0.27	0.22	0.05	0.108	0.359
J1	33	0.32	0.34	0.02	0.694	0.481
F1	33	0.43	0.53	0.10	0.003**	0.005**
C2	33	0.45	0.43	0.02	0.463	0.804
D1	33	0.52	0.63	0.11	0.022*	0.011*
N1	33	0.57	0.48	0.09	0.006**	0.215
D2	33	0.62	0.63	0.01	0.604	1.000
C4	33	0.63	0.58	0.05	0.355	0.424
H2	33	0.68	0.64	0.04	0.150	0.230
H1	33	0.70	0.71	0.01	0.737	1.000
E1	33	0.84	0.79	0.05	0.028*	0.011*
A1	20	0.88	0.86	0.02	0.212	0.332
A2	20	0.88	0.83	0.05	0.104	0.031*
JM	33	0.88	0.86	0.02	0.293	0.185
G1	33	0.90	0.91	0.01	0.594	0.442
JB	33	0.92	0.87	0.05	<0.001**	0.004**
G3	33	0.93	0.90	0.03	0.058	0.076
F2	33	0.94	0.93	0.01	0.340	0.308
C3	33	0.96	0.91	0.05	<0.001**	<0.001**
B2	33	0.97	0.93	0.04	0.001**	0.007**
All	733	0.64	0.63	0.01	0.051	<0.001

* significant at $P \leq 5\%$.
** significant at $P \leq 1\%$.

TABLE 10. Summary of analyses comparing observers' measurements from the moosehorn

Test	Significance of difference *P*
On individual observations: n=733/person	
ANOVA	0.102
Ranked Anova	0.017
On plot means: n=23/person	
ANOVA	0.085
Friedman	0.095
Wilcoxon rank-sum	0.134

plot means were analyzed ($P > 0.05$). Plot means for the two observers are graphed against ranked plot in Figure 16.

For the moosehorn the greatest difference between means of observers occurred in the mid-canopy range. The canopy variance also peaked in this range (Figure 11). Paired tests within plots were more sensitive to deviations at the low and high canopies than at mid-canopies because of the pattern of variation with estimated MCC.

4.5 Technique Effects

Analyses were performed to test for differences among techniques. Initially all observations for techniques with continuous or nearly continuous distributions were included in the analysis. Further analyses were performed on small subsets of similar techniques to identify where interactions were occurring. The final analysis of technique effects is on plot means without the test for technique x plot interactions.

4.5.1 ANOVA on individual observations

Analysis of variance was computed using individual observations of techniques generating continuous variables: moosehorn, spherical densiometer, 50 mm and 100 mm photography, diffuse and direct site factor estimates, and five concentric grids. Each observer was treated as a different technique for the moosehorn and spherical densiometer. All data for this and further ANOVA's were

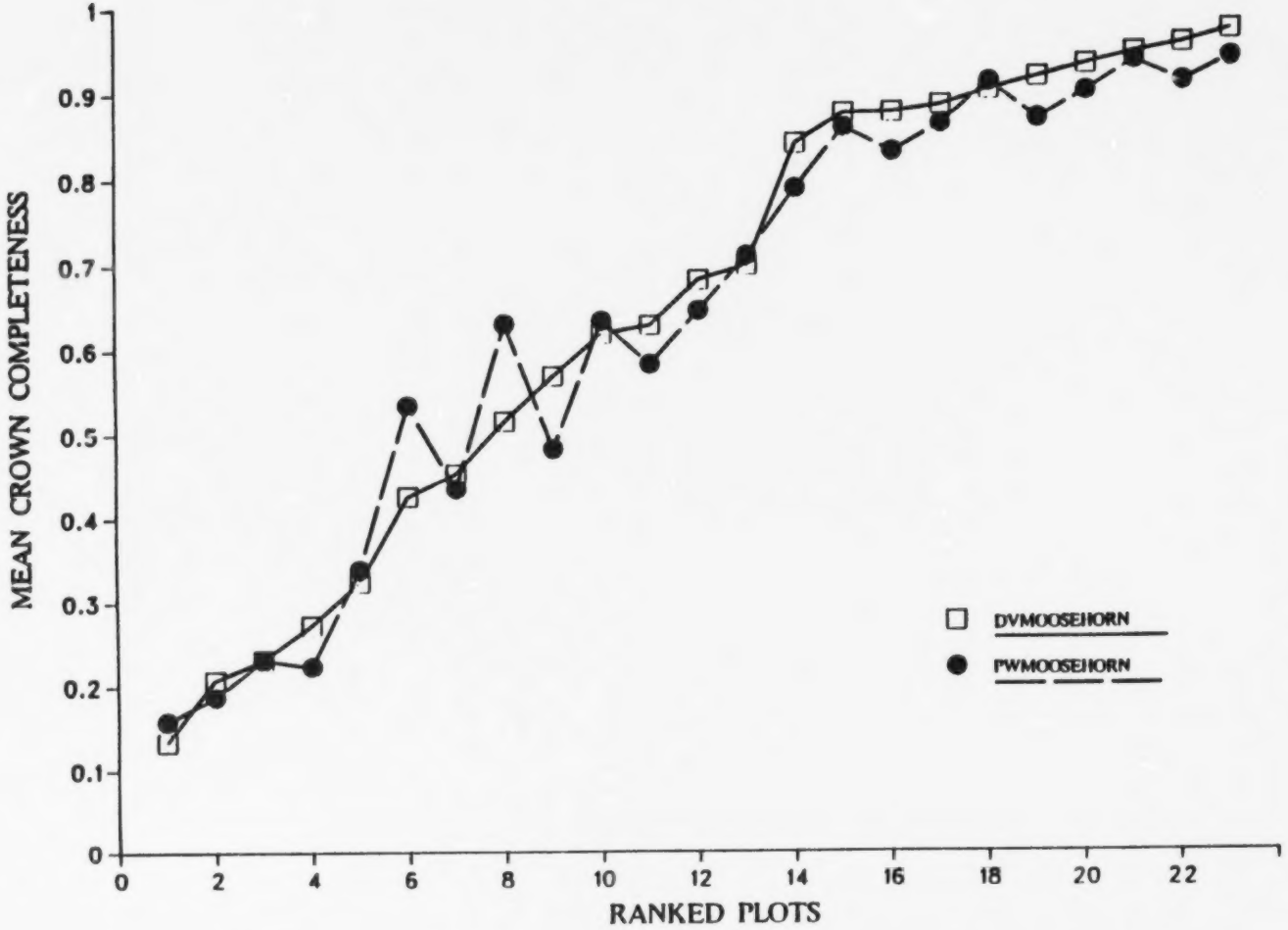

FIGURE 16. Measurements of mean crown completeness versus ranked plots for two observers using the moosehorn. Plot ranking follows DV.

angular transformed. Probabilities for F-tests were highly significant for differences in plots, "techniques", and technique x plot interaction (Table 11). All factors were heteroscedastic.

Because plots were selected to encompass a range of MCC, it was expected that there would be a significant difference between plots. Techniques were also expected to be significantly different. The significant interaction indicates that different techniques give inconsistent differences in mean values across plots.

Duncan's multiple range test at 5% probability indicated four overlapping, homogeneous subsets of techniques (Table 12). To further examine interactions and relationships among techniques, and to confirm the results of Duncan's test, additional analyses were carried out on small sets of techniques with similar projection angles (see Table 1) being grouped and compared. The comparisons included: 1) 50 mm with 100 mm photography; 2) moosehorn (2 observers) with 100 mm photography; 3) moosehorn (2 observers) with concentric grids; 4) diffuse with direct site factors; and 5) diffuse site factor with spherical densiometer (2 observers).

The 50 mm and 100 mm photography techniques were compared by analysis of variance (Table 13). Significant differences were found among plots and between the two lenses ($P < 0.01$). The wider angle 50 mm photos gave higher plot means than the 100 mm. Tests for equality of variance showed

TABLE 11. ANOVA comparing techniques generating continuous variables. Data were angular transformed.

Source	df	MSE	*F*-ratio	*P*	Test term
Ecotype	2	11.07	0.83	0.452	Plot
Plot(ecotype)	20	13.41	189.90	<0.001	Residual
Technique	12	3.56	20.40	<0.001	Technique x plot
Tech x ecotype	24	0.06	0.35	0.998	Technique x plot
Technique x plot	240	0.17	2.47	<0.001	Residual
Residual	3368	0.07			
Total	3666				

TABLE 12. Means, standard deviations, and Duncan's multiple range test at 5% probability for all techniques using individual observations as input

Duncan's test	Technique[a]	N	Observed mean (backtransformed)	Standard dev. (backtransformed)
	PWmoosehorn	733	0.64	0.236
	DVmoosehorn	733	0.66	0.249
	10°	46	0.69	0.232
	20°	46	0.70	0.181
	30°	46	0.72	0.139
	100 mm photos	207	0.74	0.136
	40°	46	0.74	0.112
	50°	46	0.76	0.095
	50 mm photos	206	0.79	0.080
	Diffuse	46	0.80	0.012
	DVsph. dens.	733	0.83	0.067
	PWsph. dens.	733	0.86	0.051
	Direct	46	0.87	0.017

[a]DV and PW refer to observers used.

TABLE 13. ANOVA comparing 50 mm and 100 mm photographic lenses. Data were angular transformed.

Source	df	MSE	*F*-ratio	*P*	Test term
Ecotype	2	0.47	0.30	0.721	Plot
Plot(ecotype)	20	1.43	32.40	<0.001	Residual
Lens	1	0.40	15.50	0.001	Lens x plot
Lens x ecotype	2	0.002	0.07	0.929	Lens x plot
Lens x plot	20	0.03	0.60	0.922	Residual
Residual	367	0.04			
Total	412				

	50 mm	100 mm
Number of observations	206	207
Observed mean (backtransformed)	0.790	0.737
Standard deviation (backtransformed)	0.080	0.136

heteroscedasticity. Paired tests by plot (Table 14) show that in seven of 23 plots (t-test), lenses differed significantly at 5% probability (only two plots differed by the Wilcoxon test). Only one plot showed a significant difference at higher MCC's (>0.82).

Table 15 presents an ANOVA table for parametric and ranked analyses comparing two observers' measurements from using the moosehorn with the 100 mm photographic lens. Plots were significantly different ($P < 0.01$) and the significance of the techniques depended upon the analysis. Duncan's multiple range test at 5% indicated differences between the moosehorn and 100 mm lens, but not between observers.

The MCC's of five concentric rings on hemispherical photos were compared to moosehorn estimates of two observers. Plots and techniques differed ($P < 0.01$) and there was a technique x ecotype interaction (Table 16). The 10° and 20° rings had the lowest means in one ecotype, followed by DV, PW moosehorn, and 30°, 40°, and 50° angles. In the other two ecotypes, the order was the same as presented in Table 16. Variance was heteroscedastic. Duncan's multiple range test at 5% indicated three homogeneous subsets. Because sample sizes within plots were very unequal between moosehorn and concentric grids, an ANOVA was computed including moosehorn measurements taken only at the point where hemispherical photographs were taken (N = 2/plot). There was a total of 46 samples for each technique, with 321 total degrees of freedom.

TABLE 14. Paired comparisons of 50 mm and 100 mm photographic estimations of mean crown completeness for all plots

Plot	N	Plot MCC		Diff	*P*	
		50 mm	100 mm		*t*-test	Wilcoxon
J2	7	0.27	0.17	0.10	0.236	0.688
M1	8	0.38	0.26	0.12	0.027*	0.289
J1	8	0.41	0.34	0.07	0.028*	0.070
C2	8	0.50	0.46	0.04	0.205	0.125
N2	8	0.50	0.40	0.10	0.039*	0.289
C1	8	0.53	0.40	0.13	0.005**	0.008**
N1	8	0.73	0.75	0.02	0.432	0.727
D2	8	0.76	0.65	0.11	0.018*	0.070
D1	8	0.76	0.67	0.09	0.082	0.289
F1	8	0.77	0.65	0.12	0.044*	0.070
C4	8	0.77	0.72	0.05	0.247	0.289
H1	8	0.81	0.75	0.06	0.300	0.727
H2	7	0.82	0.73	0.09	0.166	1.000
A2	8	0.88	0.89	0.01	0.532	0.289
E1	8	0.89	0.87	0.02	0.521	1.000
JM	8	0.89	0.88	0.01	0.012*	0.016*
G3	32	0.91	0.90	0.01	0.061	0.215
G1	8	0.92	0.92	0.00	0.976	1.000
A1	8	0.92	0.91	0.01	0.575	1.000
C3	8	0.92	0.91	0.01	0.299	0.453
F2	8	0.93	0.91	0.02	0.112	0.727
B2	8	0.94	0.93	0.01	0.360	0.219
JB	8	0.94	0.93	0.01	0.410	1.000
All	206	0.77	0.72	0.05	<0.001	<0.001

* significant at $P \leq 5\%$.
** significant at $P \leq 1\%$.

TABLE 15. ANOVA comparing observers' measurements from the moosehorn with those from 100 mm photography

A. Parametric analysis

Source	df	MSE	*F*-ratio	*P*	Test term
Ecotype	2	5.41	0.53	0.598	Plot
Plot(ecotype)	20	10.26	80.88	<0.001	Residual
Technique	2	0.27	3.12	0.055	Technique x plot
Technique x ecotype	4	0.16	1.92	0.126	Technique x plot
Technique x plot	40	0.09	0.67	0.942	Residual
Residual	1604	0.13			
Total	1672				

	PWmoosehorn	DVmoosehorn	100 mm
Number of observations	733	733	207
Observed mean (backtransformed)	0.638	0.663	0.737
Standard deviation (backtransformed)	0.237	0.255	0.136

B. Ranked observations

Ecotype	2	22.79	0.72	0.497	Plot
Plot(ecotype)	20	31.53	68.14	<0.001	Residual
Technique	2	2.00	5.39	0.008	Technique x plot
Technique x ecotype	4	0.75	2.01	0.111	Technique x plot
Technique x plot	40	0.37	0.80	0.807	Residual
Residual	1604	0.46			
Total	1672				

TABLE 16. ANOVA comparing observers' measurements from the moosehorn with those from concentric grids of hemispherical photos

A. Parametric analysis

Source	df	MSE	*F*-ratio	*P*	Test term
Ecotype	2	4.84	0.46	0.639	Plot
Plot(ecotype)	20	10.57	80.17	<0.001	Residual
Technique	6	0.23	5.06	<0.001	Technique x plot
Technique x ecotype	12	0.09	1.99	0.031	Technique x plot
Technique x plot	120	0.04	0.34	1.000	Residual
Residual	1535	0.13			
Total	1695				

	PWmoose	DVmoose	10°	20°	30°	40°	50°
Duncan's range test at 5%							
No. observations	733	733	46	46	46	46	46
Observed mean (backtransformed)	0.64	0.66	0.69	0.70	0.72	0.74	0.76
Standard deviation (backtransformed)	0.25	0.24	0.23	0.18	0.14	0.11	0.10

B. Ranked observations

Ecotype	2	18.41	0.56	0.581	Plot
Plot(ecotype)	20	32.99	69.79	<0.001	Residual
Technique	6	0.60	2.59	0.021	Technique x plot
Technique x ecotype	12	0.65	2.81	0.002	Technique x plot
Technique x plot	120	0.23	0.49	1.000	Residual
Residual	1535	0.47			
Total	1695				

The results were the same as shown in Table 16, except there was no technique x ecotype interaction and Duncan's multiple range test indicated three homogeneous subsets of: 1) DV and PWmoosehorn (about 10°), 2) 10°-40°, and 3) 30°-50°.

Diffuse and direct site factor MCC's were compared using ANOVA. The results indicate differences in plots and techniques ($P < 0.01$; Table 17). The direct site factor had a higher overall mean than the diffuse. Variances were homogeneous.

Different observervations made using the spherical densiometer were compared to diffuse site factor estimates from hemispherical photos (Table 18). Significant differences were found in plots and techniques ($P < 0.01$) and a significant technique x plot interaction was indicated ($P < 0.01$). Layard's test for equal variances showed heteroscedascity. Duncan's multiple range test at 5% probability showed no significant difference between one observer's observations with the spherical densiometer and the diffuse site factor estimates. When these two were compared with ANOVA, the F-test indicated no significant difference between them ($P = 0.28$), but a significant interaction ($P < 0.01$).

4.5.2 ANOVA on plot means

An analysis of variance also was computed for all observers' measurements and all techniques that used plot

TABLE 17. ANOVA comparing diffuse and direct site factors

Source	df	MSE	*F*-ratio	*P*	Test term
Ecotype	2	0.01	0.26	0.771	Plot
Plot(ecotype)	20	0.05	18.17	<0.001	Residual
Site factor	1	0.18	44.26	<0.001	Site factor x plot
Site factor x ecotype	2	0.002	0.49	0.618	Site factor x plot
Site factor x plot	20	0.004	1.38	0.182	Residual
Residual	46	0.003			
Total	91				

	Diffuse	Direct
Number of observations	46	46
Observed mean (backtransformed)	0.802	0.868
Standard deviation (backtransformed)	0.012	0.017

TABLE 18. ANOVA comparing observers' measurements from the spherical densiometer with diffuse site factor

Source	df	MSE	*F*-ratio	*P*	Test term
Ecotype	2	4.84	1.60	0.222	Plot
Plot(ecotype)	20	2.97	253.60	<0.001	Residual
Technique	2	0.48	7.20	0.002	Technique x plot
Technique x ecotype	4	0.08	1.20	0.315	Technique x plot
Technique x plot	40	0.07	5.60	<0.001	Residual
Residual	1443	0.01			
Total	1511				

Duncan's range test at 5%	Diffuse s.f.	DVsph. dens.	PWsph. dens.
Number of observations	46	733	733
Observed mean (backtransformed)	0.80	0.83	0.86
Standard deviation (backtransformed)	0.012	0.067	0.051

means rather than individual observations. This approach aggregates the repeated observations within plots used to generate the error term in previous analyses so there can be no test of technique x plot interaction. An additional assumption of additivity is sometimes invoked when there is only one observation per cell. The additivity assumption is of little concern in the analysis of plot means, because it enters directly only in the test for a plot effect. Plots are different (Table 11). The test for a technique effect, using the mean square error of plots x techniques as the test term, is legitimate whether there is nonadditivity or additivity (J. Petkau, pers. comm., University of B.C.). Interactions with ecotypes can be tested. The analysis allows plot means for ocular and gimbal sight to be compared with plot means for other techniques (J. Petkau, pers. comm., University of B.C.; A. Kozak, pers. comm., University of B.C.).

Differences in plots and techniques were highly significant ($P < 0.01$; Table 19). Backtransformed values and Duncan's multiple range test at 5% probability are presented in Table 20. Examination of residuals indicated normality. The standard deviation of the residuals for techniques differed by a factor of 3.5, indicating heteroscedasticity. When the analysis is computed without the diffuse and direct site factors, tests for equal variances show homogeneity and the ANOVA results and multiple range tests are unchanged. Appendix 1 contains paired t-tests and paired rank statistics

TABLE 19. ANOVA comparing all techniques across all plots, using plot means. Data are angular transformed.

Source	df	MSE	*F*-ratio	*P*	Test term
Ecotype	2	0.25	0.20	0.820	Plot
Plot(ecotype)	20	1.25	88.60	<0.001	Residual
Technique	17	0.20	14.47	<0.001	Residual
Technique x ecotype	34	0.01	0.87	0.672	Residual
Residual	337	0.01			
Total	410				

TABLE 20. Overall means, standard deviations, and Duncan's multiple range test at 5% probability for all techniques using plot means as input

Duncan's test	Technique[a]	N	Observed mean (backtransformed)	Standard dev. (backtransformed)
	BWgimbal	20	0.61	0.083
	DVocular	23	0.61	0.072
	DVgimbal	23	0.62	0.083
	PWmoosehorn	23	0.65	0.087
	PWocular	23	0.66	0.082
	PWgimbal	23	0.66	0.094
	DVmoosehorn	23	0.67	0.099
	10°	23	0.69	0.156
	20°	23	0.70	0.133
	30°	23	0.72	0.110
	100 mm photo	23	0.72	0.073
	40°	23	0.74	0.093
	50°	23	0.76	0.083
	50 mm photo	23	0.77	0.056
	Diffuse s.f.	23	0.80	0.012
	DVsph. dens.	23	0.83	0.057
	PWsph. dens.	23	0.86	0.039
	Direct s.f.	23	0.87	0.014

[a]DV, BW, and PW refer to observers used.

for all paired combinations of plot means.

4.6 Means and Confidence Intervals

Sample size, means, standard deviation's, 95% confidence intervals, measurements of skewness and kurtosis, standard errors, and coefficients of variation for each untransformed technique over all plots are summarized in Table 21. Table 22 presents the same statistics, but only for points at which hemispherical photographs were taken. Statistics by plot can be found in Appendix 2.

4.7 Sample Size Estimates

Sample size estimates for most techniques were obtained from untransformed plot variances. For techniques with continuous variables, Stauffer's (1982) convergent iteration procedure for simple random sampling was used. Sample size estimates for a binomial distribution are from Cochran (1977:75). Estimates of required sample sizes for a precision of ± 5% MCC at 95% confidence are illustrated for means observed in this study (Figs. 17-22). Because sample size is dependent on variance, the graphs of sample size versus plot mean look similar to the variance versus mean graph (see, for example, Fig. 10 for the moosehorn). A boundary around the outer edge of the plotted points will provide the most conservative estimate of required sample sizes. Bonnor (1967) drew a curve on the outer edge of the size estimates because a

TABLE 21. Univariate statistics on untransformed observations for all techniques across all plots, ranked from lowest to highest MCC

Technique[a]	N	Min.	Max.	Mean	Std. Dev.	Skewness	Kurtosis	0.95 Conf. int. half width	Std. Err.	Coeff. of var. (%)
BWgimbal	660	0.	1.00	0.592	0.49176	N/A	N/A	0.038	0.019	83
DVocular	733	0.	1.00	0.596	0.49100	N/A	N/A	0.036	0.018	82
Gimmp	420	0.	1.00	0.601	0.36419	-0.437	-1.162	0.035	0.018	61
DVgimbal	733	0.	1.00	0.603	0.48961	N/A	N/A	0.036	0.018	78
PWmoosehorn	733	0.	1.00	0.626	0.36671	-0.705	-1.111	0.027	0.014	59
PWgimbal	733	0.	1.00	0.629	0.48342	N/A	N/A	0.035	0.018	77
PWocular	733	0.	1.00	0.632	0.48269	N/A	N/A	0.035	0.018	76
DVmoosehorn	733	0.	1.00	0.637	0.37830	-0.705	-1.168	0.027	0.014	59
10°	46	0.	1.00	0.665	0.36191	-0.874	-0.765	0.108	0.053	54
20°	46	0.	1.00	0.672	0.33148	-0.932	-0.476	0.098	0.049	49
30°	46	0.	0.99	0.689	0.30357	-1.022	-0.189	0.090	0.045	44
40°	46	0.	0.99	0.710	0.27903	-1.091	0.240	0.083	0.041	39
100 mm photo	207	0.	0.97	0.725	0.28808	-1.484	0.961	0.040	0.020	40
50°	46	0.	0.99	0.732	0.26007	-1.157	0.193	0.077	0.038	36
50 mm photo	206	0.	0.99	0.768	0.23560	-1.761	2.241	0.032	0.016	31
Diffuse s.f.	46	0.443	0.92	0.796	0.09677	-2.039	4.520	0.024	0.014	12
DVsph. dens.	733	0.125	1.00	0.798	0.21487	-1.586	1.607	0.016	0.001	27
PWsph. dens.	733	0.125	1.00	0.837	0.18601	-2.090	3.682	0.013	0.007	22
Direct s.f.	46	0.419	0.97	0.857	0.10242	-2.425	6.702	0.061	0.015	12

[a]DV, BW, and PW refer to observers used.

TABLE 22. Univariate statistics on untransformed observations measured at hemispherical photo points only, across all plots

Technique[a]	N	Min.	Max.	Mean	Std. Dev.	Skewness	Kurtosis	0.95 Conf. int. half width	Std. Err.	Coeff. of var. (%)
DVgimbal	46	0.	1.00	0.435	0.5012	N/A	N/A	0.149	0.0739	115
DVocular	46	0.	1.00	0.522	0.5051	N/A	N/A	0.150	0.0745	97
PWocular	46	0.	1.00	0.543	0.5036	N/A	N/A	0.150	0.0743	93
PWmoosehorn	46	0.	1.00	0.569	0.3682	-0.481	-1.382	0.109	0.0543	65
DVmoosehorn	46	0.	1.00	0.573	0.3782	-0.412	-1.508	0.112	0.0558	66
PWgimbal	46	0.	1.00	0.587	0.4978	N/A	N/A	0.148	0.0734	85
10°	46	0.	1.00	0.665	0.3619	-0.874	-0.765	0.108	0.0534	54
20°	46	0.	1.00	0.672	0.3315	-0.932	-0.476	0.098	0.0489	49
30°	46	0.	0.99	0.689	0.3036	-1.022	-0.189	0.090	0.0448	44
40°	46	0.015	0.99	0.710	0.2790	-1.091	0.024	0.083	0.0411	39
50°	46	0.048	0.99	0.732	0.2601	-1.157	0.193	0.077	0.0383	36
DVsph. dens.	46	0.177	0.99	0.783	0.2280	-1.566	1.461	0.068	0.0336	29
Diffuse s.f.	46	0.443	0.92	0.796	0.0968	-2.039	4.520	0.024	0.0143	12
PWsph. dens.	46	0.229	0.97	0.818	0.1971	-1.844	2.297	0.059	0.0291	24
Direct s.f.	46	0.419	0.97	0.857	0.1024	-2.425	6.702	0.061	0.0151	12

[a]DV and PW refer to observers used.

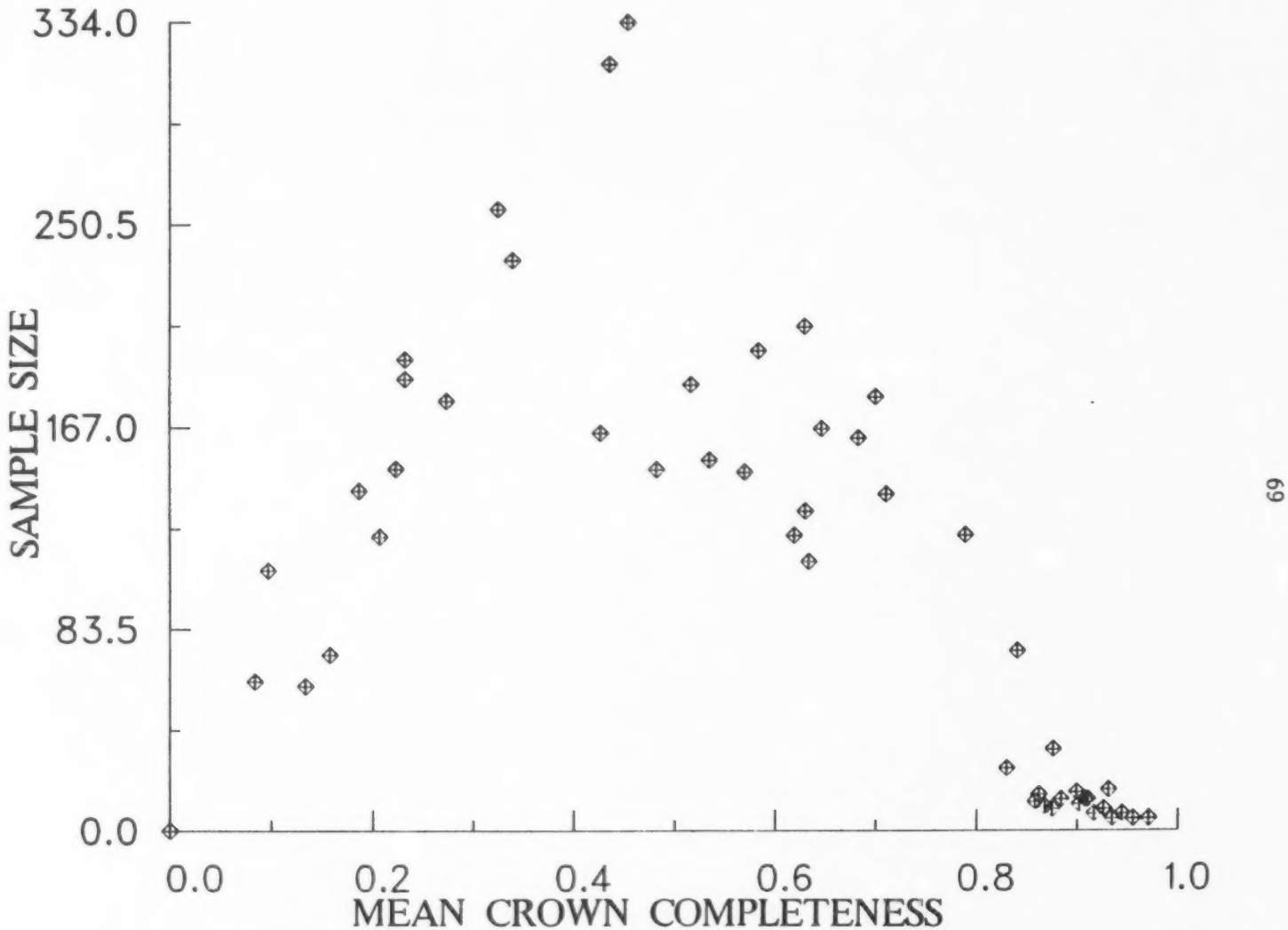

FIGURE 17. Influence of mean crown completeness on the estimated number of moosehorn samples necessary for a precision of ± 5% with 95% confidence.

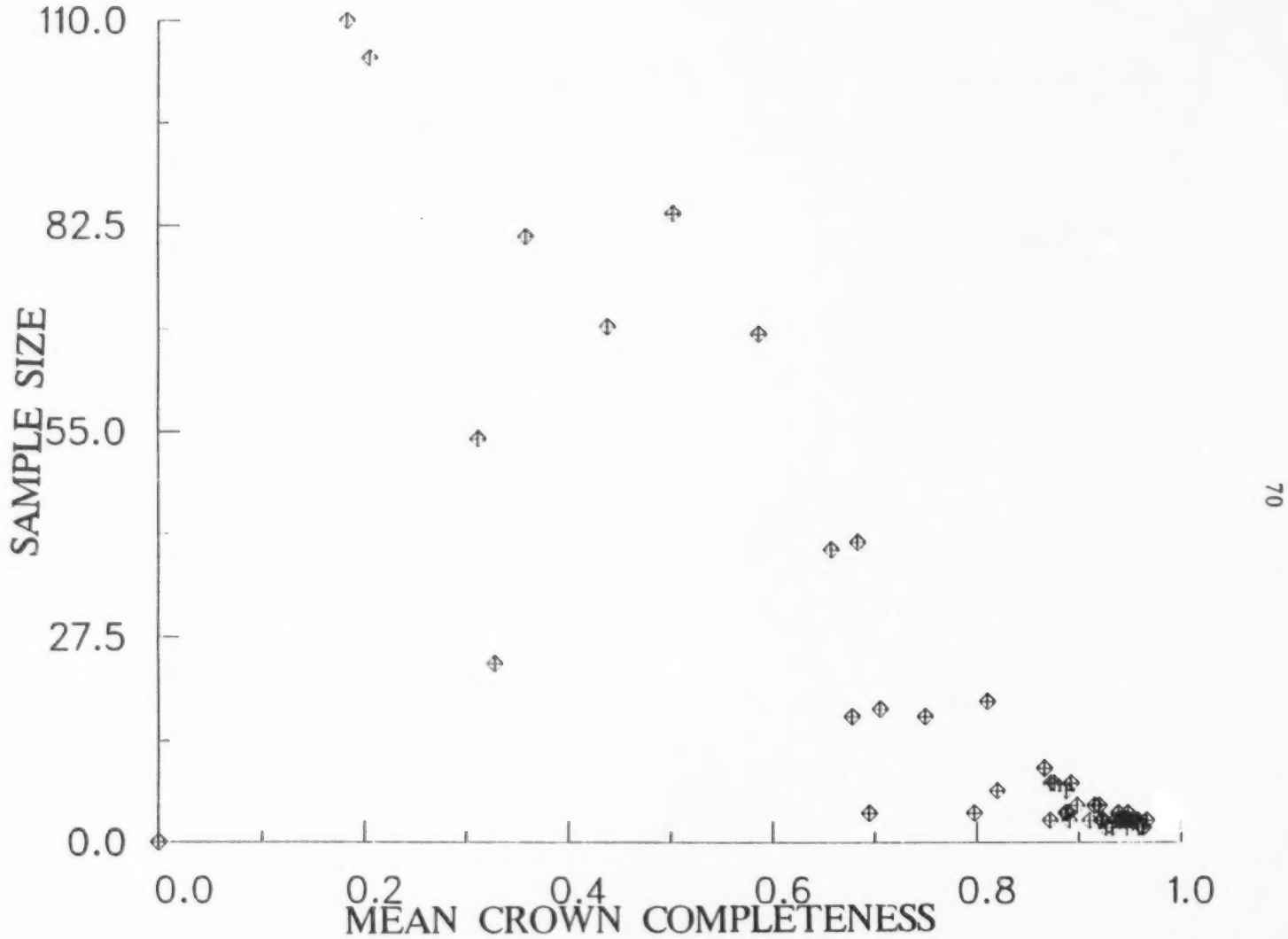

FIGURE 18. Influence of mean crown completeness on the estimated number of spherical densiometer samples necessary for a precision of ± 5% with 95% confidence.

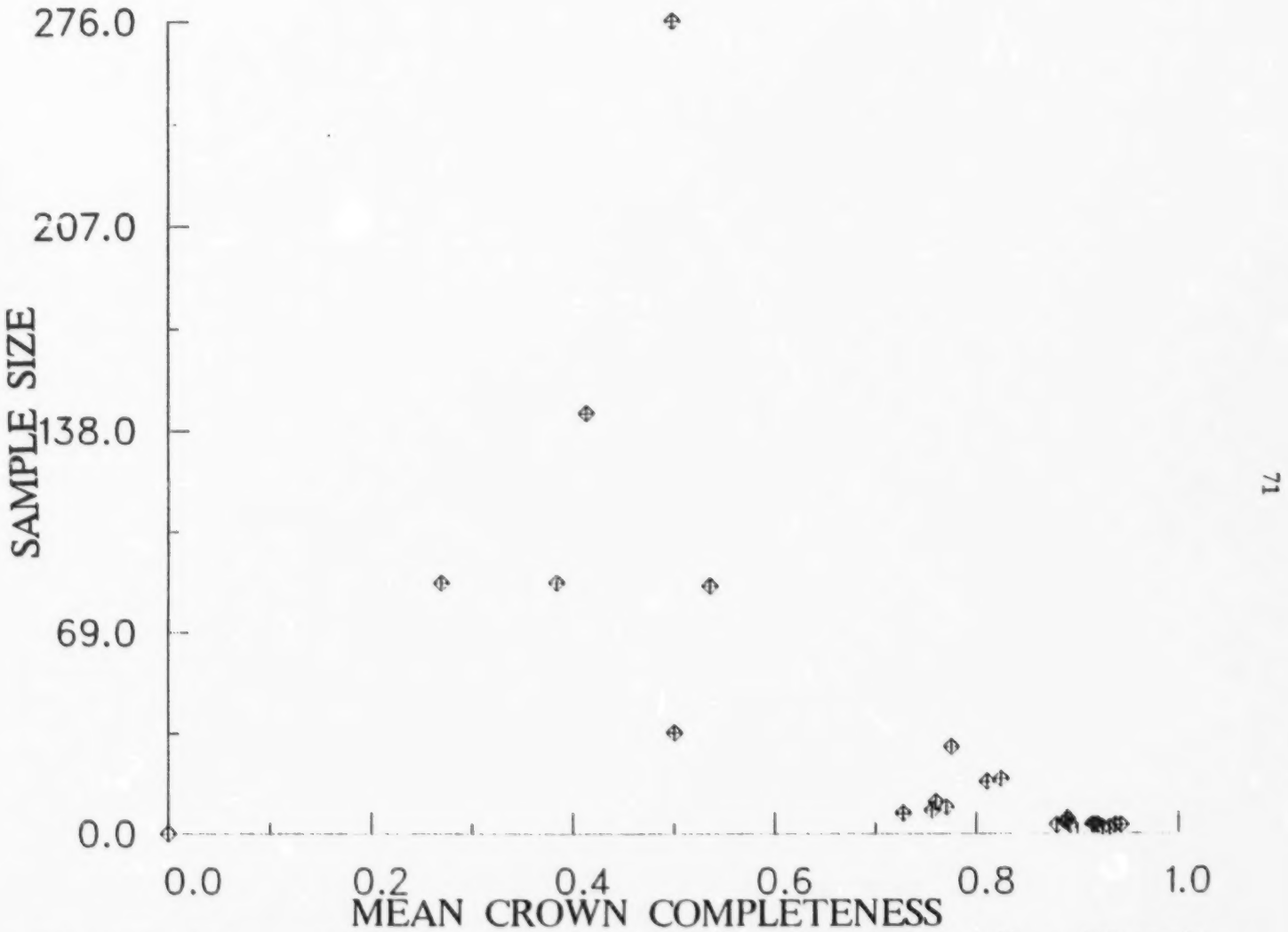

FIGURE 19. Influence of mean crown completeness on the estimated number of 50 mm photography samples necessary for a precision of ± 5% with 95% confidence.

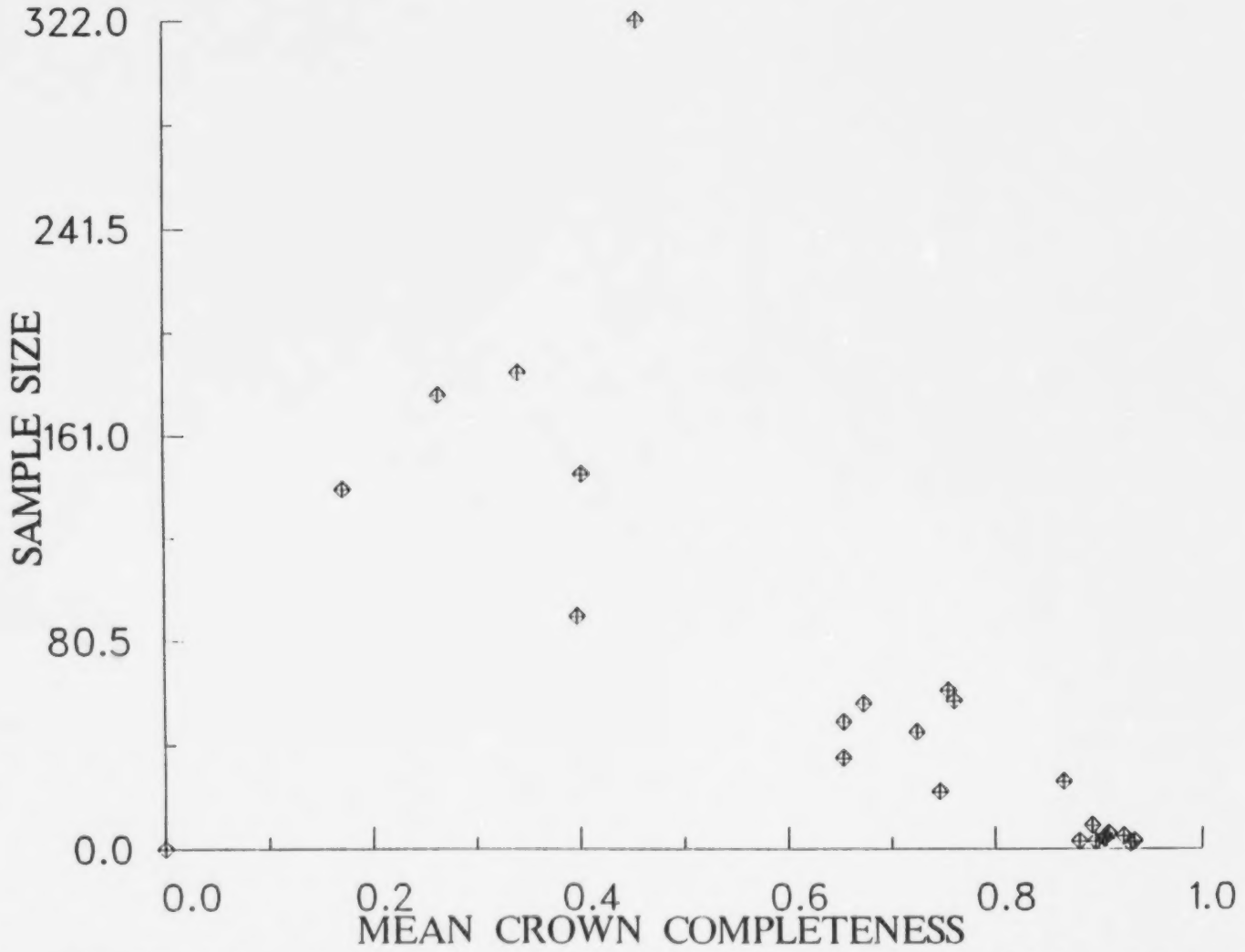

FIGURE 20. Influence of mean crown completeness on the estimated number of 100 mm photography samples necessary for a precision of ± 5% with 95% confidence.

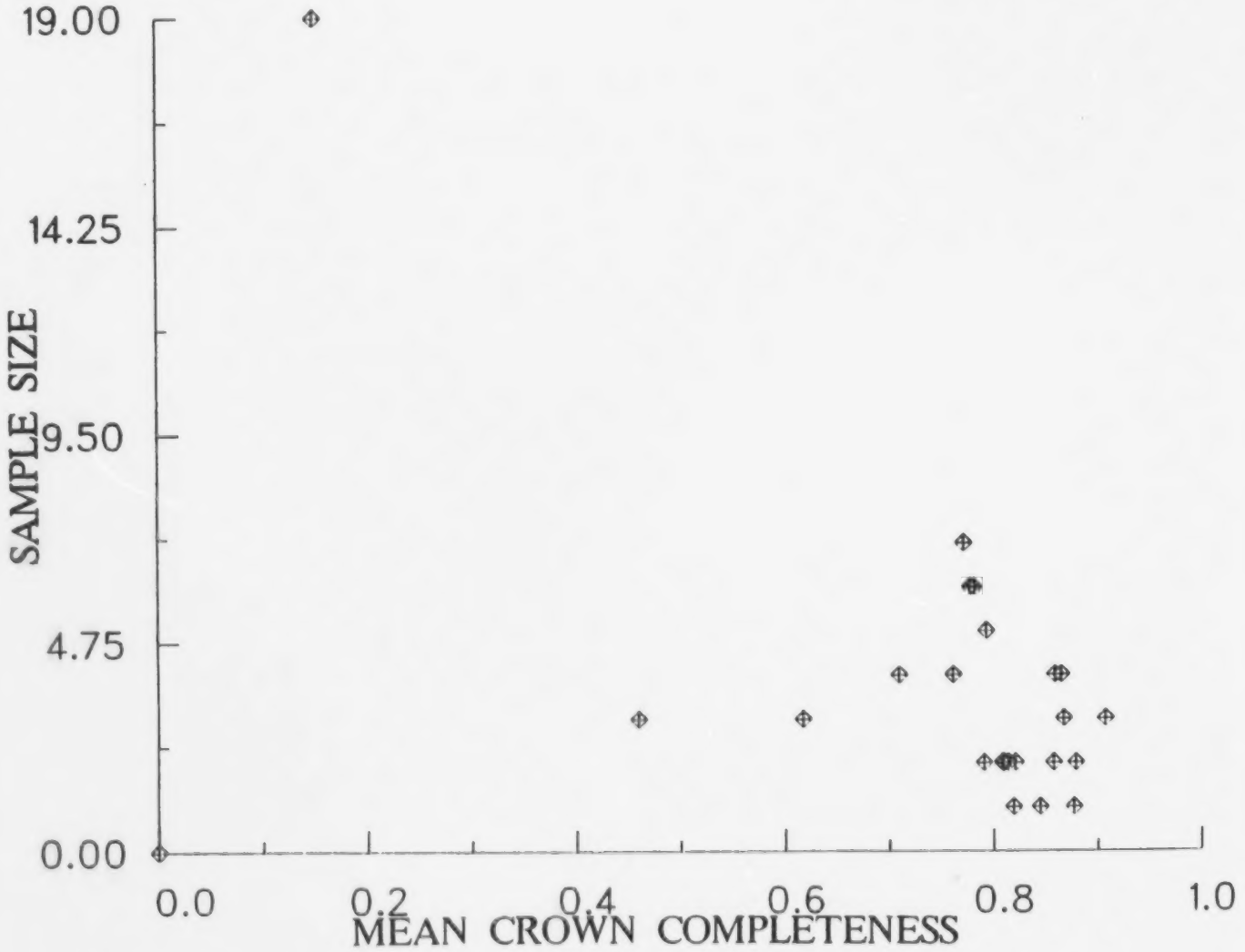

FIGURE 21. Influence of mean crown completeness on the estimated number of diffuse site factor samples necessary for a precision of ± 5% with 95% confidence.

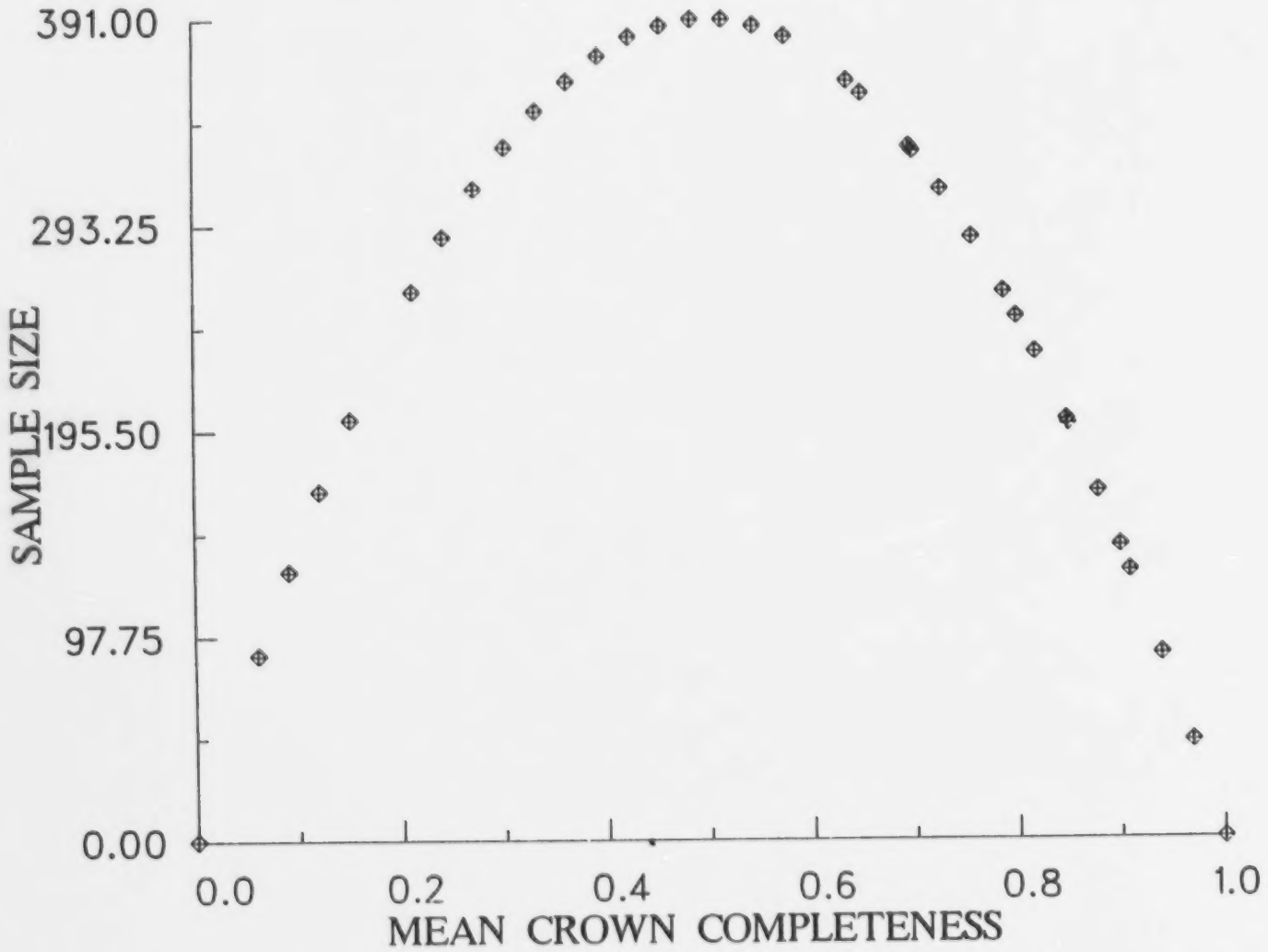

FIGURE 22. Influence of mean crown completeness on the estimated number of ocular and gimbal sight samples necessary for a precision of ± 5% with 95% confidence.

particular canopy distribution cannot be known in advance of sampling. Ocular and gimbal sample sizes follow the binomial distribution (Fig. 22). Table 23 presents size estimates in 10% MCC increments for selected techniques. Because a wide range of means for the spherical densiometer and diffuse site factor were not obtained, maximum sample size estimates are not presented for all possible means. Sample sizes within plots in this study are below the calculated ones in Table 23. Combined over all plots, however, sample sizes were slightly below (50 and 100 mm lens) or well above (moosehorn and gimbal sight) the ones in Table 23.

4.8 Correlation Of Horizontal Plane of Interception with Means and Standard Deviations

Overall, wider angle techniques gave generally higher means and lower standard deviations than narrow angle techniques. Spearman's rank correlation coefficient was used to examine the relationship of projected angle with mean and standard deviation. The HPI for each technique given in Table 1 was used as a measure of angle, and means and standard deviations are from Table 21. The results, both significant ($\underline{P} < 0.05$), indicated a correlation between mean and HPI of 0.90 and between standard deviation and HPI of -0.94.

TABLE 23. Approximate maximum sample sizes for selected techniques to obtain a precision of ± 5% mean crown completeness at 95% confidence

Technique	MCC% 10	20	30	40	50	60	70	80	90
Moosehorn	95	200	275	310	336	310	275	200	95
Spherical dens.	74	104						104	74
50 mm photos	80	170	230	260	277	260	230	170	80
100 mm photos	110	200	265	305	340	305	265	200	110
Diffuse s.f.	13								13
Gimbal sight	135	240	320	370	391	370	320	240	135

4.9 Variation in Relation to Height to Base of Live Crown

The previous analysis indicated an inverse relationship between variance and the HPI among techniques. For a single technique it was hypothesized that as the HBLC increased, the HPI increased, and thus a decrease in variance would result. For this analysis it was necessary to select MCC ranges in which the variance was not related to the mean (see Fig. 11). Potential correlations were examined over appropriate ranges of MCC: 35-65% for the moosehorn, 30-70% for the spherical densiometer, and >70% for both instruments separately. The moosehorn and spherical densiometer showed a slight linear correlation of variance and HBLC in the mid-range ($r = -0.71$, $\underline{P} = 0.095$ moosehorn; $r = -0.81$, $\underline{P} = 0.053$ spherical densiometer; $n=6$ for both), but no relationship in the >70% range.

5 DISCUSSION

All ANOVA's were performed on angular transformed data. This is an appropriate transformation for proportions (Sokal and Rohlf 1981:427). Variances were slightly less heteroscedastic (lower Layard Chi-square) than for untransformed data. Normality over all the observations was not attained with the angular transformation.

Caution should be used when ANOVA's that are not highly significant are interpreted (i.e., $0.01 \leq \underline{P} \leq 0.10$). ANOVA's with probabilities near rejection were repeated using rank

transformed data. In some cases there was a difference in results between the unranked and ranked analyses (Tables 8 and 15), and in another case there was no difference (Table 16). Where differences between the two types of analyses are not found, the results are conclusive. Where there are differences, interpretation is difficult. In these cases, consideration must be given to sample sizes and whether or not the assumptions were met, and to the resulting influence on the F-test. Normal scores of ranked observations gave normality for all techniques, even the moosehorn, because ties were broken randomly.

The non-normal distributions within and among plots may result from the inclusion of zero as a valid measurement. With the moosehorn, many observations recorded either high canopy or zero, but there were few readings in the mid-range. The zero reading reflects gaps in the canopy which are larger than the HPI of the instrument. Provided operator error is small, the variation seen in the data reflects variation in the canopy. The distribution of observations within a plot reflects the distribution of the canopy, but it is unknown which technique is the true index of the canopy. In general, had the two clearcuts been included in the analyses, techniques would have had bimodal distributions of MCC measurements if point data for all plots were combined.

The assumption of randomness was violated because plots were selected for a range of MCC, and point samples within

plots were taken systematically. Most plots had a higher MCC than expected and therefore a large proportion of plots with high MCC was measured. Canopy estimates may be high because natural forest stands tend toward canopy closure. Natural openings in the stand resulting from disease and windthrow increase variability in the canopy. Depending on the size of the plot, the variability may have an effect on the MCC of the plot. Bonnor (1967) used larger plots than were used in this study, and found a similar pattern between the variance and mean.

Because the area of HPI depends on HBLC and, to some extent, on crown depth, it was expected there might be some relationship among HBLC, crown depth, and plot variance within techniques. Emlen (1967) applied a correction factor for height and diameter of typical trees when estimating MCC with an instrument having a 4° angle, although he did not state why. He eliminated the factor when a single point was used. But when potential relationships between variance and tree height were examined from the data in this study, no clear relationship was found. The relationship of variance to the mean may be stronger than the variance to HBLC relationship. Without a large number of samples with identical means and a range of HBLC's, the proposed variance versus HBLC relationship is difficult to test.

No difference was found between observers' ocular estimates and gimbal sight readings. The results were

confirmed by the two-way and multi-way analyses and the analysis of plot means. The results with the gimbal sight support findings of Ormerod (1968).

The ANOVA's with the spherical densiometer showed observer x plot interactions and significant differences between observers. To simulate the results of two independent samples on the same canopy, the two persons using the instrument did not discuss the technique before or during the field measurements. Lemmon (1956) tested for an observer x forest interaction, using analysis of variance. He found no interaction based on a sample size of 28. The results presented here involved considerably more samples (733 observations per person over all plots). Lemmon's conclusion was that operators need training in using the spherical densiometer. No doubt, training would help to standardize results within a study. Comparisons of overstory measurements made with the spherical densiometer by different observers for different studies should be interpreted carefully. Because there are no dots on the grid, different observers would have different interpretations of dots falling on openings in the canopy.

Analyses of the moosehorn showed that there was no plot x person interaction, but the tests of observer differences were less clear. Parametric analyses over all plots showed no difference; ranked analyses indicated otherwise. Analysis of plot means showed no difference between observers. During

sampling, observers tried to stand at the same point for canopy readings. These points were clearly marked, however, there may have been differences where each person stood. As well, the moosehorn used had no device for leveling or holding it vertically, and thus different readings between observers may have been due to the way the instrument was held. Observers tried to be consistent in the way the instrument was held (e.g., resting the viewing tube against the brim of a baseball cap), but slope, downed trees, and holes affected the posture of the person and thus the way the instrument was held. A new version of the moosehorn with a circular spirit level built into the grid has been produced and should eliminate vertical projection problems, although the problem remains of holding it steady.

Time and cost constraints did not allow for a test of differences among persons interpreting photos. Null (1969), Brown and Worley (1965), and J.B. Nyberg (pers. comm., B.C. Ministry of Forests) reported differences among interpreters of photographs. Different persons have different definitions of MCC, and therefore consistent results should not be expected without standardization. Additionally, the 50 mm and 100 mm photos could be analyzed using different angles from the center of each photo.

All analyses indicated no difference among ecotypes when plot effects were considered. Only the moosehorn - concentric grid analyses showed an ecotype x technique interaction. The

interaction showed a minor change of order of rank for techniques in one ecotype compared to the other two ecotypes and overall. Ecotypes were classified by differences in soil and topographic characteristics (Klinka 1976) rather than by forest characteristics.

Significant differences in means were found between techniques tested. Cost and time constraints limited the number of photographs taken per plot, especially for hemispherical photographs. This resulted in highly unbalanced analyses. Interpretation of analyses with only two hemispherical photographs per plot should be done with caution. The computer program GENLIN (general linear models) uses the maximal method algorithm for analyzing unbalanced models. Analyses of plot means are unaffected by unbalanced sample size within plots, provided samples within each plot are an adequate representation of the overstory. However, the ANOVA's computed on plot means did not account for variation within plots. Using plot means for comparison is valid and preferred for unbalanced sample sizes within plots and non-randomly selected samples within plots (J. Petkau, pers. comm., University of B.C.; S.M. Northway, pers. comm., MacMillan Bloedel). As well, plot means can be used to compare discrete variables with continuous variables (A. Kozak, pers. comm., University of B.C.).

The study was designed to test MCC interpretation with diffuse and direct site factor grids. Because of their wide

angles and small size of the plot, it was unnecessary to take more than two photographs per plot. The use of the concentric grids was opportunistic, exploiting a limited and potentially inadequate number of samples. For the size of the plot used and location of photo points, concentric grid angles of 20° and larger would give 100% coverage of the canopy directly above a plot for HBLC's greater than 18 m. A 20° angle would give a 3.4-m radius for 20-m tall canopy; from the photo points, this radius extends beyond the edges of the plot. Wider angles were needed to give full coverage for a canopy HBLC less than 18 m. More samples with the hemispherical lens would probably be necessary if there is to be confidence in the results for concentric grid angles less than 30°. Many plots had an average HBLC of less than 18 m, but the minimum was 11 m.

Within plots and overall, techniques that projected wide angles had higher means and smaller standard deviations than narrow angle techniques. McNay (1985) reported similar results. The higher means may be due to the wide angle averaging out scattered gaps in the canopy, whereas narrow angles may project through a gap at one position, and at another be completely intercepted by canopy. Higher means for wide angles may result from the inclusion of tree boles in the field of view (L.D. Peterson, pers. comm., B.C. Ministry of Forests). Projections intercept the canopy principally at the base of the live crown. When an angle is projected from a

point, the outer edge intercepts the canopy at an angle. Essentially what is recorded is an angular view of the canopy rather than overhead MCC. J.B. Nyberg (pers. comm., B.C. Ministry of Forests) has suggested that higher means and lower variances may result from wide angles that include much of the depth of crowns of surrounding trees rather than just the tree crowns directly overhead.

Wider angles, measured the same distance apart as narrow angle techniques, have more overlap. The moosehorn, spherical densiometer, and photographic techniques had varying degrees of overlap on the plots. Measurements were made 1 m apart, and completely covered the canopy above the plot. The amount of HPI overlap between points is a function of height to base of live crown.

If MCC is simply defined as an angle projected vertically, then techniques or angles that give means different than the technique with the defined angle would be biased. A necessary assumption is that the defined instrument used to index MCC accurately measures the canopy. Bonnor (1967) assumed the true plot MCC was measured with single vertical dot projection. If plot mean MCC was defined as measured by the moosehorn, then techniques different from this would be biased. If the gimbal sight was assumed to be the true, unbiased measuring device, then techniques with means different from this would be biased. Of the techniques used, the gimbal sight is the closest approximation of a single

vertical dot projection estimate of MCC.

The most precise technique over all plots (ignoring differences in sample sizes) was the spherical densiometer, while the least precise was the 10° arc on hemispherical photos. Table 21 summarized standard errors and coefficients of variation for all techniques across all plots. When comparisons were restricted to common locations (Table 22), the diffuse site factor estimate was the most precise, while techniques with discrete measurements were least precise. Only 46 points were considered in the calculation of the statistics of Table 22. It should be noted that a large number of smaller angle measurements are required to view the same area of the canopy as that viewed by a few wide-angle measurements. Table 22 does show that the 10° arc on the hemispherical photographs is more precise than the similarly angled moosehorn, possibly because there are 50 dots on the 10° grid and 25 on the moosehorn grid, or because more time is taken to assess the photos. If the true, unbiased MCC is indexed with the gimbal sight, then all techniques other than ocular and the moosehorn were biased with respect to MCC within a 0.67° angle (Table 20 and Section 4.5.1 on moosehorn-concentric grid point ANOVA). The most precise, unbiased instrument showing no interaction is the moosehorn, with an arc of 10.2° (5.1° from vertical). Bonnor (1967) found that angles projected beyond 7.2° of vertical (14.4° arc) gave biased estimates of MCC.

Of the techniques evaluated, ocular and gimbal sight were the quickest to use. Measurement of the canopy above a point takes only about 5 seconds. The gimbal sight is small, easily carried, and its measurements are little affected by variable weather conditions. The moosehorn estimates require less than 30 seconds per point. The instrument, however, is slightly bulky. Modifications could be made to shorten the viewing tube while keeping the same projection angle. Rain on the plexiglass grid can obscure dots. Spherical densiometer readings require a maximum of 45 seconds per point depending upon canopy structure. Highly irregular canopies with large gaps and low MCC take longer to measure. The total time per plot (33 measurements) for gimbal sight and ocular estimates was 3 minutes each; 10 minutes were required for the moosehorn; and the spherical densiometer took 15 minutes per plot to measure the canopy. The moosehorn costs approximately $75 and the spherical densiometer, $50.

All of the photographic techniques are time consuming and costly, and the equipment is bulky. Each hemispherical photo costs about $8 per photo to print, and a roll of 36 exposure film costs about $10 to purchase and develop. Diffuse estimates require 20 minutes per photograph to interpret. Direct site factor MCC and concentric ring MCC each take 10 minutes per photograph. The Nikon equipment used in this study cost about $2500 (CDN) to purchase new. The tripod and protective camera case are bulky and not easily carried

through heavy understory or up steep slopes. Setup for each photograph takes a few minutes. Conditions for photographs are not always ideal. Direct sunlight shining on the lens must be avoided. Raindrops on the hemispherical lens show up on the printed photograph, so photography during rain should not be attempted. Overall, the time per plot (two photos) required 90 minutes and cost $17, but a permanent record of the canopy was retained.

Mean crown completeness estimates with the 50 mm and 100 mm focal length lenses are slightly less expensive per photo than with the hemispherical photos. A roll of 36 exposure black and white film costs about $20 to purchase, develop, and print (or $0.55 per photograph). Dot grid estimates of MCC for each photo required about 5 minutes. To give the same coverage as hemispherical photographs, more photos are needed. Field setup at each point takes as long as for hemispherical photos. Total time and cost of a large sample may exceed that for hemispherical photos. Direct light and variable weather conditions affect standard photographs the same as they affect hemispherical photos. The lenses are lighter and more portable than the fisheye lens. A good quality 35 mm camera body and 50 mm lens can be purchased for $400. Total time and photo cost (excluding salaries) per plot (eight photos) in this study were 90 minutes and $4.50 for each of the 50 mm and 100 mm techniques.

To correctly compare the efficiency and cost

effectiveness among techniques, sample size estimates for identical precision, time per sample, cost per sample, and capital equipment investment must be taken into account.

Instrument design should include the following: 1) an instrument should be small and light for portability and ease of holding it steady; 2) an instrument should include a leveling device or means for pointing it vertically; 3) dots on grids (either moosehorn or photo grids) should be small and contrast with foliage; and 4) an instrument should be designed to minimize observer effects, i.e., there should be no question between observers on what is open or closed canopy.

A sample design to index MCC should be efficient in sample selection (e.g., random, systematic), sample size, precision, and cost. The purpose of an MCC estimate and its relationship to an auxiliary variable are critical factors for selecting a sample design. Mean crown completeness estimates on small research plots are not likely to be representative of a stand average unless a number of plots are located in the same stand. Small plots can be intensively sampled for complete canopy coverage above the plot. Stand averages can be derived from a number of plots or samples within the stand. The distribution of a large number of sample points will be less normal (Figs. 5 and 6) than the distribution of means derived from a number of sample plots.

Random selection of samples is a basic assumption for most statistical analyses, but is often violated in favour of

ease and efficiency of sampling. Randomly locating points within a plot or stand is time consuming and requires considerable travel from point to point. Systematic samples along transects can be considered as clusters and analyzed with cluster sample techniques, but with a loss in the degrees of freedom. Analyses of canopy measurements here have been treated with simple random sampling formulas. Where natural populations are randomly distributed, systematic sampling can be safely recommended (Cochran 1977).

The necessary distance between sample points to eliminate overlap can be computed from the average HBLC of trees within a plot and instrument angle. The required number of points needed to give 100% coverage of the canopy on small plots can be calculated from area of HPI. Sample point spacing can then be calculated.

Table 23 presented sample size requirements for desired precision. The sample size estimates for the moosehorn were nearly identical to Bonnor's (1967) estimates with the same precision. Table 22 would suggest that sample size requirements for the 10° concentric grid would be slightly less than the moosehorn. Computing a running mean during sampling is another method for determining sample size (Mueller-Dombois and Ellenberg 1974; Greig-Smith 1984).

6 CONCLUSION

Even though there is a lot of variation in the canopy, most techniques were adequately precise at estimating MCC over all plots. Confidence widths of ± 0.03-0.10 MCC over all plots are favorable. Confidence widths within plots are considerably wider because of the small sample sizes in each plot. Wide angle techniques give higher mean MCC than do narrow angle techniques. Wide angle techniques (>10° arc) are biased with respect to estimating MCC within a 0.67° angle. The moosehorn had the best combination of least bias, greatest precision, ease of use, and lowest cost for the sample design used in this study. Individual canopy measurements do not follow a normal distribution. Variance is related to MCC but the amount of variation is dependent upon canopy structure. There is a slight relationship between variance and tree height to base of live crown for individual techniques. Provided operator errors are small, the distribution of canopy measurements reflects the distribution of the forest canopy.

7 LITERATURE CITED

Anderson, M.C. 1964. Studies of the woodland light climate. I. The photographic computation of light conditions. J. Ecol. 52:27-41.

Bonnor, G.M. 1967. Estimation of ground canopy density from ground measurements. J. For. 65(8):544-547.

Brown, H.E. and D.P. Worley. 1965. Some applications of the canopy camera in forestry. J. For. 63(9):674-680.

Bunnell, F.L., R.S. McNay, and C.C. Shank. 1985. Trees and snow: the deposition of snow on the ground - a review and quantitative synthesis. Research, Ministries of Environment and Forests. IWIFR-17. Victoria, B.C.

Church, J.E. 1912. The conservation of snow: its dependence on forests and mountains. Sci. Am. Suppl. 74:152-155.

Cochran, W.G. 1977. Sampling techniques. John Wiley and Sons, Inc., Toronto, Ont.

Conover, W.J. and R.L. Iman. 1981. Rank transformations as a bridge between parametric and nonparametric statistics. The Am. Statistician. 35(3):124-133.

Dodd, C.J.H., A. McLean, and V.C. Brink. 1972. Grazing values as related to tree-crown covers. Can. J. For. Res. 2:185-189.

Emlen, J.T. 1967. A rapid method for measuring arboreal canopy cover. Ecology. 48:158-160.

Evans, G.C. and D.E. Coombe. 1959. Hemispherical and woodland canopy photography and the light climate. J. Ecol. 47:103-113.

Garrison, G.A. 1949. Uses and modifications for "moosehorn" crown closure estimation. J. For. 47:733-735.

Greig-Smith, P. 1983. Quantitative plant ecology. 3rd ed. University of California Press, Berkeley, Cal.

Hale, A.M. 1980. An optical canopy cover instrument. Ohio J. Sci. 80(3):125-128.

Harestad, A.S. and F.L. Bunnell. 1981. Prediction of snow-water equivalents in coniferous forests. Can. J. For. Res. 11(4):854-857.

Hill, R. 1924. A lens for whole sky photographs. Quart. J. R. Meteorol. Soc. 50:227-235.

Jones, D. 1984. Use, misuse, and role of multiple-comparison procedures in ecological and agricultural entomology. Environ. Entomol. 13:635-649.

Kittredge, J. 1948. Forest influences. McGraw-Hill Book Co., Inc., Toronto, Ont.

Klinka, K. 1976. Ecosystem units, their classification, interpretation and mapping in the University of British Columbia Research Forest. Ph.D. thesis, Univ. B.C., Vancouver, B.C.

Lemmon, P.E. 1956. A spherical densiometer for estimating forest overstory density. For. Sci. 2:314-320.

Lindroth, A. and K. Perttu. 1981. Simple calculation of extinction coefficients of forest stands. Agric. Meteorol. 25(2):97-110.

McNay, R.S. 1985. Forest crowns, snow interception, and management of black-tailed deer winter habitat. M.Sc. thesis. Univ. B.C., Vancouver, B.C.

Miller, D.H. 1959. Transmission of insolation through pine forest canopy, as it affects the melting of snow. Mitt. Schweiz. Anst. Forstl. Versuchswesen, 35(1):57-79.

Mueller-Dombois, D. and H. Ellenberg. 1974. Aims and methods of vegetation ecology. John Wiley and Sons, Toronto, Ont.

Null, W.S. 1969. Photographic intrepretation of canopy density - a different approach. J. For. 67(3):175-177.

Olsson, L., K. Carlsson, H. Grip, and K. Perttu. 1982. Evaluation of forest-canopy photographs with diode-array scanner OSIRIS. Can. J. For. Res. 12(4):822-828.

Ormerod, D.W. 1968. Improved instrumentation for estimating tree crown horizontal dimensions by vertical projection. B.SF. thesis. Univ. B.C., Vancouver, B.C.

Robinson, M.W. 1947. An instrument to measure forest crown cover. For. Chron. 23:222-225.

Scheirer, C.J., W.S. Ray, and N. Hare. 1976. The analysis of ranked data derived from completely randomized factorial designs. Biometrics. 32:429-434.

Smith, J.H.G. 1969. Studies of crown development are improving Canadian forest management. Proc. 6th World For. Cong., Madrid. Vol. II, pp. 2309-2316.

Sokal, R.R. and F.J. Rohlf. 1981. Biometry. W.H. Freeman and Co., San Francisco, Cal.

Stauffer, H.B. 1982. A sample size table for forest sampling. Forest Sci. 28:777-784.

Steyn, D.G. 1980. The calculation of view factors from fisheye-lens photographs. Atmosphere Ocean. 18(3):254-258.

Walters, J. and J. Soos. 1962. The gimbal sight for the projection of crown radius. Univ. B.C., Faculty of Forestry, Vancouver, B.C. Research Note No. 39.

Young, J.A., D.W. Hedrick, and R.F. Keniston. 1967. Forest cover and logging- herbage and browse production in the mixed coniferous forest of northeastern Oregon. J. For. 65(11):807-813.

Appendix 1. Paired *t*-tests and Wilcoxon rank-sum statistics for plot means and all pair combinations[a]

	BVgimb	DVoc	DVgimb	DVmoose	DVsd	PVoc	PVgimb	PVmoose	PVsd	50mm	100mm	Diffuse	10°	20°	30°	40°	50°	Direct
Gimmp	0.20	0.46	0.67	0.49	0.00	0.69	0.46	0.69	0.00	0.00	0.01	0.00	0.33	0.21	0.06	0.01	0.00	0.00
	0.81	0.38	0.66	0.19	0.03	0.19	0.26	0.38	0.00	0.00	0.03	0.03	0.19	1.00	0.38	0.08	0.00	0.00
BVgimbal		0.38	0.30	0.04	0.00	0.04	0.06	0.07	0.00	0.00	0.00	0.00	0.05	0.02	0.00	0.00	0.00	0.00
		0.61	0.19	0.00	0.00	0.06	0.48	0.26	0.00	0.00	0.03	0.04	0.03	0.03	0.00	0.00	0.00	0.00
DVocular			0.53	0.00	0.00	0.00	0.07	0.02	0.00	0.00	0.00	0.00	0.02	0.00	0.00	0.00	0.00	0.00
			0.83	0.02	0.00	0.00	0.48	0.21	0.00	0.00	0.00	0.01	0.02	0.00	0.00	0.00	0.00	0.00
DVgimbal				0.01	0.00	0.04	0.04	0.02	0.00	0.00	0.00	0.00	0.02	0.00	0.00	0.00	0.00	0.00
				0.02	0.00	0.02	0.03	0.09	0.00	0.00	0.00	0.03	0.06	0.02	0.00	0.00	0.00	0.00
DVmoosehorn					0.00	0.51	0.65	0.25	0.00	0.00	0.01	0.01	0.35	0.20	0.05	0.01	0.00	0.00
					0.00	0.40	1.00	0.13	0.00	0.01	0.02	0.40	0.15	0.15	0.15	0.06	0.02	0.02
DVsph. dens.						0.00	0.00	0.00	0.01	0.00	0.00	0.83	0.00	0.00	0.00	0.00	0.00	0.08
						0.00	0.00	0.00	0.01	0.00	0.00	0.40	0.31	0.15	0.06	0.06	0.06	0.84
PVocular							0.97	0.87	0.00	0.00	0.01	0.00	0.27	0.15	0.04	0.01	0.00	0.00
							0.45	0.40	0.00	0.00	0.40	0.09	0.09	0.03	0.00	0.00	0.00	0.01
PVgimbal								0.85	0.00	0.00	0.01	0.00	0.31	0.19	0.05	0.01	0.00	0.00
								1.00	0.00	0.00	0.09	0.21	0.40	0.68	0.21	0.03	0.01	0.00
PVmoosehorn									0.00	0.00	0.00	0.00	0.25	0.11	0.02	0.00	0.00	0.00
									0.00	0.00	0.00	0.09	0.40	0.21	0.01	0.00	0.00	0.01
PVsph. dens.										0.00	0.00	0.08	0.00	0.00	0.00	0.00	0.00	0.49
										0.00	0.00	0.00	0.09	0.01	0.00	0.01	0.03	1.00
50 mm											0.00	0.11	0.02	0.01	0.02	0.08	0.49	0.00
											0.00	0.68	0.84	0.06	0.54	0.84	0.84	0.06
100 mm												0.02	0.28	0.32	0.74	0.44	0.04	0.00
												0.68	1.00	1.00	1.00	0.31	0.06	0.09
Diffuse s.f													0.01	0.01	0.02	0.04	0.09	0.00
													0.68	0.68	0.68	0.68	0.68	0.00
10°														0.53	0.12	0.02	0.00	0.00
														0.52	1.00	0.54	0.23	0.23
20°															0.02	0.00	0.00	0.00
															0.54	0.11	0.04	0.11
30°																0.00	0.00	0.00
																0.03	0.02	0.11
40°																	0.00	0.00
																	0.00	0.11
50°																		0.00
																		0.23

[a]DV, BV, and PV refer to observers used

APPENDIX 2. Descriptive statistics for all techniques on untransformed observations for plot G1

Variable	N	Minimum	Maximum	Mean	Std dev	Skewness	Kurtosis	95% Confidence Int.
BWgimbal	33	0.	1.0000	0.84848	0.36411	-1.944	1.779	(.71938,.97759)
DVocular	33	0.	1.0000	0.84848	0.36411	-1.944	1.779	(.71938,.97759)
Gimmp	20	0.50000	1.0000	0.77500	0.17355	-0.140	-0.960	(.69097,.85903)
DVgimbal	33	0.	1.0000	0.87879	0.33143	-2.321	3.388	(.76127,.99631)
PWmoosehorn	33	0.68000	1.0000	0.91030	0.84871 -1	-0.973	0.459	(.88021,.94040)
PWgimbal	33	0.	1.0000	0.84848	0.36411	-1.944	1.779	(.71938,.97758)
PWocular	33	0.	1.0000	0.93939	0.24231	-3.683	11.565	(.85348,1.0253)
DVmoosehorn	33	0.72000	1.0000	0.90182	0.78798 -1	-0.193	-0.922	(.87388,.92976)
10°	2	0.96000	0.98000	0.97000	0.14142 -1	0.000	-2.000	(.84294,1.0971)
20°	2	0.94000	0.95000	0.94500	0.70711 -2	0.000	-2.000	(.88147,1.0085)
30°	2	0.93333	0.94667	0.94000	0.94328 -2	0.000	-2.000	(.85525,1.0248)
40°	2	0.91000	0.94000	0.92500	0.21213 -1	0.000	-2.000	(.73441,1.1156)
100 mm photos	8	0.85714	0.95893	0.92411	0.39030 -1	-0.722	-1.013	(.89148,.95674)
50°	2	0.92000	0.94000	0.93000	0.14142 -1	0.000	-2.000	(.80294,1.0571)
50 mm photos	8	0.90536	0.93750	0.92455	0.10314 -1	-0.657	-0.478	(.91593,.93318)
Diffuse s.f.	2	0.81000	0.81700	0.81350	0.49497 -2	0.000	-2.000	(.76903,.85797)
DVsph. dens.	33	0.88542	0.97917	0.94223	0.20520 -1	-0.654	0.334	(.93496,.94951)
Direct s.f.	2	0.85000	0.87500	0.86250	0.17678 -1	0.000	-2.000	(.70367,1.0213)
PWsph. dens.	33	0.89583	0.97917	0.94949	0.18252 -1	-0.872	0.881	(.94302,.95597)

APPENDIX 2. Descriptive statistics for all techniques on untransformed observations for plot G3

Variable	N	Minimum	Maximum	Mean	Std dev	Skewness	Kurtosis	95% Confidence Int.
BWgimbal	33	0.	1.0000	0.78788	0.41515	-1.408	-0.016	(.64067,.93508)
DVocular	33	0.	1.0000	0.81818	0.39167	-1.650	0.722	(.67930,.95706)
Gimmp	20	0.25000	1.0000	0.76250	0.23613	-0.484	-0.894	(.65199,.87301)
DVgimbal	33	0.	1.0000	0.90909	0.29194	-2.846	6.100	(.80557,1.0126)
PWmoosehorn	33	0.64000	1.0000	0.89939	0.94932 -1	-1.405	1.449	(.86573,.93306)
PWgimbal	33	1.0000	1.0000	1.0000				
PWocular	33	0.	1.0000	0.84848	0.36411	-1.944	1.779	(.71938,.97759)
DVmoosehorn	33	0.60000	1.0000	0.93091	0.98133 -1	-2.007	3.681	(.89576,.96606)
10°	2	0.84000	0.94000	0.89000	0.70711 -1	0.000	-2.000	(.25469,1.5253)
20°	2	0.87000	0.92000	0.89500	0.35355 -1	0.000	-2.000	(.57734,1.2127)
30°	2	0.86000	0.93333	0.89666	0.51852 -1	0.000	-2.000	(.43079,1.3625)
40°	2	0.87000	0.94000	0.90500	0.49497 -1	0.000	-2.000	(.46028,1.3497)
100 mm photos	32	0.83393	0.95000	0.90474	0.28331 -1	-0.744	0.076	(.89463,.91486)
50°	2	0.88000	0.93600	0.90800	0.39598 -1	0.000	-2.000	(.55223,1.2638)
50 mm photos	32	0.86429	0.94286	0.91429	0.19630 -1	-0.681	-0.094	(.90721,.92136)
Diffuse s.f.	2	0.81800	0.82000	0.81900	0.14142 -2	0.000	-2.000	(.80629,.83171)
DVsph. dens.	33	0.91667	1.0000	0.95739	0.17149 -1	0.019	0.473	(.95131,.96347)
Direct s.f.	2	0.83125	0.90625	0.86875	0.53033 -1	0.000	-2.000	(.39227,1.3452)
PWsph. dens.	33	0.88542	0.96875	0.94602	0.19910 -1	-1.591	2.930	(.93896,.95308)

APPENDIX 2. Descriptive statistics for all techniques on untransformed observations for plot F1

Variable	N	Minimum	Maximum	Mean	Std dev	Skewness	Kurtosis	95% Confidence Int.
SWgimbal	33	0.	1.0000	0.51515	0.50752	-0.061	-1.996	(.33519,.69511)
DVocular	33	0.	1.0000	0.45455	0.50565	0.183	-1.967	(.27525,.63384)
Gimmp	20	0.	1.0000	0.56250	0.24164	-0.157	0.231	(.44941,.67559)
DVgimbal	33	0.	1.0000	0.54545	0.50565	-0.183	-1.967	(.36616,.72475)
PWmoosehorn	33	0.	0.96000	0.53333	0.31427	-0.281	-1.173	(.42190,.64477)
PWgimbal	33	0.	1.0000	0.63636	0.48850	-0.567	-1.679	(.46315,.80958)
PWocular	33	0.	1.0000	0.45455	0.50565	0.183	-1.967	(.27525,.63384)
DVmoosehorn	33	0.	0.96000	0.42545	0.32478	0.296	-1.356	(.31029,.54062)
10°	2	0.46000	0.58000	0.52000	0.84853 -1	0.000	-2.000	(-.24237,1.2824)
20°	2	0.45000	0.57000	0.51000	0.84853 -1	0.000	-2.000	(-.25237,1.2724)
30°	2	0.54000	0.63333	0.58666	0.65994 -1	0.	-2.000	(-.62704 -2,1.1796)
40°	2	0.63000	0.69000	0.66000	0.42426 -1	0.000	-2.000	(.27881,1.0412)
100 mm photos	8	0.35893	0.89643	0.65379	0.17349	-0.210	-0.770	(.50875,.79884)
50°	2	0.68400	0.73200	0.70800	0.33941 -1	0.000	-2.000	(.40305,1.0129)
50 mm photos	8	0.71786	0.91964	0.77009	0.65429 -1	1.654	1.592	(.71539,.82479)
Diffuse s.f.	2	0.84400	0.88500	0.86450	0.28991 -1	0.000	-2.000	(.60402,1.1250)
DVsph. dens.	33	0.82292	0.91667	0.87184	0.26234 -1	0.098	-0.849	(.86254,.88115)
Direct s.f.	2	0.89375	0.96250	0.92812	0.48614 -1	0.000	-2.000	(.49135,1.3649)
PWsph. dens.	33	0.86458	1.0000	0.91951	0.37582 -1	0.465	-0.752	(.90618,.93283)

APPENDIX 2. Descriptive statistics for all techniques on untransformed observations for plot F2

Variable	N	Minimum	Maximum	Mean	Std dev	Skewness	Kurtosis	95% Confidence Int.
BWgimbal	33	0.	1.0000	0.87879	0.33143	-2.321	3.388	(.76127,.99631)
DVocular	33	0.	1.0000	0.87879	0.33143	-2.321	3.388	(.76127,.99631)
Gimmp	20	0.50000	1.0000	0.83750	0.18629	-0.644	-0.870	(.75031,.92469)
DVgimbal	33	0.	1.0000	0.93939	0.24231	-3.683	11.565	(.85348,1.0253)
PWmoosehorn	33	0.84000	1.0000	0.93455	0.47768 -1	-0.175	-0.863	(.91761,.95148)
PWgimbal	33	0.	1.0000	0.84848	0.36411	-1.944	1.779	(.71938,.97759)
PWocular	33	0.	1.0000	0.90009	0.29194	-2.846	6.100	(.80557,1.0126)
DVmoosehorn	33	0.80000	1.0000	0.94424	0.56515 -1	-0.894	-0.061	(.92420,.96428)
10°	2	0.94000	0.98000	0.96000	0.28284 -1	0.000	-2.000	(.70588,1.2141)
20°	2	0.95000	0.96000	0.95500	0.70711 -2	0.000	-2.000	(.89147,1.0185)
30°	2	0.95333	0.95333	0.95333				
40°	2	0.94500	0.94500	0.94500				
100 mm photos	8	0.85179	0.93929	0.90692	0.29918 -1	-0.717	-0.681	(.88191,.93193)
50°	2	0.94400	0.94400	0.94400				
50 mm photos	8	0.91250	0.95536	0.93170	0.14310 -1	0.005	-0.687	(.91973,.94366)
Diffuse s.f.	2	0.79900	0.81700	0.80800	0.12728 -1	0.000	-2.000	(.69364,.92236)
DVsph. dens.	33	0.91667	0.98958	0.96622	0.18048 -1	-1.414	1.790	(.95983,.97262)
Direct s.f.	2	0.88125	0.88125	0.88125				
PWsph. dens.	33	0.93750	0.97917	0.95833	0.11934 -1	-0.253	-0.867	(.95410,.96256)

APPENDIX 2. Descriptive statistics for all techniques on untransformed observations for plot E1

Variable	N	Minimum	Maximum	Mean	Std dev	Skewness	Kurtosis	95% Confidence Int.
BWgimbal	33	0.	1.0000	0.69697	0.46669	-0.857	-1.265	(.53149,.86245)
DVocular	33	0.	1.0000	0.69697	0.46669	-0.857	-1.265	(.53149,.86245)
Gimap	20	0.	1.0000	0.65000	0.35726	-0.706	-0.726	(.48280,.81720)
DVgimbal	33	0.	1.0000	0.78788	0.41515	-1.408	-0.016	(.64067,.93508)
PWmoosehorn	33	0.16000	1.0000	0.78788	0.28080	-1.315	0.382	(.68831,.88745)
PWgimbal	33	0.	1.0000	0.75758	0.43519	-1.202	-0.555	(.60326,.91189)
PWocular	33	0.	1.0000	0.78788	0.41515	-1.408	-0.016	(.64067,.93508)
DVmoosehorn	33	0.16000	1.0000	0.84000	0.21772	-1.375	1.241	(.76280,.91720)
10°	2	0.56000	0.86000	0.71000	0.21213	0.000	-2.000	(-1.1959,2.6159)
20°	2	0.64000	0.83000	0.73500	0.13435	0.000	-2.000	(-.47209,1.9421)
30°	2	0.73333	0.84667	0.79000	0.80143 -1	0.000	-2.000	(.69939 -1,1.5101)
40°	2	0.78000	0.85500	0.81750	0.53033 -1	0.000	-2.000	(.34102,1.2940)
100 mm photos	8	0.66429	0.97143	0.86629	0.12208	-0.700	-1.041	(.76423,.96836)
50°	2	0.80800	0.87600	0.84200	0.48083 -1	0.000	-2.000	(.40999,1.2740)
50 mm photos	8	0.84464	0.94286	0.88996	0.40798 -1	0.440	-1.597	(.85585,.92406)
Diffuse s.f.	2	0.85100	0.86400	0.85750	0.91924 -2	0.000	-2.000	(.77491,.94009)
DVsph. dens.	33	0.88542	1.0000	0.94760	0.28938 -1	-0.252	-0.814	(.93734,.95786)
Direct s.f.	2	0.89375	0.92500	0.90937	0.22097 -1	0.000	-2.000	(.71084,1.1079)
PWsph. dens.	33	0.89583	1.0000	0.95455	0.24817 -1	-0.137	-0.511	(.94575,.96335)

APPENDIX 2. Descriptive statistics for all techniques on untransformed observations for plot J1

Variable	N	Minimum	Maximum	Mean	Std dev	Skewness	Kurtosis	95% Confidence Int.
BWgimbal	33	0.	1.0000	0.18182	0.39167	1.650	0.722	(.42936 -1,.32070)
DVocular	33	0.	1.0000	0.36364	0.48850	0.567	-1.679	(.19042,.53685)
Gimmp	20	0.	1.0000	0.28750	0.30645	0.765	-0.412	(.14407,.43093)
DVgimbal	33	0.	1.0000	0.33333	0.47871	0.707	-1.500	(.16359,.50308)
PWmoosehorn	33	0.	0.96000	0.33818	0.38821	0.485	-1.534	(.20053,.47584)
PWgimbal	33	0.	1.0000	0.36364	0.48850	0.567	-1.679	(.19042,.53685)
PWocular	33	0.	1.0000	0.36364	0.48850	0.567	-1.679	(.19042,.53685)
DVmoosehorn	33	0.	1.0000	0.32364	0.40514	0.545	-1.552	(.17998,.46729)
10°	2	0.	0.90000	0.45000	0.63640	0.	-2.000	(-5.2678,6.1678)
20°	2	0.10000 -1	0.89000	0.45000	0.62225	0.000	-2.000	(-5.1407,6.0407)
30°	2	0.80000 -1	0.84667	0.46333	0.54212	0.000	-2.000	(-4.4074,5.3341)
40°	2	0.16000	0.82000	0.49000	0.46669	0.	-2.000	(-3.7030,4.6830)
100 mm photos	8	0.	0.85179	0.34152	0.34553	0.454	-1.339	(.52648 -1,.63039)
50°	2	0.23200	0.80800	0.52000	0.40729	0.000	-2.000	(-3.1394,4.1794)
50 mm photos	8	0.26786 -1	0.86429	0.41205	0.30305	0.238	-1.305	(.15870,.66541)
Diffuse s.f.	2	0.68600	0.73200	0.70900	0.32527 -1	0.000	-2.000	(.41676,1.0012)
DVsph. dens.	33	0.51042	0.89583	0.70518	0.10030	-0.097	-0.609	(.66961,.74074)
Direct s.f.	2	0.74375	0.83750	0.79062	0.66291 -1	0.000	-2.000	(.19502,1.3862)
PWsph. dens.	33	0.63542	0.97917	0.81029	0.10331	-0.162	-1.160	(.77366,.84692)

APPENDIX 2. Descriptive statistics for all techniques on untransformed observations for plot J2

Variable	N	Minimum	Maximum	Mean	Std dev	Skewness	Kurtosis	95% Confidence Int.
BWgimbal	33	0.	1.0000	0.30303	0.46669	0.857	-1.265	(.13755,.46851)
DVocular	33	0.	1.0000	0.27273	0.45227	1.021	-0.958	(.11236,.43309)
Gimmp	20	0.	0.50000	0.11250	0.18979	1.283	0.030	(.23676 -1,.20132)
DVgimbal	33	0.	1.0000	0.21212	0.41515	1.408	-0.016	(.64916 -1,.35933)
PWmoosehorn	33	0.	0.96000	0.23152	0.35281	1.008	-0.745	(.10641,.35662)
PWgimbal	33	0.	1.0000	0.24242	0.43519	1.202	-0.555	(.88111 -1,.39674)
PWocular	33	0.	1.0000	0.33333	0.47871	0.707	-1.500	(.16359,.50308)
DVmoosehorn	33	0.	0.92000	0.23152	0.34594	0.957	-0.923	(.10885,.35418)
10'	2	0.	0.	0.				
20'	2	0.	0.15000	0.75000 -1	0.10607	0.	-2.000	(-.87797,1.0280)
30'	2	0.	0.20000	0.10000	0.14142	0.000	-2.000	(-1.1706,1.3706)
40'	2	0.15000 -1	0.22500	0.12000	0.14849	0.	-2.000	(-1.2142,1.4542)
100 mm photos	7	0.	0.69643	0.17219	0.29902	1.055	-0.743	(-.10435,.44874)
50'	2	0.48000 -1	0.22400	0.13600	0.12445	0.000	-2.000	(-.98215,1.2541)
50 mm photos	7	0.	0.56964	0.26913	0.23190	0.158	-1.685	(.54657 -1,.48361)
Diffuse s.f.	2	0.44300	0.47600	0.45950	0.23335 -1	0.	-2.000	(.24985,.66915)
DVsph. dens.	33	0.15625	0.67708	0.32828	0.11728	1.132	1.457	(.28670,.36987)
Direct s.f.	2	0.41875	0.59375	0.50625	0.12374	0.000	-2.000	(-.60554,1.6180)
PWsph. dens.	33	0.14583	0.96875	0.58649	0.20513	0.154	-0.505	(.51376,.65922)

APPENDIX 2. Descriptive statistics for all techniques on untransformed observations for plot H1

Variable	N	Minimum	Maximum	Mean	Std dev	Skewness	Kurtosis	95% Confidence Int.
BWgimbal	33	0.	1.0000	0.60606	0.49620	-0.434	-1.812	(.43012,.78200)
DVocular	33	0.	1.0000	0.69697	0.46669	-0.857	-1.265	(.53149,.86245)
Gimmp	20	0.25000	1.0000	0.68750	0.26748	-0.017	-1.377	(.56232,.81268)
DVgimbal	33	0.	1.0000	0.72727	0.45227	-1.021	-0.958	(.56691,.88764)
PWmoosehorn	33	0.	1.0000	0.70909	0.29904	-1.018	-0.249	(.60305,.81513)
PWgimbal	33	0.	1.0000	0.63636	0.48850	-0.567	-1.679	(.46315,.80958)
PWocular	33	0.	1.0000	0.75758	0.43519	-1.202	-0.555	(.60326,.91189)
DVmoosehorn	33	0.	1.0000	0.69818	0.33928	-0.854	-0.737	(.57788,.81848)
10'	2	0.78000	0.94000	0.86000	0.11314	0.000	-2.000	(-.15650,1.8765)
20'	2	0.74000	0.95000	0.84500	0.14849	0.000	-2.000	(-.48915,2.1792)
30'	2	0.76667	0.94667	0.85667	0.12728	0.000	-2.000	(-.28689,2.0002)
40'	2	0.77500	0.93500	0.85500	0.11314	0.000	-2.000	(-.16150,1.8715)
100 mm photos	8	0.40893	0.91607	0.75491	0.19515	-0.918	-0.808	(.59176,.91806)
50'	2	0.78400	0.92400	0.85400	0.98995 -1	0.000	-2.000	(-.35435 -1,1.7434)
50 mm photos	8	0.66071	0.92321	0.81004	0.99038 -1	-0.282	-1.401	(.72725,.89284)
Diffuse s.f.	2	0.81400	0.82700	0.82050	0.91924 -2	0.000	-2.000	(.73791,.90309)
DVsph. dens.	33	0.71875	0.96875	0.86616	0.66451 -1	-0.480	-0.754	(.84260,.88972)
Direct s.f.	2	0.85000	0.94375	0.89687	0.66291 -1	0.000	-2.000	(.30127,1.4925)
PWsph. dens.	33	0.75000	0.95833	0.87247	0.58174 -1	-0.277	-1.000	(.85185,.89310)

APPENDIX 2. Descriptive statistics for all techniques on untransformed observations for plot H2

Variable	N	Minimum	Maximum	Mean	Std dev	Skewness	Kurtosis	95% Confidence Int.
BWgimbal	33	0.	1.0000	0.63636	0.48850	-0.567	-1.679	(.46315,.80958)
DVocular	33	0.	1.0000	0.63636	0.48850	-0.567	-1.679	(.46315,.80958)
Gimmp	20	0.25000	1.0000	0.75000	0.22942	-0.419	-0.813	(.64263,.85737)
DVgimbal	33	0.	1.0000	0.57576	0.50189	-0.307	-1.906	(.39780,.75372)
PWmoosehorn	33	0.	1.0000	0.64485	0.32677	-0.481	-1.152	(.52898,.76071)
PWgimbal	33	0.	1.0000	0.60606	0.49620	-0.434	-1.812	(.43012,.78200)
PWocular	33	0.	1.0000	0.60606	0.49620	-0.434	-1.812	(.43012,.78200)
DVmoosehorn	33	0.40000 -1	1.0000	0.68121	0.32318	-0.690	-0.990	(.56662,.79581)
10°	2	0.18000	0.98000	0.58000	0.56569	0.000	-2.000	(-4.5025,5.6625)
20°	2	0.40000	0.89000	0.64500	0.34648	0.000	-2.000	(-2.4680,3.7580)
30°	2	0.54000	0.81333	0.67666	0.19327	0.000	-2.000	(-1.0598,2.4132)
40°	2	0.64000	0.80000	0.72000	0.11314	0.000	-2.000	(-.29650,1.7365)
100 mm photos	8	0.45714	0.96071	0.76071	0.18849	-0.549	-1.054	(.60313,.91830)
50°	2	0.70800	0.82400	0.76600	0.82024 -1	0.000	-2.000	(.29040 -1,1.5030)
50 mm photos	7	0.71250	0.99286	0.82398	0.10322	0.576	-1.027	(.72852,.91944)
Diffuse s.f.	2	0.87500	0.87900	0.87700	0.28284 -2	0.000	-2.000	(.85[illegible].90241)
DVsph. dens.	33	0.80208	0.96875	0.88763	0.50480 -1	0.063	-1.125	(.86973,.90553)
Direct s.f.	2	0.86875	0.88750	0.87812	0.13258 -1	0.000	-2.000	(.75900,.99725)
PWsph. dens.	33	0.84375	0.98958	0.89804	0.38340 -1	0.959	-0.059	(.88445,.91164)

APPENDIX 2. Descriptive statistics for all techniques on untransformed observations for plot A1

Variable	N	Minimum	Maximum	Mean	Std dev	Skewness	Kurtosis	95% Confidence Int.
BWgimbal	0							
DVocular	20	0.	1.0000	0.65000	0.48936	-0.629	-1.604	(.42097,.87903)
Gimmp	20	0.75000	1.0000	0.90000	0.12566	-0.408	-1.833	(.84119,.95881)
DVgimbal	20	0.	1.0000	0.80000	0.41039	-1.500	0.250	(.60793,.99207)
PWmoosehorn	20	0.68000	1.0000	0.86200	0.93110 -1	-0.155	-0.804	(.81842,.90558)
PWgimbal	20	0.	1.0000	0.90000	0.30779	-2.667	5.111	(.75595,1.0441)
PWocular	20	0.	1.0000	0.70000	0.47016	-0.873	-1.238	(.47996,.92004)
DVmoosehorn	20	0.68000	1.0000	0.88400	0.86960 -1	-0.951	0.006	(.84330,.92470)
10°	2	0.88000	0.96000	0.92000	0.56569 -1	0.000	-2.000	(.41175,1.4282)
20°	2	0.86000	0.93000	0.89500	0.49497 -1	0.000	-2.000	(.45028,1.3397)
30°	2	0.86667	0.91333	0.89000	0.32994 -1	0.000	-2.000	(.59356,1.1864)
40°	2	0.88500	0.91500	0.90000	0.21213 -1	0.000	-2.000	(.70941,1.0906)
100 mm photos	8	0.82321	0.96786	0.90937	0.45021 -1	-0.704	-0.206	(.87174,.94701)
50°	2	0.90000	0.92000	0.91000	0.14142 -1	0.000	-2.000	(.78294,1.0371)
50 mm photos	8	0.88929	0.93393	0.91652	0.17697 -1	-0.710	-1.102	(.90172,.93131)
Diffuse s.f.	2	0.80300	0.81600	0.80950	0.91924 -2	0.000	-2.000	(.72691,.89209)
DVsph. dens.	20	0.83333	0.93750	0.88906	0.27513 -1	0.050	-0.649	(.87619,.90194)
Direct s.f.	2	0.90000	0.91250	0.90625	0.88388 -2	0.000	-2.000	(.82684,.98566)
PWsph. dens.	20	0.84375	0.91667	0.89062	0.19851 -1	-0.562	-0.306	(.88133,.89992)

APPENDIX 2. Descriptive statistics for all techniques on untransformed observations for plot A2

Variable	N	Minimum	Maximum	Mean	Std dev	Skewness	Kurtosis	95% Confidence Int.
BWgimbal	0							
DVocular	20	0.	1.0000	0.85000	0.36635	-1.960	1.843	(.67854,1.0215)
Gimmp	20	0.50000	1.0000	0.82500	0.16424	-0.366	-0.706	(.74813,.90187)
DVgimbal	20	0.	1.0000	0.80000	0.41039	-1.500	0.250	(.60793,.99207)
PWmoosehorn	20	0.52000	0.96000	0.83000	0.12507	-0.992	0.193	(.77147,.88853)
PWgimbal	20	0.	1.0000	0.85000	0.36635	-1.960	1.843	(.67854,1.0215)
PWocular	20	0.	1.0000	0.85000	0.36635	-1.960	1.843	(.67854,1.0215)
DVmoosehorn	20	0.52000	1.0000	0.87600	0.14387	-1.330	0.734	(.80867,.94333)
10'	2	0.68000	0.98000	0.83000	0.21213	0.000	-2.000	(-1.0759,2.7359)
20'	2	0.72000	0.93000	0.82500	0.14849	0.000	-2.000	(-.50915,2.1592)
30'	2	0.72667	0.86667	0.79667	0.98995 -1	0.000	-2.000	(-.92765 -1,1.6861)
40'	2	0.75000	0.86000	0.80500	0.77782 -1	0.000	-2.000	(.10616,1.5038)
100 mm photos	8	0.73929	0.94643	0.89375	0.66068 -1	-1.798	1.993	(.83852,.94898)
50'	2	0.78000	0.87200	0.82600	0.65054 -1	0.000	-2.000	(.24151,1.4105)
50 mm photos	8	0.85893	0.91964	0.87969	0.22363 -1	0.786	-0.759	(.86099,.89838)
Diffuse s.f.	2	0.78600	0.79500	0.79050	0.63640 -2	0.000	-2.000	(.73332,.84768)
DVsph. dens.	20	0.89583	0.94792	0.92656	0.14526 -1	-0.268	-0.572	(.91976,.93336)
Direct s.f.	2	0.88125	0.90625	0.89375	0.17678 -1	0.000	-2.000	(.73492,1.0526)
PWsph. dens.	20	0.88542	0.95833	0.91042	0.18634 -1	0.620	0.484	(.90170,.91914)

APPENDIX 2. Descriptive statistics for all techniques on untransformed observations for plot C1

Variable	N	Minimum	Maximum	Mean	Std dev	Skewness	Kurtosis	95% Confidence Int.
BWgimbal	33	0.	1.0000	0.12121	0.33143	2.321	3.388	(.36908 -2,.23873)
DVocular	33	0.	1.0000	0.24242	0.43519	1.202	-0.555	(.88111 -1,.39674)
Gimmp	20	0.	0.75000	0.21250	0.26000	0.879	-0.480	(.90817 -1,.33418)
DVgimbal	33	0.	1.0000	0.21212	0.41515	1.408	-0.016	(.54916 -1,.35933)
PWmoosehorn	33	0.	0.92000	0.22303	0.30984	1.282	0.155	(.11316,.33290)
PWgimbal	33	0.	1.0000	0.27273	0.45227	1.021	-0.958	(.11236,.43309)
PWocular	33	0.	1.0000	0.24242	0.43519	1.202	-0.555	(.88111 -1,.39674)
DVmoosehorn	33	0.	0.96000	0.27273	0.33741	0.906	-0.724	(.15309,.39237)
10'	2	0.12000	0.92000	0.52000	0.56569	0.000	-2.000	(-4.5625,5.6025)
20'	2	0.17000	0.91000	0.54000	0.52326	0.000	-2.000	(-4.1613,5.2413)
30'	2	0.23333	0.88667	0.56000	0.46198	0.000	-2.000	(-3.5907,4.7107)
40'	2	0.31500	0.88000	0.59750	0.39952	0.000	-2.000	(-2.9920,4.1870)
100 mm photos	8	0.	0.82321	0.40223	0.30465	-0.165	-1.352	(.14754,.65692)
50'	2	0.37200	0.87600	0.62400	0.35638	0.000	-2.000	(-2.5780,3.8260)
50 mm photos	8	0.13214	0.82679	0.53482	0.23102	-0.522	-0.836	(.34169,.72796)
Diffuse s.f.	2	0.76300	0.82200	0.79250	0.41719 -1	0.000	-2.000	(.41767,1.1673)
DVsph. dens.	33	0.56250	0.89583	0.67771	0.94612 -1	0.718	-0.505	(.64417,.71126)
Direct s.f.	2	0.75625	0.85625	0.80625	0.70711 -1	0.000	-2.000	(.17094,1.4416)
PWsph. dens.	33	0.59375	0.96875	0.74937	0.97298 -1	0.150	-0.517	(.71487,.78387)

APPENDIX 2. Descriptive statistics for all techniques on untransformed observations for plot C2

Variable	N	Minimum	Maximum	Mean	Std dev	Skewness	Kurtosis	95% Confidence Int.
BVgimbal	33	0.	1.0000	0.24242	0.43519	1.202	-0.555	(.88111 -1,.39674)
DVocular	33	0.	1.0000	0.48485	0.50752	0.061	-1.996	(.30489,.66481)
Gimmp	20	0.	1.0000	0.47500	0.34317	0.308	-1.069	(.31439,.63561)
DVgimbal	33	0.	1.0000	0.42424	0.50189	0.307	-1.906	(.24628,.60220)
PWmoosehorn	33	0.	1.0000	0.43394	0.44979	0.186	-1.830	(.27445,.59343)
PWgimbal	33	0.	1.0000	0.48485	0.50752	0.061	-1.996	(.30489,.66481)
PWocular	33	0.	1.0000	0.48485	0.50752	0.061	-1.996	(.30489,.66481)
DVmoosehorn	33	0.	1.0000	0.45212	0.46157	0.083	-1.906	(.28846,.61579)
10'	2	0.	0.80000	0.40000	0.56569	0.	-2.000	(-4.6825,5.4825)
20'	2	0.10000 -1	0.65000	0.33000	0.45255	0.000	-2.000	(-3.7360,4.3960)
30'	2	0.66670 -1	0.57333	0.32000	0.35826	0.	-2.000	(-2.8989,3.5389)
40'	2	0.15500	0.54500	0.35000	0.27577	0.000	-2.000	(-2.1277,2.8277)
100 mm photos	6	0.	0.94464	0.45670	0.45552	-0.000	-1.932	(.75868 -1,.83752)
50'	2	0.23600	0.56800	0.40200	0.23476	0.000	-2.000	(-1.7072,2.5112)
50 mm photos	6	0.	0.92500	0.49598	0.42138	-0.120	-1.814	(.14370,.84827)
Diffuse s.f.	2	0.74000	0.78200	0.76100	0.29698 -1	0.000	-2.000	(.49417,1.0278)
DVsph. dens.	33	0.38542	0.91667	0.65720	0.15359	0.246	-1.314	(.60274,.71166)
Direct s.f.	2	0.76875	0.81875	0.79375	0.35355 -1	0.000	-2.000	(.47609,1.1114)
PWsph. dens.	33	0.41667	0.93750	0.68340	0.15584	0.153	-0.853	(.62814,.73865)

APPENDIX 2. Descriptive statistics for all techniques on untransformed observations for plot C3

Variable	N	Minimum	Maximum	Mean	Std dev	Skewness	Kurtosis	95% Confidence Int.
BWgimbal	33	0.	1.0000	0.93939	0.24231	-3.683	11.565	(.85348,1.0253)
DVocular	33	0.	1.0000	0.87879	0.33143	-2.321	3.388	(.76127,.99631)
Gimmp	20	0.50000	1.0000	0.95000	0.13079	-2.534	5.391	(.88879,1.0112)
DVgimbal	33	0.	1.0000	0.84848	0.36411	-1.944	1.779	(.71938,.97759)
PWmoosehorn	33	0.68000	1.0000	0.91030	0.85458 -1	-0.948	0.072	(.88000,.94061)
PWgimbal	33	0.	1.0000	0.90909	0.29194	-2.846	6.100	(.80557,1.0126)
PWocular	33	0.	1.0000	0.93939	0.24231	-3.683	11.565	(.85348,1.0253)
DVmoosehorn	33	0.84000	1.0000	0.95515	0.45560 -1	-0.791	-0.310	(.93900,.97131)
10'	2	0.94000	0.98000	0.96000	0.28284 -1	0.000	-2.000	(.70588,1.2141)
20'	2	0.94000	0.97000	0.95500	0.21213 -1	0.000	-2.000	(.76441,1.1456)
30'	2	0.95333	0.96667	0.96000	0.94328 -2	0.000	-2.000	(.87525,1.0448)
40'	2	0.96000	0.96000	0.96000				
100 mm photos	8	0.86250	0.95536	0.90692	0.34248 -1	0.256	-1.045	(.87829,.93555)
50'	2	0.96000	0.96400	0.96200	0.28284 -2	0.000	-2.000	(.93659,.98741)
50 mm photos	8	0.89821	0.94643	0.91964	0.18085 -1	0.177	-1.332	(.90452,.93476)
Diffuse s.f.	2	0.81100	0.83000	0.82050	0.13435 -1	0.000	-2.000	(.69979,.94121)
DVsph. dens.	33	0.89583	1.0000	0.93561	0.22471 -1	0.390	0.277	(.92764,.94357)
Direct s.f.	2	0.86250	0.89375	0.87812	0.22097 -1	0.000	-2.000	(.67959,1.0767)
PWsph. dens.	33	0.90625	1.0000	0.94476	0.19744 -1	0.333	0.647	(.93776,.95176)

APPENDIX 2. Descriptive statistics for all techniques on untransformed observations for plot C4

Variable	N	Minimum	Maximum	Mean	Std dev	Skewness	Kurtosis	95% Confidence Int.
BWgimbal	33	0.	1.0000	0.45455	0.50565	0.183	-1.967	(.27525,.63384)
DVocular	33	0.	1.0000	0.51515	0.50752	-0.061	-1.996	(.33519,.69511)
Gimmp	20	0.	1.0000	0.52500	0.43604	-0.095	-1.717	(.32093,.72907)
DVgimbal	33	0.	1.0000	0.48485	0.50752	0.061	-1.996	(.30489,.66481)
PWmoosehorn	33	0.	1.0000	0.58182	0.35680	-0.362	-1.397	(.45530,.70834)
PWgimbal	33	0.	1.0000	0.54545	0.50565	-0.183	-1.967	(.36616,.72475)
PWocular	33	0.	1.0000	0.54545	0.50565	-0.183	-1.967	(.36616,.72475)
DVmoosehorn	33	0.	1.0000	0.62788	0.36531	-0.708	-1.095	(.49835,.75741)
10°	2	0.20000 -1	0.82000	0.42000	0.56569	0.000	-2.000	(-4.6625,5.5025)
20°	2	0.12000	0.77000	0.44500	0.45962	0.	-2.000	(-3.6845,4.5745)
30°	2	0.28000	0.79333	0.53666	0.36298	0.000	-2.000	(-2.7246,3.7979)
40°	2	0.39500	0.81500	0.60500	0.29698	0.000	-2.000	(-2.0633,3.2733)
100 mm photos	8	0.42321	0.85714	0.72455	0.16598	-0.994	-0.651	(.58579,.86332)
50°	2	0.49200	0.84000	0.66600	0.24607	0.000	-2.000	(-1.5449,2.8769)
50 mm photos	8	0.56250	0.91429	0.77455	0.13205	-0.574	-1.129	(.66416,.88495)
Diffuse s.f.	2	0.75000	0.81200	0.78100	0.43841 -1	0.000	-2.000	(.38711,1.1749)
DVsph. dens.	33	0.73958	0.96875	0.89236	0.56136 -1	-0.750	-0.121	(.87246,.91227)
Direct s.f.	2	0.91875	0.91875	0.91875				
PWsph. dens.	33	0.82292	0.96875	0.91540	0.40825 -1	-0.594	-0.609	(.90093,.92988)

APPENDIX 2. Descriptive statistics for all techniques on untransformed observations for plot D2

Variable	N	Minimum	Maximum	Mean	Std dev	Skewness	Kurtosis	95% Confidence Int.
BWgimbal	33	0.	1.0000	0.42424	0.50189	0.307	-1.906	(.24628,.60220)
DVocular	33	0.	1.0000	0.57576	0.50189	-0.307	-1.906	(.39780,.75372)
Gimmp	20	0.	1.0000	0.38750	0.32922	0.456	-0.883	(.23342,.54158)
DVgimbal	33	0.	1.0000	0.54545	0.50565	-0.183	-1.967	(.36616,.72475)
PWmoosehorn	33	0.40000	-1 0.96000	0.63273	0.26748	-0.812	-0.475	(.53788,.72757)
PWgimbal	33	0.	1.0000	0.45455	0.50565	0.183	-1.967	(.27525,.63384)
PWocular	33	0.	1.0000	0.60606	0.49620	-0.434	-1.812	(.43012,.78200)
DVmoosehorn	33	0.12000	1.0000	0.61818	0.28037	-0.442	-1.073	(.51877,.71760)
10°	2	0.30000	0.94000	0.62000	0.45255	0.000	-2.000	(-3.4460,4.6860)
20°	2	0.47000	0.86000	0.66500	0.27577	0.000	-2.000	(-1.8127,3.1427)
30°	2	0.58667	0.85333	0.72000	0.18856	0.000	-2.000	(-.97412,2.4141)
40°	2	0.67000	0.86000	0.76500	0.13435	0.000	-2.000	(-.44209,1.9721)
100 mm photos	8	0.40179	0.81786	0.65335	0.14500	-0.551	-0.838	(.53213,.77457)
50°	2	0.72800	0.88000	0.80400	0.10748	0.000	-2.000	(-.16167,1.7697)
50 mm photos	8	0.65714	0.84107	0.75580	0.55949 -1	-0.247	-0.428	(.70903,.80258)
Diffuse s.f.	2	0.86800	0.88900	0.87850	0.14849 -1	0.000	-2.000	(.74508,1.0119)
DVsph. dens.	33	0.77083	1.0000	0.87595	0.58426 -1	0.266	-0.886	(.85523,.89666)
Direct s.f.	2	0.86250	0.88750	0.87500	0.17678 -1	0.000	-2.000	(.71617,1.0338)
PWsph. dens.	33	0.87500	0.98958	0.93845	0.29734 -1	-0.077	-0.691	(.92790,.94899)

APPENDIX 2. Descriptive statistics for all techniques on untransformed observations for plot D1

Variable	N	Minimum	Maximum	Mean	Std dev	Skewness	Kurtosis	95% Confidence Int.
BWgimbal	33	0.	1.0000	0.72727	0.45227	-1.021	-0.958	(.56691,.88764)
DVocular	33	0.	1.0000	0.51515	0.50752	-0.061	-1.996	(.33519,.69511)
Gimmp	20	0.50000	1.0000	0.83750	0.20318	-0.708	-1.054	(.74241,.93259)
DVgimbal	33	0.	1.0000	0.54545	0.50565	-0.183	-1.967	(.36616,.72475)
PWmoosehorn	33	0.	1.0000	0.62909	0.29194	-0.274	-0.978	(.52557,.73261)
PWgimbal	33	0.	1.0000	0.60606	0.49620	-0.434	-1.812	(.43012,.78200)
PWocular	33	0.	1.0000	0.48485	0.50752	0.061	-1.996	(.30489,.66481)
DVmoosehorn	33	0.	1.0000	0.51515	0.34377	0.016	-1.482	(.39326,.63705)
10°	2	0.38000	0.54000	0.46000	0.11314	0.	-2.000	(-.55650,1.4765)
20°	2	0.56000	0.60000	0.58000	0.28284 -1	0.000	-2.000	(.32588,.83412)
30°	2	0.64000	0.64667	0.64333	0.47164 -2	0.000	-2.000	(.60096,.68571)
40°	2	0.68500	0.70000	0.69250	0.10607 -1	0.000	-2.000	(.59720,.78780)
100 mm photos	8	0.35000	0.87857	0.67299	0.18606	-0.719	-0.830	(.51744,.82854)
50°	2	0.72800	0.74800	0.73800	0.14142 -1	0.000	-2.000	(.61094,.86506)
50 mm photos	8	0.65000	0.88036	0.75960	0.74756 -1	-0.160	-0.620	(.69710,.82210)
Diffuse s.f.	2	0.84300	0.84600	0.84450	0.21213 -2	0.000	-2.000	(.82544,.86356)
DVsph. dens.	33	0.72917	1.0000	0.82008	0.53260 -1	1.263	2.399	(.80119,.83896)
Direct s.f.	2	0.91250	0.91250	0.91250				
PWsph. dens.	33	0.82292	1.0000	0.88699	0.35336 -1	0.839	1.519	(.87447,.89952)

APPENDIX 2. Descriptive statistics for all techniques on untransformed observations for plot B2

Variable	N	Minimum	Maximum	Mean	Std dev	Skewness	Kurtosis	95% Confidence Int.
BWgimbal	33	0.	1.0000	0.93939	0.24231	-3.683	11.565	(.85348,1.0253)
DVocular	33	0.	1.0000	0.93939	0.24231	-3.683	11.565	(.85348,1.0253)
Gimap	20	0.75000	1.0000	0.92500	0.11754	-0.873	-1.238	(.86999,.98001)
DVgimbal	33	0.	1.0000	0.90909	0.29194	-2.846	6.100	(.80557,1.0126)
PWmoosehorn	33	0.76000	1.0000	0.92606	0.67913 -1	-0.668	-0.445	(.90198,.95014)
PWgimbal	33	0.	1.0000	0.93939	0.24231	-3.683	11.565	(.85348,1.0253)
PWocular	33	0.	1.0000	0.96970	0.17408	-5.480	28.031	(.90797,1.0314)
DVmoosehorn	33	0.80000	1.0000	0.97091	0.47194 -1	-1.934	3.655	(.95417,.98764)
10°	2	0.96000	1.0000	0.98000	0.28284 -1	0.000	-2.000	(.72588,1.2341)
20°	2	0.96000	0.99000	0.97500	0.21213 -1	0.000	-2.000	(.78441,1.1656)
30°	2	0.96000	0.98000	0.97000	0.14142 -1	0.000	-2.000	(.84294,1.0971)
40°	2	0.96000	0.98000	0.97000	0.14142 -1	0.000	-2.000	(.84294,1.0971)
100 mm photos	8	0.90179	0.94821	0.93058	0.14893 -1	-0.915	-0.205	(.91813,.94303)
50°	2	0.96000	0.98000	0.97000	0.14142 -1	0.000	-2.000	(.84294,1.0971)
50 mm photos	8	0.90536	0.96071	0.93705	0.16717 -1	-0.696	-0.091	(.92308,.95103)
Diffuse s.f.	2	0.83600	0.88100	0.85850	0.31820 -1	0.000	-2.000	(.57261,1.1444)
DVsph. dens.	33	0.93750	0.98958	0.96307	0.14521 -1	0.060	-0.600	(.95792,.96822)
Direct s.f.	2	0.86250	0.91875	0.89062	0.39775 -1	0.000	-2.000	(.53326,1.2480)
PWsph. dens.	33	0.90625	0.95833	0.93277	0.14046 -1	-0.292	-0.793	(.92778,.93775)

APPENDIX 2. Descriptive statistics for all techniques on untransformed observations for plot M1

Variable	N	Minimum	Maximum	Mean	Std dev	Skewness	Kurtosis	95% Confidence Int.
BWgimbal	33	0.	1.0000	0.39394	0.49620	0.434	-1.812	(.21800,.56988)
DVocular	33	0.	1.0000	0.27273	0.45227	1.021	-0.958	(.11236,.43309)
Gimmp	20	0.	0.75000	0.32500	0.25777	-0.331	-1.481	(.20436,.44564)
DVgimbal	33	0.	1.0000	0.24242	0.43519	1.202	-0.555	(.88111 -1,.39674)
PWmoosehorn	33	0.	1.0000	0.18667	0.30028	1.605	1.330	(.80193 -1,.29314)
PWgimbal	33	0.	1.0000	0.30303	0.46669	0.857	-1.265	(.13755,.46851)
PWocular	33	0.	1.0000	0.30303	0.46669	0.857	-1.265	(.13755,.46851)
DVmoosehorn	33	0.	0.96000	0.20727	0.27901	1.345	0.654	(.10834,.30620)
10°	2	0.	0.68000	0.34000	0.48083	0.	-2.000	(-3.9801,4.6601)
20°	2	0.20000 -1	0.58000	0.30000	0.39598	0.000	-2.000	(-3.2577,3.8577)
30°	2	0.86670 -1	0.54667	0.31667	0.32527	0.	-2.000	(-2.6058,3.2391)
40°	2	0.16500	0.52500	0.34500	0.25456	0.000	-2.000	(-1.9421,2.6321)
100 mm photos	8	0.	0.80000	0.26451	0.33705	0.951	-0.824	(-.17275 -1,.54629)
50°	2	0.22400	0.52400	0.37400	0.21213	0.000	-2.000	(-1.5319,2.2799)
50 mm photos	8	0.14107	0.74821	0.38304	0.23294	0.855	-0.885	(.18829,.57778)
Diffuse s.f.	2	0.60300	0.63100	0.61700	0.19799 -1	0.	-2.000	(.43911,.79489)
DVsph. dens.	33	0.12500	0.77083	0.31187	0.18164	1.124	0.033	(.24746,.37627)
Direct s.f.	2	0.60625	0.73125	0.66875	0.88388 -1	0.000	-2.000	(-.12539,1.4629)
PWsph. dens.	33	0.12500	0.87500	0.35859	0.22553	1.333	0.395	(.27862,.43855)

APPENDIX 2. Descriptive statistics for all techniques on untransformed observations for plot N1

Variable	N	Minimum	Maximum	Mean	Std dev	Skewness	Kurtosis	95% Confidence Int.
BWgimbal	33	0.	1.0000	0.48485	0.50752	0.061	-1.996	(.30489,.66481)
DVocular	33	0.	1.0000	0.48485	0.50752	0.061	-1.996	(.30489,.66481)
Gimmp	20	0.	1.0000	0.76250	0.31908	-1.030	-0.193	(.61317,.91183)
DVgimbal	33	0.	1.0000	0.57576	0.50189	-0.307	-1.906	(.39780,.75372)
PWmoosehorn	33	0.	1.0000	0.48121	0.30959	0.040	-1.168	(.37143,.59099)
PWgimbal	33	0.	1.0000	0.69697	0.46669	-0.857	-1.265	(.53149,.86245)
PWocular	33	0.	1.0000	0.63636	0.48850	-0.567	-1.679	(.46315,.80958)
DVmoosehorn	33	0.	0.96000	0.56848	0.30883	-0.326	-1.270	(.45898,.67799)
10°	2	0.68000	0.78000	0.73000	0.70711 -1	0.000	-2.000	(.94689 -1,1.3653)
20°	2	0.66000	0.75000	0.70500	0.63640 -1	0.000	-2.000	(.13322,1.2768)
30°	2	0.64667	0.73333	0.69000	0.61278 -1	0.000	-2.000	(.13944,1.2406)
40°	2	0.65000	0.70500	0.67750	0.38891 -1	0.	-2.000	(.32808,1.0269)
100 mm photos	8	0.53036	0.84464	0.74665	0.11075	-1.130	-0.221	(.65406,.83924)
50°	2	0.65200	0.70000	0.67600	0.33941 -1	0.000	-2.000	(.37105,.98095)
50 mm photos	8	0.63929	0.76964	0.72746	0.52097 -1	-1.110	-0.670	(.68390,.77101)
Diffuse s.f.	2	0.74200	0.81200	0.77700	0.49497 -1	0.000	-2.000	(.33228,1.2217)
DVsph. dens.	33	0.60417	0.73958	0.69444	0.35770 -1	-0.822	-0.101	(.68176,.70713)
Direct s.f.	2	0.85625	0.95000	0.90312	0.66291 -1	0.000	-2.000	(.30752,1.4987)
PWsph. dens.	33	0.73958	0.87500	0.79766	0.28172 -1	0.440	0.337	(.78767,.80765)

APPENDIX 2. Descriptive statistics for all techniques on untransformed observations for plot N2

Variable	N	Minimum	Maximum	Mean	Std dev	Skewness	Kurtosis	95% Confidence Int.
BWgimbal	0							
DVocular	33	0.	1.0000	0.90909 -1	0.29194	2.846	6.100	(-.12607 -1,.19443)
Gimmp	20	0.	0.25000	0.75000 -1	0.11754	0.873	-1.238	(.19989 -1,.13001)
DVgimbal	33	0.	1.0000	0.90909 -1	0.29194	2.846	6.100	(-.12607 -1,.19443)
PWmoosehorn	33	0.	0.68000	0.15758	0.21493	1.177	-0.044	(.81366 -1,.23379)
PWgimbal	33	0.	1.0000	0.60606 -1	0.24231	3.683	11.565	(-.25312 -1,.14652)
PWocular	33	0.	1.0000	0.12121	0.33143	2.321	3.388	(.36908 -2,.23873)
DVmoosehorn	33	0.	0.72000	0.13333	0.19485	1.430	1.022	(.64242 -1,.20242)
10°	2	0.	0.44000	0.22000	0.31113	0.000	-2.000	(-2.5754,3.0154)
20°	2	0.	0.40000	0.20000	0.28284	0.	-2.000	(-2.3412,2.7412)
30°	2	0.33330 -1	0.40000	0.21666	0.25927	0.000	-2.000	(-2.1128,2.5462)
40°	2	0.95000 -1	0.43500	0.26500	0.24042	0.000	-2.000	(-1.8951,2.4251)
100 mm photos	8	0.	0.70893	0.39754	0.23807	-0.357	-1.004	(.19851,.59658)
50°	2	0.17200	0.47200	0.32200	0.21213	0.000	-2.000	(-1.5839,2.2279)
50 mm photos	8	0.23214	0.67143	0.50000	0.14443	-0.494	-0.446	(.37926,.62074)
Diffuse s.f.	2	0.73500	0.80700	0.77100	0.50912 -1	0.000	-2.000	(.31358,1.2284)
DVsph. dens.	33	0.12500	0.76042	0.43845	0.20774	0.130	-1.318	(.36479,.51211)
Direct s.f.	2	0.88750	0.96875	0.92812	0.57452 -1	0.000	-2.000	(.41194,1.4443)
PWsph. dens.	33	0.20833	0.86458	0.50253	0.23016	0.229	-1.488	(.42092,.58414)

APPENDIX 2. Descriptive statistics for all techniques on untransformed observations for plot JM

Variable	N	Minimum	Maximum	Mean	Std dev	Skewness	Kurtosis	95% Confidence Int.
BWgimbal	33	0.	1.0000	0.75758	0.43519	-1.202	-0.555	(.60326,.91189)
DVocular	33	0.	1.0000	0.81818	0.39167	-1.650	0.722	(.67930,.95706)
Gimmp	0							
DVgimbal	33	0.	1.0000	0.84848	0.36411	-1.944	1.779	(.71938,.97759)
PWmoosehorn	33	0.68000	1.0000	0.85818	0.83121 -1	-0.030	-0.698	(.82871,.88766)
PWgimbal	33	0.	1.0000	0.87879	0.33143	-2.321	3.388	(.76127,.99631)
PWocular	33	0.	1.0000	0.87879	0.33143	-2.321	3.388	(.76127,.99631)
DVmoosehorn	33	0.64000	1.0000	0.87515	0.67644 -1	-0.949	2.681	(.85117,.89914)
10°	2	0.94000	0.98000	0.96000	0.28284 -1	0.000	-2.000	(.70588,1.2141)
20°	2	0.96000	0.99000	0.97500	0.21213 -1	0.000	-2.000	(.78441,1.1656)
30°	2	0.94000	0.99333	0.96666	0.37710 -1	0.000	-2.000	(.62785,1.3055)
40°	2	0.95000	0.99000	0.97000	0.28284 -1	0.000	-2.000	(.71588,1.2241)
100 mm photos	8	0.84107	0.91607	0.88125	0.23729 -1	-0.053	-0.577	(.86141,.90109)
50°	2	0.95200	0.98800	0.97000	0.25456 -1	0.000	-2.000	(.74129,1.1987)
50 mm photos	8	0.87143	0.93036	0.89263	0.20325 -1	0.670	-0.564	(.87564,.90963)
Diffuse s.f.	2	0.85100	0.88300	0.86700	0.22627 -1	0.	-2.000	(.66370,1.0703)
DVsph. dens.	33	0.87500	0.97917	0.92172	0.26700 -1	-0.135	-0.600	(.91225,.93118)
Direct s.f.	2	0.85000	0.90000	0.87500	0.35355 -1	0.000	-2.000	(.55734,1.1927)
PWsph. dens.	33	0.90625	0.97917	0.94697	0.16339 -1	-0.243	0.154	(.94118,.95276)

APPENDIX 2. Descriptive statistics for all techniques on untransformed observations for plot JB

Variable	N	Minimum	Maximum	Mean	Std dev	Skewness	Kurtosis	95% Confidence Int.
BWgimbal	33	0.	1.0000	0.90909	0.29194	-2.846	6.100	(.80557,1.0126)
DVocular	33	0.	1.0000	0.84848	0.36411	-1.944	1.779	(.71938,.97759)
Gimmp	0							
DVgimbal	33	0.	1.0000	0.78788	0.41515	-1.408	-0.016	(.64067,.93508)
PWmoosehorn	33	0.72000	1.0000	0.86788	0.73814 -1	-0.061	-0.729	(.84171,.89405)
PWgimbal	33	0.	1.0000	0.81818	0.39167	-1.650	0.722	(.67930,.95706)
PWocular	33	0.	1.0000	0.87879	0.33143	-2.321	3.388	(.76127,.99631)
DVmoosehorn	33	0.76000	1.0000	0.91636	0.56003 -1	-0.739	0.427	(.89651,.93622)
10'	2	1.0000	1.0000	1.0000				
20'	2	1.0000	1.0000	1.0000				
30'	2	0.98000	0.99333	0.98666	0.94257 -2	0.000	-2.000	(.90198,1.0714)
40'	2	0.98500	0.98500	0.98500				
100 mm photos	8	0.89286	0.95893	0.93437	0.22011 -1	-0.619	-0.429	(.91597,.95278)
50'	2	0.98400	0.98800	0.98600	0.28284 -2	0.000	-2.000	(.96059,1.0114)
50 mm photos	8	0.92143	0.96964	0.94263	0.20145 -1	0.265	-1.651	(.92579,.95948)
Diffuse s.f.	2	0.89500	0.91900	0.90700	0.16971 -1	0.000	-2.000	(.75453,1.0595)
DVsph. dens.	33	0.92708	0.98958	0.96212	0.16015 -1	-0.368	-0.112	(.95644,.96780)
Direct s.f.	2	0.92500	0.96250	0.94375	0.26517 -1	0.000	-2.000	(.70551,1.1820)
PWsph. dens.	33	0.88542	0.96875	0.94003	0.18603 -1	-0.505	0.535	(.93343,.94662)